CELLULAR STIFFNESS REGULATES METASTASIS OF HEPATOCELLULAR CARCINOMA THROUGH JNK

JUNFAN WANG

M.Phil.

The Hong Kong Polytechnic University

2021

The Hong Kong Polytechnic University

Department of Biomedical Engineering

Cellular Stiffness Regulates Metastasis of Hepatocellular Carcinoma through JNK

Junfan Wang

A thesis submitted in partial fulfillment of the requirements for the degree of Master of Philosophy

January 2021

CERTIFICATE OF ORIGINALITY

I hereby declare that this thesis is my own work and that, to the best of my knowledge and belief, it reproduces no material previously published or written, nor material that has been accepted for the award of any other degree or diploma, except where due acknowledgement has been made in the text.

_____ (Signed)

WANG Junfan (Name of student)

Acknowledgement

Firstly, I would like to express my sincerest gratitude to my supervisor Dr. Youhau Tan. He provided me an opportunity to explore the field of biomechanics and cancer research. Dr. Tan gave me persistent encouragement and patient guidance during my study period, and I could not finish this project without his experimental platform. I will never forget Dr. Tan's teaching, spirit and encouragement.

During my M.Phil. study, I would also like to give my gratitude to all of the technicians and my group members. There are two friends who are special to me and also gave me a lot of help during last two years. Miss Li Keming, who has the firm attitude and determination to pursue pure academic research continually and convincingly, her encouragement and accompanying prompted me to insist on doing research. Miss Xin Ying, who has great intelligence and high standard requirement on experiments has made some achievements on her project. Both of them gave me many constructive suggestions on my project and helped me to solve problems when I encountered difficulties, so, I am also very grateful to Miss Li and Miss Xin.

Being a research student, it is required to work hard and keep making progress on studies. I spent almost all of my time in laboratory, even during public holidays and weekends, so the time I spent to accompany my parents was very limited, for which I feel very guilty to them. However, my parents give me all of their love, understanding and patience, continuously encouraging me to insist on doing research and they always play a role as mentors and close

friends of my life. No matter what I encountered, they always stand by my side at the first time. My fiancé, Mr. Guan Yingqin is the ‘Phospherus’ in my life, it is my great honor to possess his true love and admire. Mr. Guan always comforts me and cheer me up when I feel frustrated and painful while reminds me not to be cocky when I make progress. We are not only friends and lovers, but also soulmates because he could understand all my feelings and thoughts. Although I did little for my families, they gave all of their love to me, and I would not insist till now and finish the study without their unswerving support. Finally, please allow me to consecrate my sincerest and deepest gratitude and love to my families.

There are still lots of cute people I would like to express thanks to, but the vocabularies and language are limited and powerless. It is very lucky for me to enjoy this journey along with all of you for last two years and thanks all of you very much.

Abstract

Distant metastases rather than the primary tumor from which these malignant lesions were initially caused are responsible for more than 90% of human mortality from carcinomas. Hepatocellular carcinoma (HCC), a primary type of liver cancer, has become one of the most prevalent cancer and one of the leading causes of cancer deaths around the whole world. Most HCC cases are distributed in Asia, more than 50% of all cases occur in China alone. Although great advance has been achieved, it remains quite challenging in the prognosis and effective treatment of HCC, due to the nature of chemoresistance, recurrence, and metastasis. Accumulating evidence suggests that HCC contained a subset of cancer cells with the ability to form tumors and give rise to multiple tumor cells, which is called cancer stem cells (CSCs). CSCs are highly invasive and able to spread to other organs and generate secondary tumors. These cells are resistant to chemotherapy and radiotherapy and speculated to play a key role in cancer metastasis and relapse. Therefore, CSCs have been proposed to drive tumor progression and metastasis. To develop effective therapeutic strategies against HCC metastasis, understanding the mechanisms underlying high metastatic ability of HCC is essential and necessary.

It is known that significant alterations in cellular cytoskeleton could induce

changes in cell mechanics, which are associated with tumor progression. Compared to cells of normal tissue, cancer cells, especially CSCs exhibit lower cellular stiffness in many types of cancer, which is correlated with malignancy and poor clinical outcomes. However, it remains largely elusive whether cellular stiffness could regulate metastatic potential and the underlying mechanism. In this study, we aimed to dissect the regulatory effect of cellular stiffness on HCC metastasis. For this purpose, we employed different HCC cell lines and firstly confirm the correlation between their cellular stiffness and metastatic ability. Different methods were used to change cellular stiffness, including activators, inhibitors, plasmids and small interfering RNAs (siRNA)s targeting several molecules that directly related to cytoskeleton. Upon the confirmation of the correlation between cellular stiffness and metastatic ability in HCC cell lines and the efficiency of methods to change cellular stiffness, we examined the functional effect of cellular stiffness on metastasis. We found decreasing cellular stiffness could enhance metastatic ability of HCC cells and in contrast metastasis was impaired when increasing cellular stiffness. These phenomena were proved both in 2D migration and 3D invasion condition. Not only in HCC cells, we also further confirmed the findings in CSCs obtained from 3D soft-fibrin method, metastatic potential was obviously decreased when stiffening CSCs. Our results confirmed

the regulatory roles of cancer cell stiffness in HCC metastasis. To better understand the mechanism underlying the finding that cellular stiffness could regulate metastatic ability, we analysed several related signalling pathways through qPCR and found JNK might play an important role. It is known that JNK functions as activated state by phosphorylation at the site of T183 and Y185, so we examined the change of phosphorylated JNK at protein level by western blotting assay and found phosphorylated JNK was reduced after decreasing cellular stiffness. On the contrary, phosphorylated JNK was augmented when increasing cellular stiffness. Except for the alterations at protein level, we performed rescue experiments to prove it at the functional level. Increasing phosphorylation of JNK through activator Anisomycin could decrease metastasis after soften HCC cells and inhibitor SP600125 that decreases phosphorylation of JNK could conversely increase metastasis. In conclusion, our study proved the regulatory role of cellular stiffness on metastatic ability through JNK pathway. The outcomes of this study may provide new evidence to support the opinion that cancer may be not only a genetic disease but also related to mechanics. The causal role of low mechanical stiffness in promoting metastasis may identify cellular stiffness as a mechanical marker as a therapeutic target for liver cancer metastasis treatment, which will facilitate the development of novel strategies against cancer

cell stiffness and eventually benefit patients with liver cancer.

Table of Contents

List of Figures and Tables

List of Abbreviations

AFM	Atomic Force Microscopy
BCLC	Barcelona Clinic Liver Cancer
CA	Constitutive active
cDNA	Complimentary DNA
CSC	Cancer stem cell
CytoD	Cytochalasin D
DMEM	Dulbecco's modified eagle's medium
DMSO	Dimethyl sulfoxide
DNA	Deoxyribonucleic acid
dNTP	Deoxyribonucleic triphosphates
Doxy	Doxycycline
EGFR	Epidermal growth factor receptor
EMT	Epithelial-Mesenchymal Transition
FAK	Focal adhesion kinase
FBS	Foetal bovine serum
HCC	Hepatocellular carcinoma
IARC	International Agency for Research on Cancer
JNK	c-Jun N-terminal kinase

MAPK	Mitogen-activated protein kinase
mDia1	Diaphanous-related formin-1
MKK4	Mitogen-activated protein kinase kinase 4
MKK7	Mitogen-activated protein kinase kinase 7
MLCK	Myosin light-chain kinase
PBS	Phosphate buffered saline
PS	Penicillin-Streptomycin
qPCR	Quantitative polymerase chain reaction
RhoA	Ras homolog family member A
RNA	Ribonucleic acid
ROCK	Rho-associated protein kinase
RT	Room temperature
siRNA	Small interference RNA
TACE	Transarterial chemoembolization
Thr	Threonine
Tyr	Tyrosine
WHO	World Health Organization

Chapter 1 Introduction

1.1 Hepatocellular Carcinoma (HCC)

It was published on the official website of World Health Organization (WHO) that cancer has become the second leading cause of human deaths and it was reported that there were around 9.6 million cancer-related deaths in 2018 globally (Bray et al., 2018). After two years only, according to the observation results published by International Agency for Research on Cancer (IARC) of WHO, there were more than 19 million new cases of cancer and the number of cancer-caused deaths reached at nearly 10 million during 2020.

Fig 1.1 Global Cancer Observatory published on IARC official website in 2020

Liver is one of the most important organs in human body, which mainly functions to break down and avoid accumulation of toxins. It plays an essential role in maintaining homeostasis of living body. Liver cancer is one of the most prevalent cancers, especially in China, and its incidence is rising steadily worldwide. From 1990 to 2015, it was reported that the growth rate of liver cancer reached at 75% (Global Burden of Disease Liver Cancer) and nearly 0.8 million of patients were diagnosed with

liver cancer yearly (Aragonès et al., 2012). It is also claimed in Figure 1 that nearly 5% of new cancer-related cases were liver cancer, which ranked as the third leading cause of cancer-related death in the whole world in 2018.

Liver cancer is regarded as one of the deadliest cancers because patients with liver cancer at the advanced stage are lower than 10% for 5-year survival (Kulik & El-Serag, 2019). Unless diagnosed at earlier stage, liver cancer threatens lives owing to its high malignancy. Pathologically, liver cancer contains 4 different sub-types: hepatocellular carcinoma (HCC), hepatoblastoma, liver angiosarcoma and cholangiocarcinoma. Among the 4 sub-types of liver cancer, approximately 80% diagnosed liver cancer cases are HCC around the world (Kulik & El-Serag, 2019). The distribution of HCC cases has geographical characteristics. It is reported that the majority of HCC cases are in east and southeast Asia and Sub-Saharan Africa. Asia is the high-risk region of HCC cases, notably, in which approximately 50% to 55% of the total incidence of HCC occur in China alone (Lai, Ratziu, Yuen, & Poynard, 2003; Park et al., 2015). The nature of high chemoresistance, cancer recurrence, and metastasis in HCC shortens the overall survival. Notably, most patients are diagnosed with HCC at advanced stages, of which only 25% are amenable to surgery and the 5-year-recurrence rate reaches 70% after tumor resection (Llovet et al., 2016). So far, many researchers have devoted to the studies of HCC and various methods of prevention and treatments

for HCC have been identified. However, the rate of incidence around the world remains steady except Hong Kong where the incidence cases of HCC are on the rise no matter in males or females every year (Zhu, Seto, Lai, & Yuen, 2016). The Hong Kong Cancer registry claimed in 2015 that liver cancer was identified as the third most common cause of cancer-related deaths and it also ranked as the fifth most common cancer incidence in Hong Kong. Although some significant breakthroughs have been achieved, it is still a big challenge for the prognosis and effective treatment of HCC.

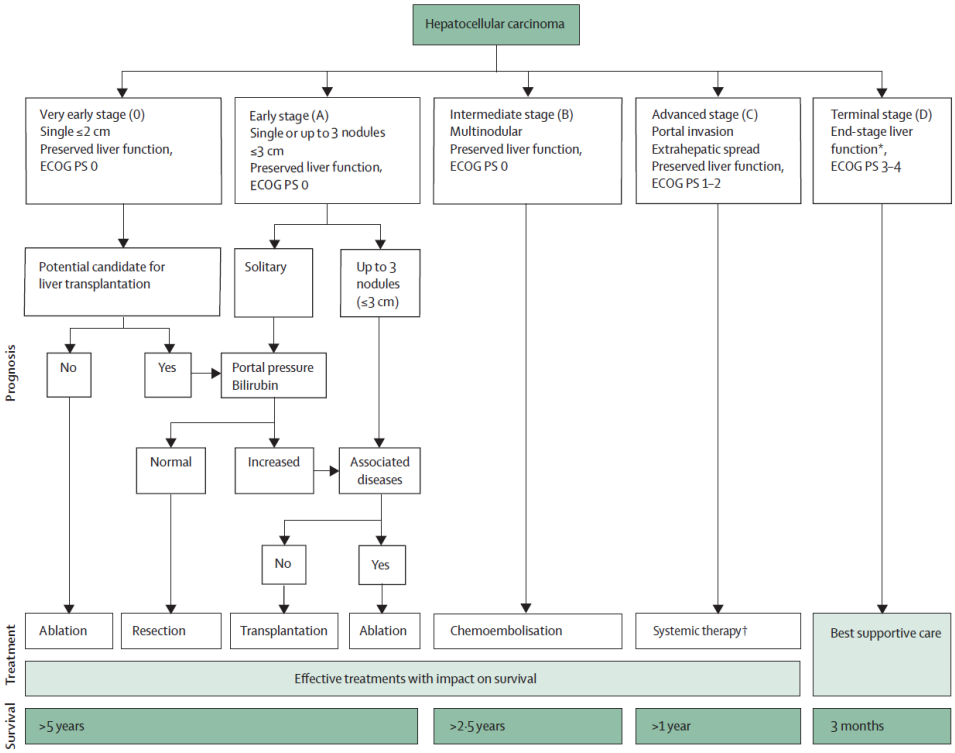

Fig 1.2 Barcelona Clinic Liver Cancer (BCLC) staging and treatment strategy (Forner, Reig, & Bruix, 2018)

1.2 Cancer Metastasis

1.2.1 Overview of cancer metastasis

Metastasis is responsible for over 90% of cancer-related deaths (Mehlen & Puisieux, 2006) and remains a big challenge in cancer biology. The term metastasis can be traced back to 1829 coined by Jean Claud Recamier (Talmadge & Fidler, 2010) and now it is defined as the dissemination of tumor cells from the primary lesion to other organs (Lambert, Pattabiraman, & Weinberg, 2017). Tumor metastasis is a complex process and contains multiple steps.

1.2.2 The invasion-metastasis cascade

Metastases are the final outcomes of a series of highly complex steps, termed as 'the invasion-metastasis cascade'. In order to form new metastatic colonization, the cells from the primary tumor need to undergo several procedures:

(1) Becoming motile and local invasion

It is necessary for cells in the primary tumor to gain a motile phenotype because this step is crucial to initiate the following steps of the invasion-metastasis cascade. There exists an intrinsic barrier to the motility of primary tumor cells with epithelial origin, which is the cell-cell junctions mediated by intercellular E-cadherins. The cell-cell junctions prevent primary tumor cells from disaggregating and dissemination. However, the epithelial-mesenchymal transition (EMT) can help transform epithelial cells with

low motile phenotype into mesenchymal-like cells with high migratory capacity (Polyak & Weinberg, 2009; Thiery, 2002). The process of EMT, which is evolutionarily conserved and commonly happens during development, allows immotile primary tumor cells to escape from the primary lesion and disseminate to distant organs.

Cell migration includes mesenchymal single cell migration, amoeboid single cell migration and collective migration. Mesenchymal single cell migration has four steps: (1) the actin-rich polarized protrusions reach out along the intended direction of migration; (2) focal adhesions mediated by integrin are formed between actin-rich polarized protrusions which are located in the forward direction of cell body and the substrate; (3) forward contraction of the cell body is induced by stress fiber-dependent actomyosin; (4) the focal adhesions located at the lagging edge of the cells are released and the whole cell body is pulled forward (Lauffenburger & Horwitz, 1996). 'Amoeboid migration' is different from the first one which is depend on integrin and actomyosin (Friedl & Wolf, 2003; Sahai, 2005). In this manner of single cell migration, the motility of cells does not rely on integrin-dependent focal adhesions and contractile forces induced by actomyosin but depends on the small GTPase Rho and the downstream regulatory kinase ROCK. Small GTPase Rho and ROCK play an important role in the formation and organization of more widely distributed patches of cortical actin. These effects allow individual cells with high motility to move along the substrate

(Friedl & Wolf, 2003; Sahai, 2005). In collective migration, cancer cells are connected together by cell-cell adhesion molecules and migrate collectively. The intact adhesions among cells allow them to complete and repeat the cyclic four-step migratory process. Cells located at the leading edge of the cell unit extend protrusions and focal adhesions are formed and contractile forces are generated, and focal adhesions at the lagging edge of cell units are released to facilitate forward migration. The process of collective migration is mediated by various integrins and actomyosin-related regulators (Friedl & Wolf, 2003; Sahai, 2005). Through three different types of migration, tumor cells could disseminate not only as individuals but also as multi-cellular units.

After primary tumor cells become motile, they gradually invade locally. In order to arrive at stromal, disseminated tumor cells need to firstly penetrate the basement membrane (Nelson & Bissell, 2006). The process of cancer cells physically squeezing into the surrounding stroma is called local invasion (Friedl & Wolf, 2003; Gupta & Massagué, 2006). Once tumor cells obtain the motility and the ability of penetrating the basement membrane, they can then enter into the neighboring stroma.

(2) Intravasation and survival in the circulation

Intravasation is the process that the locally invasive tumor cells leave their surrounding stroma and enter into the circulation system (Friedl & Wolf, 2003; Gupta & Massagué, 2006). Tumor cell dissemination is usually found in lymph nodes, and

lymphatic spread has been considered as a prognostic biomarker for tumor progression. The majority of distant metastasis of cancer cells is through the blood circulation system, which explains how metastatic cancer cells spread throughout the whole body (Gupta & Massagué, 2006).

After tumor cells enter into blood vessels, they could disseminate and spread throughout the body. However, circulating tumor cells must overcome the damage caused by hemodynamic shear stress and the monitoring of immune system. Only survived circulating tumor cells have the chance to enter into the next step (Gupta & Massagué, 2006; Nash, Turner, Scully, & Kakkar, 2002).

(3) Arrest at the distant organ site and extravasation

The microvasculature of the distant organ site is very narrow, so the survived circulating tumor cells may be trapped by these narrow blood vessels. The trapped tumor cells subsequently attempt to extravasate from these blood vessels and enter into the organ.

(4) Micro-metastasis formation and metastatic colonization

After the extravasation of tumor cells and entering into the surrounding tissue of distant secondary organ sites, the process of metastasis formation may be initiated. The first necessary and critical step for metastasis formation is that the successfully extravasated tumor cells need to adapt to the new microenvironment and survive at the

secondary organ site. The following step of micro-metastasis is the formation of metastasis colonization. In many aspects, the actual ‘metastases’ refer to those that have completed the whole procedure of metastasis colonization because these metastasis colonization are truly malignant and breaks through various complex obstacles. The formation of infinitely growing metastases indicates the endpoint of the invasion-metastasis cascade.

1.3 Cell mechanics and Cancer

1.3.1 Cytoskeleton and cellular contractility

It is known that the stiffness of a cell is determined by its cytoskeleton and cellular contractility. Cytoskeleton is a structure that helps cells maintain their shape and internal organization and also provides mechanical support that enables cells to carry out essential functions such as proliferations and movement. Alterations in cytoskeleton during tumor progression could induce changes in cell mechanics. Cell cytoskeleton also can be regarded as the scaffold in cells and contains interlinking filaments and tubules, which form a complex network extending throughout the cytoplasm from the nucleus to the plasma membrane. Besides, cell contractility is also responsible for cell stiffness. Actomyosin is a main factor to influence cell contractility and has a good correlation with cell mechanics. In conjunction with actomyosin, actin filaments can

generate contractile forces, responding to exogenous forces as well as generating endogenous forces within cells. During cancer cell metastasis, actomyosin plays an important role in this process by producing cell contractility, especially during migration. Cancer cells firstly exert tension in the cell front and actomyosin plays a key role in cell spreading, stabilization of cell polarity, and cellular direct movement (Betapudi, Licate, & Egelhoff, 2006). Finally, the rear part retracts and detaches, while stress fibers are contracted by actomyosin. It has also been reported that actomyosin regulates tumor invasion (Thomas et al., 2016). Actomyosin is directly regulated by RhoA, myosin light chain kinase (MLCK) and ROCK. RhoA is a small GTPase protein of Rho family and a crucial regulator of both actin and actomyosin. It has been found that RhoA plays a key role in F-actin formation and actomyosin activity. Besides, RhoA is an upstream and positive regulator of ROCK, MLCK and actomyosin as shown in Figure 3 (Lessey, Guilluy, & Burridge, 2012). RhoA is closely related to cell mechanical properties (Kataoka & Ogawa, 2016) and the mutation of RhoA is frequently found in various types of human primary or metastatic tumors. Thus, it is expected that cell stiffness may change because of the dysregulation of RhoA, MLCK and ROCK, which mediates the alteration in metastatic potential of cancer cells.

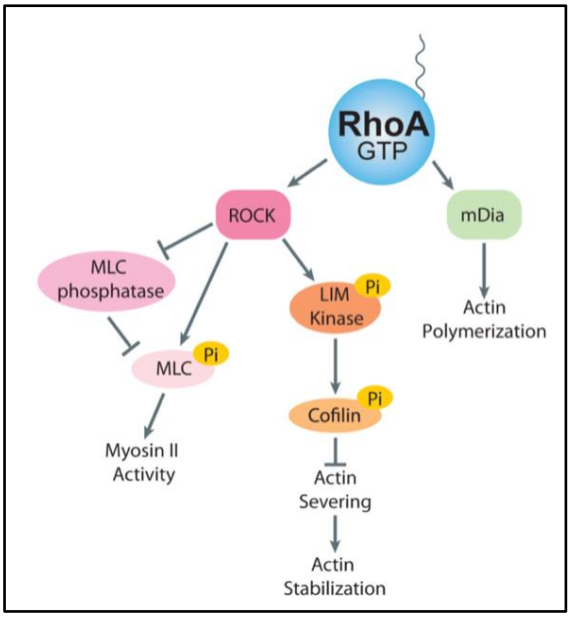

Fig 1.3 RhoA downstream pathways (Lessey et al., 2012)

1.3.2 Mechanical alterations in metastatic tumor cells

As mentioned above, cancer metastasis contained multiple and complex steps. Weaver (Kumar & Weaver, 2009) described the development of tumor metastasis as the force journey of cancer cells: (1) in the primary tumor, tumor cells need to fight with para-carcinoma tissue for space to grow; (2) some tumor cells detach from the original tumor mass and squeeze through the para-carcinoma tissue; (3) in order to metastasize to a distant organ, tumor cells would penetrate into the circulatory system and undergo shear force in blood vessel or lymph-vessel; (4) after arrested at a distant organ site, cancer cells penetrate the endothelium for extravasation and fight with matrix to form a secondary metastatic tumor. Weinberg (Valastyan & Weinberg, 2011) has summarized the tumor metastasis process as shown in Fig.4.

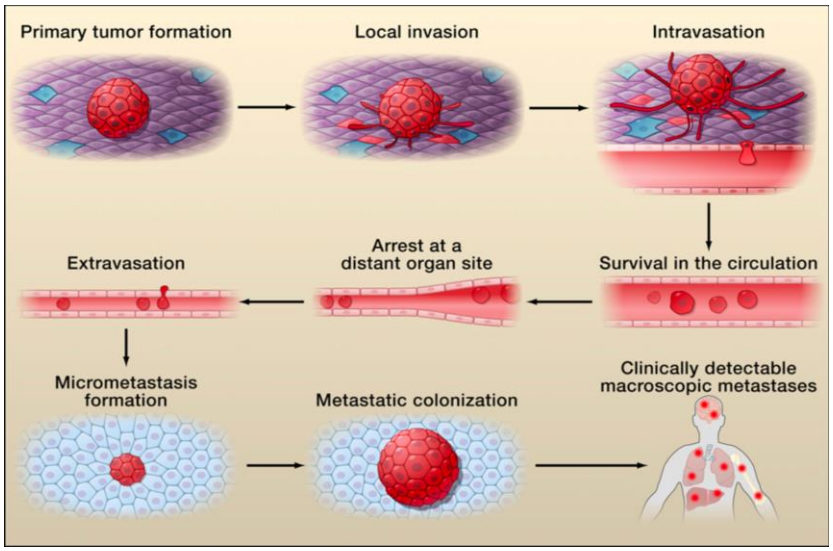

Fig 1.4 The progress of tumor metastasis (Valastyan & Weinberg, 2011)

It has been widely accepted that cancer is caused by accumulations of genetic mutations. Previous studies have mostly focused on abnormal expressions of essential genes and proteins and the activation of key biochemical pathways that are involved in tumor progression. It has been found in recent years that except genetic mutations, cell mechanical properties also play a critical role in tumor progression (Suresh, 2007). A shocking study has been reported that external forces could turn healthy epithelium into a tumor in mice (Fernández-Sánchez et al., 2015), which provides strong evidence to support the correlation between mechanics and cancer. The nanomechanical signatures of cancerous cells and tissues are different from their normal counterparts. In liver and breast cancer, it has been found that tumor tissue is usually stiffer than the normal tissue while cancer cells are softer than normal cells from the same organ (Plodinec et al., 2012; Tian et al., 2015), which is supported by the finding that the softness of resected

breast tumor tissues predicts subsequent local recurrence and metastasis (Fenner et al., 2014) Sarah E. Cross et Al. (Cross, Jin, Rao, & Gimzewski, 2007) used atomic force microscopy (AFM) to detect mechanical properties of cancer and normal cells that were collected from the same organ of cancer patients and they found that there was an obvious difference in cell stiffness between tumor cells and normal cells as shown in Table 1. It can be found that primary tumor cells from patients with lung, breast, and pancreas cancer showed ~70% lower stiffness than benign cells from the same patients. They demonstrated that tumor cells were softer than normal cells in general.

Table 1 Patient characteristics and cytological diagnosis versus mechanical measurements (Young's modulus, *E*).

Case no.	Age/sex	Clinical history	Cytological diagnosis of pleural fluid*	Stiffness (kPa): 'Tumour'	Stiffness (kPa): 'Normal'
1	52/Female	Non-small cell carcinoma of the lung	Positive for metastatic malignant cells	0.56±0.09	2.10±0.79
2	60/Female	Non-small cell carcinoma of the lung	Positive for metastatic malignant cells	0.52±0.12	2.05±0.87
3	49/Female	Breast ductal adenocarcinoma	Positive for metastatic malignant cells	0.50±0.08	1.93±0.50
4	85/Male	Pancreatic adenocarcinoma	Positive for metastatic malignant cells	0.54±0.08	0.54±0.12
5	40/Male	Liver cirrhosis	Negative for malignant cells	–	1.86±0.50
6	47/Male	Fever and hepatic failure	Negative for malignant cells	–	1.75±0.61
7	92/Female	Anasarca peripheral oedema	Negative for malignant cells	–	2.09±0.98

*Cytomorphological diagnosis was made based on morphological analysis combined with immunohistochemical analysis (see Supplementary Information). Stiffness values (*E*) represent mean±s.d.

Table1. Cell stiffness of cancer cells and normal cells

(Cross et al., 2007)

After that, cancer cells have been demonstrated to be softer than normal cells from the same tissue in many other types of cancer, including breast (Q. S. Li, Lee, Ong, & Lim, 2008), cervical (Iyer, Gaikwad, Subba-Rao, Woodworth, & Sokolov, 2009), and esophageal cancer (Fuhrmann et al., 2011). Further, it is shown that metastatic cancer cells are softer than non-metastatic cancer cells (Cross et al., 2008). The stiffness of primary tumor cells can grade their migratory and invasive potential as shown in Figure 5 (Swaminathan et al., 2011) and Figure 6 (W. Xu et al., 2012). Similar results have

also been found in skin (Watanabe et al., 2012), liver (Tian et al., 2015), and head and neck cancer (Y. Q. Chen et al., 2018). These reports suggest that cancer cells exhibit low mechanical stiffness, which can be further extended to clinical specimen. Thus, it is clear that cell stiffness is inversely correlated with metastatic potential of cancer cells. However, it remains largely elusive whether low cell stiffness is the cause or consequence of high metastatic ability of cancer cells.

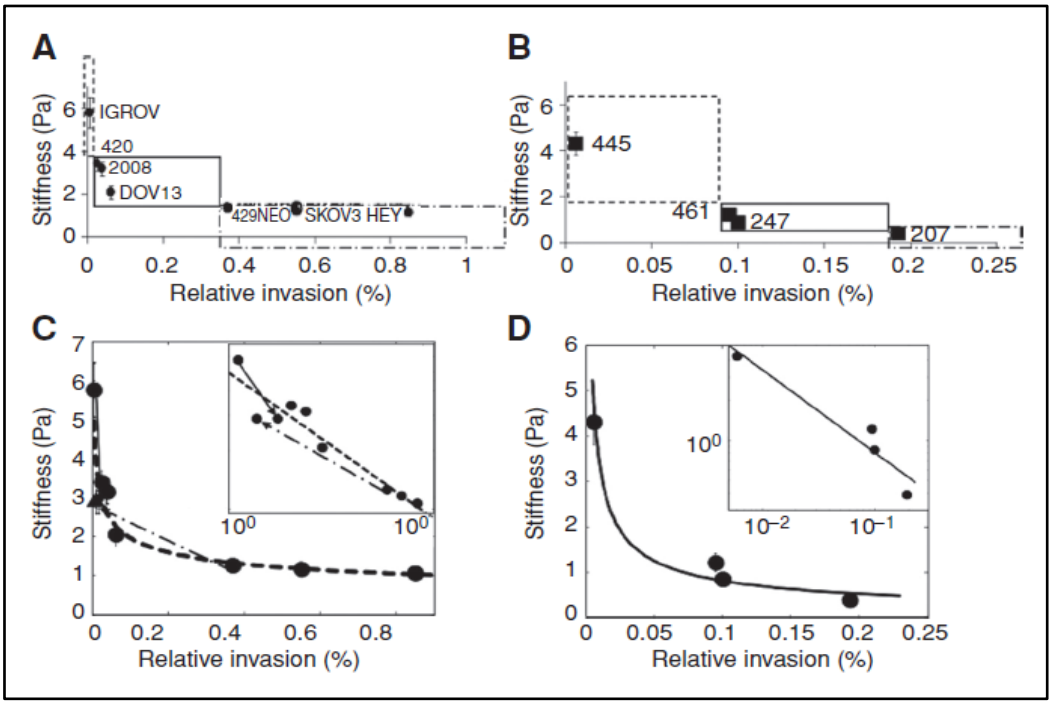

Fig 1.5 Cellular stiffness correlates with invasion (Swaminathan et al., 2011)

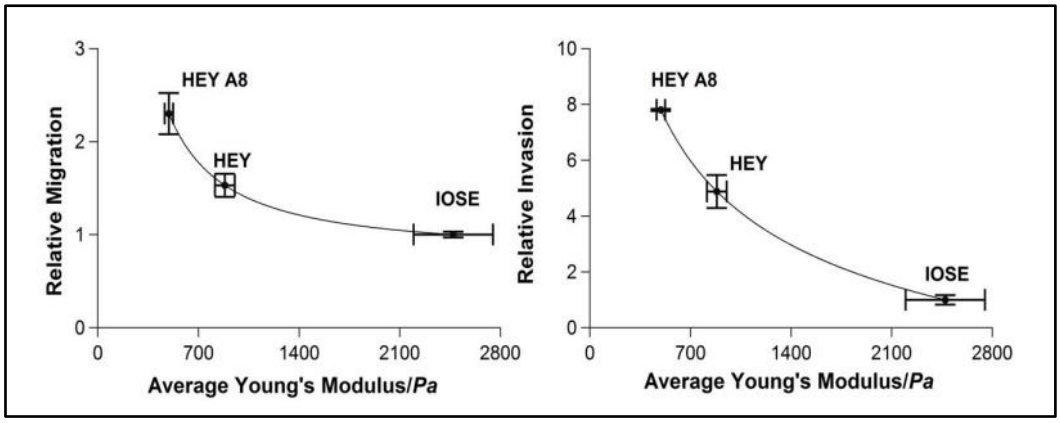

Fig 1.6 Cellular stiffness is a biomarker of metastasis potential
(Watanabe et al., 2012)

1.4 JNK and cytoskeleton

1.4.1 Overview of JNK signaling

c-Jun N-terminal kinase (JNK), also termed as stress-activated MAP kinases, is widely identified in mammals and drosophila. JNK belongs to mitogen-activated protein kinases (MAPKs) family, which also includes extracellular signal-regulated kinase 1/2 (ERK1/2) and p38 (Dhillon, Hagan, Rath, & Kolch, 2007; Noguchi, 2019). There are three subtypes of JNK proteins--JNK1, JNK2 and JNK3, encoded by jnk1 (Mapk8), jnk2 (Mapk9) and jnk3 (Mapk10) (Davis, 2000). It has been reported that JNK is essential for various cellular functions, such as cell migration, proliferation, differentiation, and apoptosis (Bode & Dong, 2007; Dhanasekaran & Reddy, 2017; Seki, Brenner, & Karin, 2012). JNK could be activated by various stimuli, including oxidative stress, ultraviolet radiation, growth factors, and cytokines.

JNK activation involves a series of phosphorylation events (Behrens, Sibilia, & Wagner,

1999; Bogoyevitch & Kobe, 2006). JNK functions as phosphorylated state, which is activated by its upstream MKK4 and MKK7. MKK4 and MKK7 belong to mitogen-activated protein kinase kinase (MAP2K) group and they directly phosphorylate JNK at the threonine 183 (Thr183) site and tyrosine 185 (Tyr185) site (Davis, 2000; Dou, Jiang, Xie, He, & Xiao, 2019). JNKs interact with MAP2Ks and substrates in the site of their N-terminus domain (Haeusgen, Herdegen, & Waetzig, 2011). JNKs mainly activate transcription factor activator protein-1 (AP-1), and AP-1 has a dimerization structure consists of Jun proteins and Fos proteins. Jun proteins contain c-Jun, JunB and JunD and the Fos proteins include c-Fos, FosB, Fra-1 and Fra-2 (Bogoyevitch & Kobe, 2006). Besides, many other factors could be regulated by JNK, for example, p53, STAT, Bcl2, Bax, Bad, c-Myc and so on, which are involved in essential cell processes. Furthermore, there exists another pathway to activate JNK signaling, which is facilitated by scaffold proteins like JNK interacting protein 1 (JIP1). JIP1 could positively regulate JNK pathway by facilitating JNKs and their activators or substrates to form a complex (Bubici & Papa, 2014; Whitmarsh, 2006).

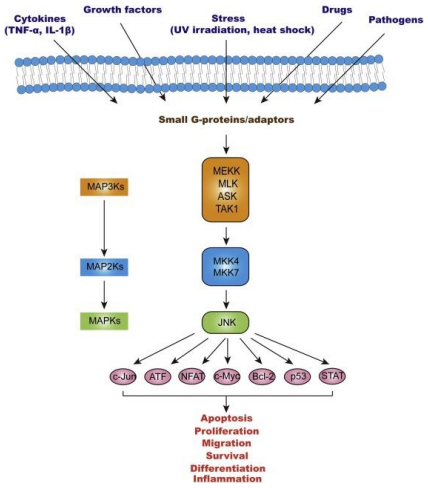

Fig 1.7 The classic JNK signaling pathways

(R. Xu & Hu, 2020)

1.4.2 JNK and cytoskeleton

There have been many studies reporting the functions of JNK, and JNKs do not only play a crucial role in maintaining the integrity and functions of cytoskeleton, but also are regulated by cytoskeleton. The well-defined substrate of JNK is microtubule-associated proteins (MAPs), and JNK could mediate microtubule dynamics (Chang, Jones, Ellisman, Goldstein, & Karin, 2003; J. Chen, Sun, Wasylyk, Wang, & Zheng, 2012). Recently, some studies in Drosophila suggested that actin cytoskeleton was controlled by JNK, as JNK is involved in the process of actin-nucleating center formation and filopodia and lamellipodia formation. JNK is also necessary for cell spreading (Kaltschmidt et al., 2002; Martin-Blanco, Pastor-Pareja, & Garcia-Bellido, 2000). The regulatory role of JNK in cytoskeleton reorganization was further observed in other cytoskeletal proteins, including profilin and cortactin (Jasper et al., 2001). Not only in Drosophila, the regulatory effect of JNK on stress fibers was also investigated

in mammalian cells (Zhang et al., 2003). The role of JNK in regulation of stress fibers in cell migration was also studied. JNK could inhibit the formation of stress fibers at cell edges in some migratory cells (Rennefahrt, Illert, Kerkhoff, Troppmair, & Rapp, 2002), and it was also reported that activation of JNK by knocking down Yap in HCC cells could promote metastasis through inhibit F-actin polymerization (Shi et al., 2018). The specific regulatory role of JNK in cytoskeleton reorganization needs to be further explored.

It is commonly accepted that intracellular MAPK signaling cascade can be regulated by mechanical force or mechanical stress, such as shear stress (S. Li et al., 1997). Actin dynamics also play an essential role in mechanical stretch induced JNK phosphorylation, and this finding has been proved in several cell types (Cheng et al., 2007; Hsu, Lee, Locke, Vanderzyl, & Kaunas, 2010; Okada et al., 1998). However, so far, whether cellular mechanics could regulate JNK signaling is unclear.

1.5 Hypothesis and Aims of this study

HCC is a prevalent and deadly disease around the world and HCC metastasis accounts for a large number of patient deaths. Currently, surgical resection is the first choice as treatment strategy for patients with early-stage HCC. However, there exists high possibility that cancer relapse occurs after tumor resection. For intermediate to advanced-stage HCC patients, systemic chemotherapy and transarterial chemoembolization (TACE) are standard treatment strategies. There are several chemotherapeutic agents commonly used in systemic chemotherapy and TACE, including doxorubicin and sorafenib. However, these chemotherapeutic agents cause side effects, such as genomic instability and multi-kinase inhibition. Although a mass of resources and energy have been devoted to the studies of anticancer drugs, metastasis is still frequently observed in HCC patients. The nature of high chemoresistance, cancer recurrence, and metastasis in HCC builds up a barrier to increasing life expectance of cancer patients and shortens their overall survival. In particular, prevention of cancer metastasis has become a grand challenge to human beings. In order to prolong survival of HCC patients, discovery of new therapeutic targets from different perspective is urgently needed. Besides, cancer metastasis is regarded as one of the biggest threatens to cancer patients and has already been studied for nearly 200 years, the process of metastasis is still controversial. The majority of the studies on metastasis have been

focusing on genetic mutation. Although considerable advance has been achieved, metastasis, however, is still far away from being treated effectively. These may suggest that it is necessary to study tumor metastasis from new perspectives, including mechanics, for the better understanding of this malignancy and the development of novel therapeutic strategies.

In the past decades, the field of mechanobiology has developed vigorously, including the advance in the physical properties of cancer cells. Although cancer biologists have dig out vast biochemical evidence, it is still unable to effectively diagnose and cure cancer, especially cancer metastasis. Physicists and biologists start to ask whether changes in biomechanical properties of cancer cells are required for tumor progression (Fritsch et al., 2010). Mechanical changes occur in tumor cells from tumor initiation, invasion to metastasis. Cancer cells, at least a subpopulation of cancer cells, are proved to be more compliant than normal cells (Fritsch et al., 2010). Although the correlation between mechanical properties and cancer progression has been found, whether mechanical change of cells is the causal factor to cancer progression, especially metastasis, has not been well demonstrated. Specifically, whether modification of cellular stiffness could regulate metastasis is still unclear.

The objectives of this study include the following:

1. To determine whether cancer cell stiffness could regulate metastatic ability in HCC.

2. To elucidate the molecular mechanism underlying the regulatory effect of cellular stiffness on metastasis.

Chapter 2: Methodology and Materials

2.1 Methodology

2.1.1 Cell culture

2.1.1.1 Cell culture medium preparation

The general culture medium contained DMEM, foetal bovine serum (FBS) and Penicillin-Streptomycin (PS). High glucose DMEM (SH30243.01, Hyclone Laboratories Corporation) was purchased from Hyclone and it contained 4.00 mM L-glutomine, 4500 mg/L glucose and sodium pyruvate. This high glucose DMEM was filtered by sterile, disposable vacuum filtration system of 0.1 um and stored at 4℃. FBS (SH30071, Hyclone Laboratories Corporation) was purchased from Hyclone and it was filtered by sterile, disposable vacuum filtration system of 40nm and it was shipped, sub-packaged to 50mL/tube and stored at -20℃. PS (15140-122, Gibco Corporation) was purchased from Gibco and each milliliter contains 10000 units of penicillin (alkali) and 10000 μg streptomycin (alkali), using 0.85% salt form of penicillin G (sodium salt) and streptomycin sulfate. The general culture medium was finally composed by high glucose DMEM, 10% FBS and 1% PS. The medium tube was tightly sealed by parafilm and stored at 4℃.

2.1.1.2 General Cell Culture

Human liver cancer cell lines (HepG2, Huh-7, MHCC97-L, PLC, Bel-7402) were donated as a gift by Professor Xinyuan YUAN of Hong Kong University. They were stored in -80℃ ultra low temperature refrigerator and the liquid nitrogen tank. Before thawing cells, water bath was set and heated to 37℃ and then made the culture medium warm up. The cryovial contained frozen cells was thawed in 37℃ water baths. After melted completely, the whole content was transferred into centrifuge tube which contained 10ml 37℃ culture medium. The centrifuge tube was placed into the centrifuge and centrifuged at 1000rpm for 5 minutes and after centrifuge the supernatant was removed completely. Moderate volume culture medium was used to re-suspended cell pellet and then cellular suspended liquid was spread into different diameter cell culture flask or plate (according to purpose). The cell culture flask or plate was transferred into incubators (Thermos) at 37℃ and supplemented with 5% CO_2. The interval of time to refresh the medium or passage cells was decided according to growth cycle of different types of cells. When passage cells, phosphate buffered saline (PBS) and trypsin-EDTA would be used. 1X PBS (SH30256.01, Hyclone Laboratories Corporation) was purchased from Hyclone which did not contain Calcium and Magnesium and filtered by sterile, disposable vacuum filtration system of 0.1uM. Trypsin-EDTA (25200-072, Gibco Corporation) was purchased from Gibco and it was

used as a concentration of 0.25% and stored at -20℃ for long term but at 4℃ for short time.

When the density of liver cancer cells reached confluence (~10^7 cells in diameter 75cm^2 cell culture flask), the old culture medium was discarded. 3ml 1X sterile phosphate buffered saline was used to wash the cells for 3 times. 2ml Trypsin-EDTA was added to the flask and the flask was placed into 37℃ incubators supplemented with CO_2 for 3-5 minutes. After incubated, 2ml cell culture medium with 10% foetal bovine serum and 1% Penicillin-Streptomycin was added to the flask to neutralize the function of Trypsin-EDTA, the cell suspension was added into a 15ml centrifuge tube and centrifuged at 1000RPM for 5 minutes. After centrifuged, the supernatant was discarded completely. 2ml fresh cell culture medium was added into the centrifuge tube and continuous pipetting was carried out to re-suspend the cell pellet. Moderate volume of cell suspension was spread to cell culture flask or dish with fresh cell culture medium. The flask or dish was eddied gently to distribute the cells evenly. The cell culture flask or dish was transferred to 37℃ incubators supplemented with CO_2. The culture cycle was repeated until around 15 passage.

When cryopreserved cells, cells were re-suspended by foetal bovine serum (FBS), 900ul of cell suspension and 100ul sterile dimethyl sulfoxide (DMSO) were totally mixed and added into sterile cryogenic vial. The vial was fixed on an automatic cooling

frozen storage box and stored in -80℃ ultra low temperature refrigerator for around 24-48 hours and the cryogenic vials were transferred to a liquid nitrogen tank for long term stocking.

2.1.2 3D Fibrin Gel

Liver cancer cells should be cultured and maintained in a standard and good growth condition. Liver cancer cells were cultured in culture flask or plate using DMEM cell culture medium which contained 10% FBS and 1% PS, and after the number of cells was enough, they would be detached from the bottom of the flask or plate and suspended in DMEM without FBS. The density of suspended cells was adjusted to 10^4/ml. Before started to mix the cell suspended liquid and fibrinogen, T7 buffer was preparation firstly. T7 buffer contained 50mM Tris and 150Mm sodium chloride, they were dissolved by deionized water and then adjusted to pH7.4 precisely. T7 buffer was stored at 4℃. Fibrinogen (SEA) was thawed completely at room temperature and diluted the concentration into 2mg/ml using T7 buffer. Suspended cell solution and fibrinogen solution was mixed gently with same volume respectively to make 1:1 fibrinogen and cell solution mixture, resulting in 1mg/ml fibrinogen and 5000 cells/ml density in the mixture. Thrombin was purchased from SEA. 6ul thrombin was pre-added into every well of 24 well-plate as the concentration of 100U/ml and then 300ul

fibrinogen and cell solution mixture was taken out and gently mixed by pipetting up and down once or twice, and then swirling to spread the gel throughout the whole well. After mixing all gels into the well, the plate was transferred to cell culture incubator supplement by 5% CO_2 at 37℃ and the solutions could continuously to form gel for 10 to 15 minutes. After that, 1ml warm cell culture medium contained 10% FBS and 1%PS was added on the top of the gel to the wells. The 3D fibrin gel and cells were cultured at 37℃ and the cell culture medium was refreshed every 2 days.

Multicellular spheroids were formed during the culture periods (at least 5 days), after moderate culture periods, single cells could be harvested from the fibrin gel. Before taking out cells from fibrin gel, fibrinase should be prepared at first. Fibrinase was composed by 0.08g Collagenase (Sigma-Aldrich) and 0.4g Dispaseli (Sigma-Aldrich) and 10ml PBS was used to dissolve them, after dissolved completely, the solution was filtered by sterile, disposable vacuum filtration system and stored at -20℃. Cell culture medium was removed completely at first, after that, 10X fibrinase solution was diluted into 1X by PBS and then 500ul fibrinase solution was added to every well contained fibrin gel. The plate with fibrinase was transferred into 37℃ cell culture incubators supplemented with 5% CO_2 for 30 minutes. After incubated for 30 minutes, the solution in every well was blew gently by a liquid transfer gun for some time and then 7ul EDTA was added to every well, then the plate was transferred to 37℃ cell culture incubators

supplemented with 5% CO_2 for 15 minutes. After incubated for 15 minutes again, all solutions were together collected to the centrifuge tube. The centrifuge tube was centrifuged at 1000×rpm for 5 minutes and supernatant was removed. The same volume of PBS was added to the centrifuge tube to re-suspend cells and chelate EDTA, after homogeneous mixing, the centrifuge tube was centrifuged at 1000RPM for 5 minutes, this process was repeated 3 times and finally cells were harvested from 3D fibrin gel.

2.1.3 Atomic force microscopy (AFM)

At first, HCC cells were seeded on a gelatin coated culture dish before experiment and incubated at 37°C for at least 12 h until well attached. Cellular stiffness was measured by an AFM (Bruker Catalyst) combined with an inverted microscope (Nikon). Soft silicon nitride cantilevers and indenters with pyramid-type tips were used as the AFM probe and the spring constant of indenters was 0.02 N/m (MLCT, Bruker). Before stiffness measurement, the probe sensitivity and spring constant were at first calibrated in culture medium based on thermal vibration of the cantilever. Then, HCC cells were visualized under the inverted microscope. The cells were indented in the sites around the middle of the connecting line between the cell edge and the nucleus. Five different sites near the indentation area were automatically chosen to obtain the force-indentation curves. To avoid cell damage and substrate effect, the indentation depth was set as 500 nm and cell strain in the indentation direction was thus around 10%. The loading rate

was 1 μm/s at room temperature. For each condition, at least 40-50 cells were measured, and Young's modulus of the cells was determined by fitting the force-indentation curves under Sneddon's model. The values of cellular stiffness were averaged, and the distribution of the values was analyzed and displayed in histone graph.

2.1.4 Metastatic ability characterization

2.1.4.1 Migration

2.1.4.1.1 Wound healing assay

(1) For cells transfected by plasmid: A diluted cell suspension will be prepared and seeded into a 24-well plate at 5×10^5 cells per well and cultured until 90%-100% confluence. The monolayer will be wounded with a straight scratch using a 20 μl pipette tip, and then cells will be washed by PBS for at least 3 times to remove cell debris and cultured in medium with 1% FBS and doxycycline. The wound edges and area will be observed under an inverted microscope (4×), pictures will be taken at 0h, 24h and 48 h respectively and then measured using NIH ImageJ software.

(2) For cells pretreated by chemical drugs: A diluted cell suspension will be prepared and seeded into a 24-well plate at 5×10^5 cells per well and cultured until 90%-100% confluence. Drugs will be diluted precisely to appropriate concentration by medium with 1% FBS and then add the mix into wells. The monolayer will be wounded with a

straight scratch using a 100 μl pipette tip, and then cells will be washed by PBS for at least 3 times to remove cell debris and cultured in medium with 1% FBS. The wound edges and area will be observed under an inverted microscope (4×), pictures will be taken at 0h, 24h and 48 h respectively and then measured using NIH ImageJ software.

2.1.4.1.2 Transwell migration

In vitro invasion assays will be examined using Transwell cell culture chambers (5-8 μm pore size). Cells (1×10^5) were placed into the upper chamber with DMEM while the down chamber filled with full cell culture medium. After incubated at 37 °C, 5% CO2 for 24 h, the chambers were stained with 0.1% crystal violet for 1 h. Cells that migrated toward the outer chamber were counted in five representative (10×) fields per insert.

2.1.4.2 Invasion

2.1.4.2.1 Transwell invasion assay

In vitro invasion assays will be examined using Transwell cell culture chambers (5-8 μm pore size). Upper membranes will be coated with Matrigel as a barrier (50 μg/well) for invasion assay. Cells (1×10^5) were placed into the upper chamber with DMEM while the down chamber filled with full cell culture medium. After incubated at 37 °C, 5% CO_2 for 48 h, the chambers were stained with 0.1% crystal violet for 1 h. Cells that migrated toward the outer chamber were counted in five representative (10×) fields per

insert.

2.1.4.2.2 3D tumor spheroid collagen invasion

(1) Tumor spheroid formation

When cells grew to moderate density and number, cells were washed by 1X PBS for three times and then trypsin-EDTA was used to make cells suspended in the medium, they were collected in suspension together and counted at a concentration of $5x10^5$ cells/ml.

Every 20ul could form a drop, so drops of the cell suspension were places on the covers of 100mm cell culture dishes, which were inverted over cell culture dishes and contains 10-12ml DMEM.

Drops were left without shaking for 48 hours and spheroids would form during that period.

(2) Embedding tumor spheroid in collagen

10X DMEM was prepared in advance, 2g DMEM powder (Hyclone) was dissolved into 15ml ultrapure H_2O and after dissolved completely, the solution was filtered by sterile, disposable vacuum filtration system through 0.22um filters. Fresh 0.1M and 0.01M NaOH and 0.1M HCl was prepared and filtered by 0.22um filters. Insulin solution (Sigma-Aldrich) was purchased from Sigma-Aldrich Corporation and Collagen I (Invitrogen) was purchased from Corporation.

A box of ice was packed up and all solutions and liquids were cooled down to 4°C, all performance was held on ice when working with collagen in order to prevent unwanted polymerization. Collagen I was prepared at a final collagen concentration of 1.0 mg/ml, which was in a solution condition containing 10% 10X DMEM, 1% human insulin solution (Sigma-Aldrich), and sterilized PBS. The pH was adjusted to 7.4 by gradually adding 0.1M NaOH. Detailed recipe of 1.0mg/ml was listed below.

The bottom of each well of a 96-well cell culture plate was coated with a minimum volume of 50 µl neutralized collagen I solution. The coated 96-well cell culture plate was transferred to an incubator at 37°C supplemented with 5% CO_2 for at least 30 minutes until the collagen was polymerized, remaining neutralized collagen was still stored on ice temporarily. Remaining neutralized Collagen I was placed into 200ul centrifuge tubes equally at volume of 60ul. Pre-formed spheroids were collected using p1,000 filter tips into 200ul centrifuge tubes. Pre-formed spheroids were pipetted slowly and avoided repeating or excessive pipetting to minimize the side effects of fluid-shearing on the spheroids. After pre-formed spheroids were mixed well with the neutralized Collagen I, the solution was transferred to the coated wells of 96-well cell culture plate. Entire contents would not be dispensed of pipette in order to avoid creating bubbles and dropwise pipetting reduced the chances of disturbing the collagen base layer. The spheroid-collagen mixture was carefully pipetted on top of collagen

base layer. The 96-well cell culture plate was incubated at 37°C and 5% CO_2 until collagen was polymerized.

A minimum volume of 50µl warmed culture medium or culture medium containing desired chemo-attractants, inhibitors, or other treatments was slowly and gently added to each well of the 96-well cell culture plate. The collagen layer containing spheroids might tear if liquid was pipetted onto it too violently. Culture medium could be slowly dispensed down the side of a well to avoid disturbing the collagen.

96-well cell culture plate was incubated at 37 °C and 5% CO_2 to allow cells to invade. Cell invasion into the surrounding collagen may be observed by brightfield or fluorescence imaging and quantified by a variety of methods using epifluorescence, confocal or light sheet microscopy.

2.1.5 Total protein extraction

Total proteins from cell lysates were extracted using 1X RIPA buffer (20-188, Merck Millipore) which was diluted from 10X by PBS, containing 0.5M Tris-HCl, pH 7.4, 1.5M NaCl, 2.5% deoxycholic acid, 10% NP-40, 10mM EDTA. 1X protease inhibitor cocktail (78430, Thermo Fisher Scientific) was added to the RIPA buffer according to the total volume. The lysate with the cocktail of lysis buffer was re-

suspended using pipette and incubated on ice for 30 minutes. The protein lysates were then centrifuged at 13000 rpm for 30 minutes at 4°C. The supernatant was collected, and the protein concentration determined by BCA protein assay kit (PC0020, Solarbio Life Sciences). Under alkaline conditions, the protein reduced Cu2+ to Cu+, which formed a purple blue complex with BCA reagent. The absorption value at 562nm was measured and compared with the standard curve to calculate the concentration of the protein to be measured. BCA standard substance with known concentration was used to create standard curve using Cu^{2+} reagent. Protein was diluted in PBS solution at 1:9 ratio and 20uL BCA working solution which was prepared by BCA reagent and Cu^{2+} reagent in 50:1 ratio was added to diluted protein samples. The absorbance measured at 562nM using a microplate reader.

2.1.6 Nuclear protein extraction

Nuclear proteins from cell lysates were extracted using NE-PER nuclear and cytoplasmic extraction reagents kit (78833, Thermo Fisher Scientific). Adherent cells were harvested with trypsin-EDTA and then centrifuged at 500 × g for 5 minutes. Cell pellet was washed and suspended by PBS. Suspended cells were transferred to a 1.5mL microcentrifuge tube and pelleted by centrifugation at 500 × g for 3 minutes. Use a pipette to carefully remove and discard the supernatant, leaving the cell pellet as dry as possible. Add 1mL ice-cold CER I solution to the cell pellet. Vortex the tube with the

highest setting for 15 seconds to fully suspend the cell pellet. Incubate the tube on ice for 10 minutes and then add ice-cold 55µL CER II solution to the tube. Vortex the tube for 5 seconds on the highest setting and incubate tube on ice for 1 minute. Vortex the tube for 5 seconds on the highest setting. Centrifuge the tube for 5 minutes at maximum speed in a microcentrifuge (16,000 × g). Immediately transfer the supernatant (cytoplasmic extract) to a clean pre-chilled tube. Place this tube on ice until use or storage. Suspend the pellet produced before, which contains nuclei, in 500µL ice-cold NER solution. Vortex on the highest setting for 15 seconds. Place the sample on ice and continue vortex for 15 seconds every 10 minutes, for a total of 40 minutes. Centrifuge the tube at maximum speed (16,000 × g) in a microcentrifuge for 10 minutes. Immediately transfer the supernatant (nuclear extract) fraction to a new clean microcentrifuge tube and place on ice. Store extracts at -80°C until use.

2.1.7 Western blot assay

20-60µg of protein samples were mixed with 4× Laemmli Buffer (#1610747, Bio-Rad) and boiled at 95°C for 10 minutes. Based on the molecular weight of the proteins to be evaluated, resolving gel from 12-15% SDS polyacrylamide gel were made. Pre-stained protein ladder (26617, Thermo Fisher Scientific) was loaded parallel to the protein lanes. Gel electrophoresis was performed at constant voltage of 80-120

volts for 1.5-2.5 hours. Following electrophoresis, proteins were transferred from gel to nitrocellulose membranes (77010, Thermo Fisher Scientific) at constant voltage of 100 volts for 30 minutes. The membrane was then washed with TBS-T and blocked in 5% BSA in 0.1% TBS-T at RT for 2 hours. The blocked membrane was then incubated with respective primary antibody, diluted in 5% BSA in 0.1% TBS-T overnight at 4°C. After primary antibody probing, the membrane was washed at least five times with 0.1% TBS-T, each time for 5 minutes. The membrane was then incubated with HRP-conjugated secondary antibody, diluted in their respective diluent for 1 hour. The membrane was then washed for five times, each time for 5 minutes. Protein signal was developed using enhanced chemiluminescence (ECL) system (Bio-Rad) and then exposed on X-ray film in dark.

2.1.8 Extraction of RNA

Total RNA was extracted using The E.Z.N.A.® HP Total RNA Isolation Kit (Omega BIO-TEK) according to the manufacturer's instructions. Cells were lysed and homogenized by 700µl of GTC Lysis Buffer and incubated at room temperature (RT) for 5 minutes, during this period, the cells should be grinded all the time. Insert a RNA Homogenizer Mini Column into a 2 mL Collection Tube. After cell lysate been mixed

well, transfer all lysate samples to the prepared Mini Column and centrifuge at maximum speed for 2 minutes. The The RNA Homogenizer Mini Column could be discarded and the filtrate was collected. 700µl 70% ethanol was added to the collected filtrate in the collection tube and mixed gently. Insert a HiBind® RNA Mini Column into a 2 mL Collection Tube. Transfer all mixed samples to newly-prepared RNA Mini Column and centrifuge at 10000×g for 1 minute. The filtrate was discarded and 500µl RNA Wash Buffer I was added to the samples on the collection tube, centrifuge at 10000×g for 1 minute and discard the filtrate. DNase was dissolved in DNase Buffer with the ratio of 73.5:1.5. 75µl DNase was added to the sample on the collection tube and incubate at RT for 15 minutes. After incubation, 250µl RNA Wash Buffer II was added and incubate for 2 minutes. After incubation, centrifuge at 10000×g for 1 minute. Discard the filtrate and use 500µl RNA Wash Buffer II to wash the sample for two times at 10000 × g for 1 minute. Centrifuge at maximum speed for 2 minutes to completely dry the HiBind® RNA Mini Column. Transfer the HiBind® RNA Mini Column to a clean 1.5 mL microcentrifuge tube and 40-70 µL Nuclease-free Water to centrifuge at maximum speed for 2 minutes. RNA was dissolved using Nuclease-free Water and the quantity and quality of RNA were assessed using Nanodrop with A260/280>1.8 and A260/230>2.0.

2.1.9 Complementary DNA (cDNA) synthesis

cDNA was synthesized from total RNA extracted using RevertAid RT Reverse Transcription Kit (Thermo Scientific) according to the manufacturer's instructions. 0.1ng-5µg of RNA could be used for cDNA synthesis.

Add the following reagents into a sterile, nuclease-free tube on ice in the indicated order:

Total RNA	0.1ng-5µg
Random Hexamer primer	1µl
Water, nuclease-free	To 12µl
Total volume	12µl

Mix gently and centrifuge briefly, and incubate at 65 °C for 5 min. After incubation finished, add the following components in the indicated order:

5×Reaction Buffer	4µl
RiboLock RNase Inhibitor (20 U/µl)	1µl
10 mM dNTP Mix	2µl
RevertAid M-MuLV RT (200 U/µl)	1µl
Total volume	20µl

After mixed gently and centrifuged briefly, the reaction mixture was incubated for 5 minutes at 25°C followed by 60 min at 42°C. Terminate the reaction by heating at 70°C for 5 min.

2.1.10 Quantitative polymerase chain reaction (qPCR) analysis

Forget-Me-Not™ EvaGreen® qPCR Master Mix Kit (Biotium) was used to prepare for the reaction buffer. Reaction buffer contained 5µl 1×Forget-Me-Not buffer and 0.2µl forward and reverse qPCR primers, the reaction buffer was added to optical 96-well plate. 4.6µl Diluted cDNA was added to each well of 96-well plate, the total volume of final reaction buffer was 10µl. The reaction was performed in CFX96 Touch Deep Well Real-Time PCR System (Bio-Rad) and was monitored real time by CFX Maestro Software (Bio-Rad). The cycling reaction protocol was followed by:

Cycling Step	Temperature	Holding time	Number of cycles
Enzyme activation	95°C	2min	1
Denaturation	95°C	1min	
Annealing	55°C	30s	40
Extension / data acquisition	72°C	30s	1
Dissociation / melt curve	Set up as per instrument guidelines		

The amplification curves were analyzed using CFX Maestro Software (Bio-Rad). All qPCR samples were performed in triplicate, and the amount of target gene expression was calculated by relative quantification method with respective housekeeping gene (GAPDH) as the normalization.

2.2 Materials

2.2.1 Cell lines

Cell lines	Characteristics	Source
HepG2	HCC	HKU
Huh-7	HCC	HKU
MHCC97-L	HCC	ABCT, PolyU
Bel-7402	HCC	ABCT, PolyU

2.2.2 Antibodies

Antibodies	Source	Dilution used
F-actin Staining Kit - Green Fluorescence - Cytopainter	Abcam (ab112125)	1:1000
Invitrogen™ ProLong™ Gold Antifade Mountant with DAPI	Thermo Fisher Scientific (P36935)	——
Mouse monoclonal anti-	Abcam	1:5000

GAPDH	(ab9484)	
Rabbit anti-myosin light chain	Abcam (ab92721)	1:2000
Rabbit anti-myosin light chain2 (Ser19)	Cell signaling technology (#3671)	1:1000
Mouse monoclonal anti-LaminA+LaminC	Abcam (ab238303)	1:1000
Rabbit polyclonal anti-LaminA+C (phospho S392)	Abcam (ab58528)	1:1000
Rabbit polyclonal anti-JNK1+JNK2	Abcam (ab112501)	1:1000
Rabbit polyclonal anti-JNK1+JNK2 (phospho T183+Y185)	Abcam (ab131499)	1:500
Goat polyclonal Secondary Antibody to Mouse IgG - H&L (Alexa Fluor® 594)	Abcam (ab150116)	1:1000

Goat polyclonal Secondary Antibody to Rabbit IgG - H&L (Alexa Fluor® 594)	Abcam (ab150080)	1:1000
Goat polyclonal Secondary Antibody to Mouse IgG - H&L (Alexa Fluor® 488)	Abcam (ab150113)	1:1000
Goat polyclonal Secondary Antibody to Rabbit IgG - H&L (Alexa Fluor® 488)	Abcam (ab150077)	1:1000
Goat Anti-Rabbit IgG (H+L)-HRP Conjugate	BIO-RAD (#170-6515)	1:2000
Goat Anti-Mouse IgG (H+L)-HRP Conjugate	BIO-RAD (#170-6516)	1:2000

2.2.3 Primers

Human Gene	Forward Primer (5'-3')	Reverse Primer (3'-5')
mDia1	GGAGTTACGATAGCCGGAACA	CTTCTGTCTCCAACATGGTCTTG
MLCK	CACCGTCCATGAAAAGAAGAGTAG	GAGAGGCCCTGCAGGAAGATGG
MKK4	AGTGGACAGCTTGTGGACTCT	AACTCCAGACATCAGAGCGGA
MKK7	GCGCTACCAGGCAGA	TGCCATGAGCTCCAT
JNK2	CTGCGTCACCCATACATC	TGGCGTTGCTACTTACTGC

Chapter 3 Decreasing cellular stiffness promotes HCC metastasis

It has been found in recent years that except genetic mutations, cell mechanical properties also play a critical role in tumor progression (Suresh 2007). In 2007, atomic force microscopy (AFM) was (Cross, Jin et al. 2007) used to detect mechanical properties of tumor and normal cells from the same organ of cancer patients and the researchers found that cancer cells were softer than normal cells in general. After that, more and more studies indicated that cancer cells showed a lower mechanical stiffness and metastatic ability of cancer cells had an inverse correlation with their mechanical stiffness. However, it is still not clear whether low mechanical stiffness is the consequence or the cause of cancer metastasis in HCC.

In this chapter, the correlation between cellular stiffness and metastatic ability was established among several HCC cell lines at first. The functional role of tumor cell softening in metastatic ability of HCC was investigated in vitro. Several inhibitors of cytoskeleton protein or cytoskeleton regulators were applied to decrease cellular stiffness, including Blebbistatin and Y-27632. Except pharmacological treatment, small interfering RNAs (siRNAs) were also used to knock down the expression of cytoskeleton-related genes in order to decrease cellular stiffness. Various functional assays were performed to examine metastatic ability of HCC cells in both 2D and 3D conditions. Besides, we also established the correlation between cellular stiffness and metastatic ability of CSCs.

3.1 Establishment of the correlation between cellular stiffness and metastatic ability in HCC cell lines

In order to characterize the correlation between mechanical stiffness and metastatic ability among HCC cell lines, MHCC97-L, HepG2 and Bel-7402 with different malignancy were utilized in the study and their stiffness was measured by AFM. Young's modulus was used to describe cellular stiffness and obtained by fitting the force-indentation curve of each measurement using the Hertzian contact model **(Figure 3.1a, right)**. MHCC97-L cells exhibited the highest stiffness (approximately 4 kPa), which was followed by HepG2 cells (3 kPa) and then Bel-7402 cells (nearly 2 kPa). The histograms of Young's modulus showed the stiffness distribution, which was fitted by Gaussian functions **(Figure 3.1a, left)**. The distribution of MHCC97-L cell stiffness was broad, and the center peak value was close to 3kPa. The histogram curve of HepG2 was narrower than MHCC97-L and the peak point was shifted to around 2kPa. The histogram of Bel-7402 was the narrowest one and the peak value was 1kPa. The results indicated that the mechanical stiffness of MHCC97-L, HepG2 and Bel-7402 gradually decreased. Further, we examined metastatic ability of MHCC97-L, HepG2 and Bel-7402, including migration and invasion, which were measured by wound healing assay, transwell migration assay, and transwell invasion assay, respectively. The results of wound healing assay showed that the percentage of wound closure of MHCC97-L cells was around 50% slower than HepG2 cells **(Figure 3.1b)**, suggesting that the migration ability of MHCC97-

L cells is weaker than HepG2 cells. In transwell migration assay, the number of migrated cells of MHCC97-L, HepG2 and Bel-7402 was less than 10, around 40 and 60 **(Figure 3.1c)**, respectively. Similarly, the number of invaded cells gradually increased from MHCC97-L, HepG2 to Bel-7402 cells **(Figure 3.1d)**. These results suggest that MHCC97-L, HepG2 and Bel-7402 cells exhibit increasing migratory and invasive abilities. The results in Fig. 3.1a, c, and d demonstrate that metastatic potential of liver cancer cells is inversely correlated with cellular stiffness.

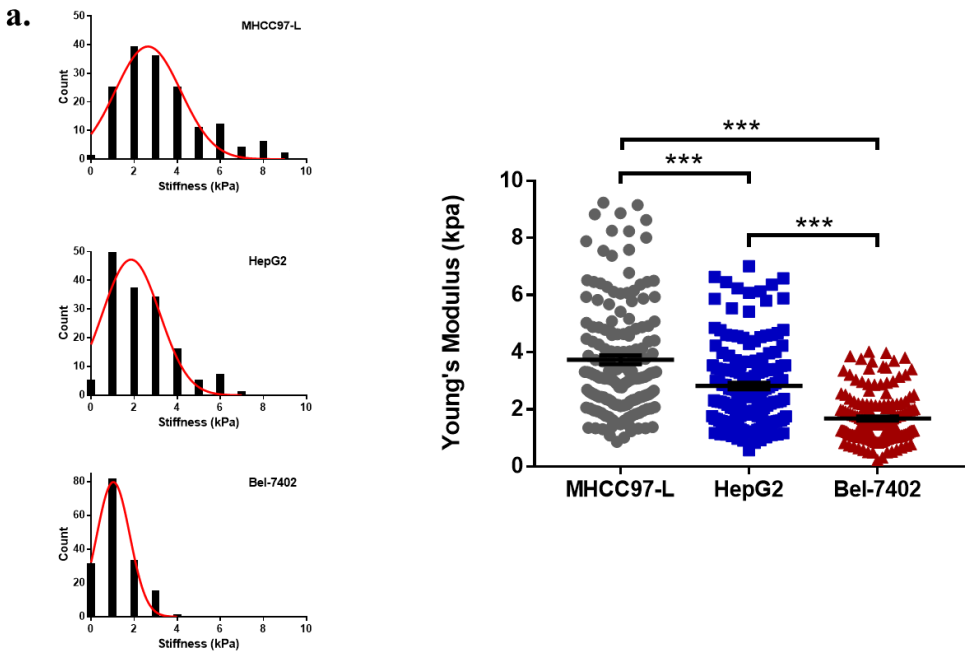

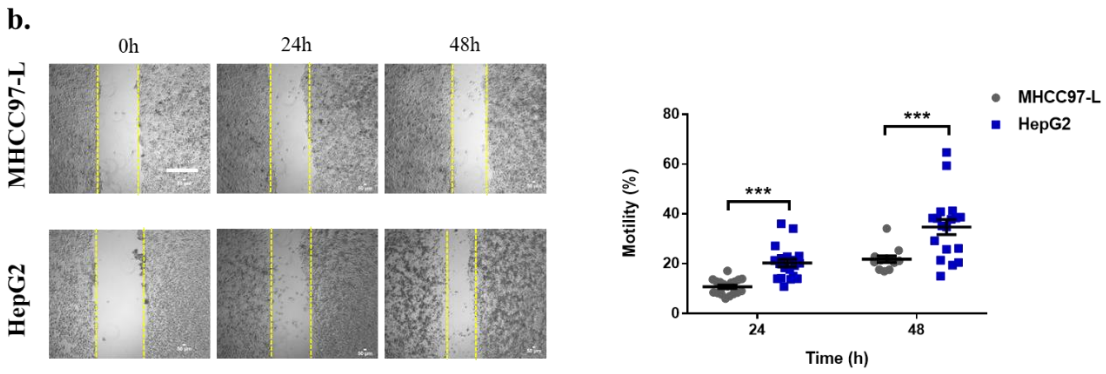

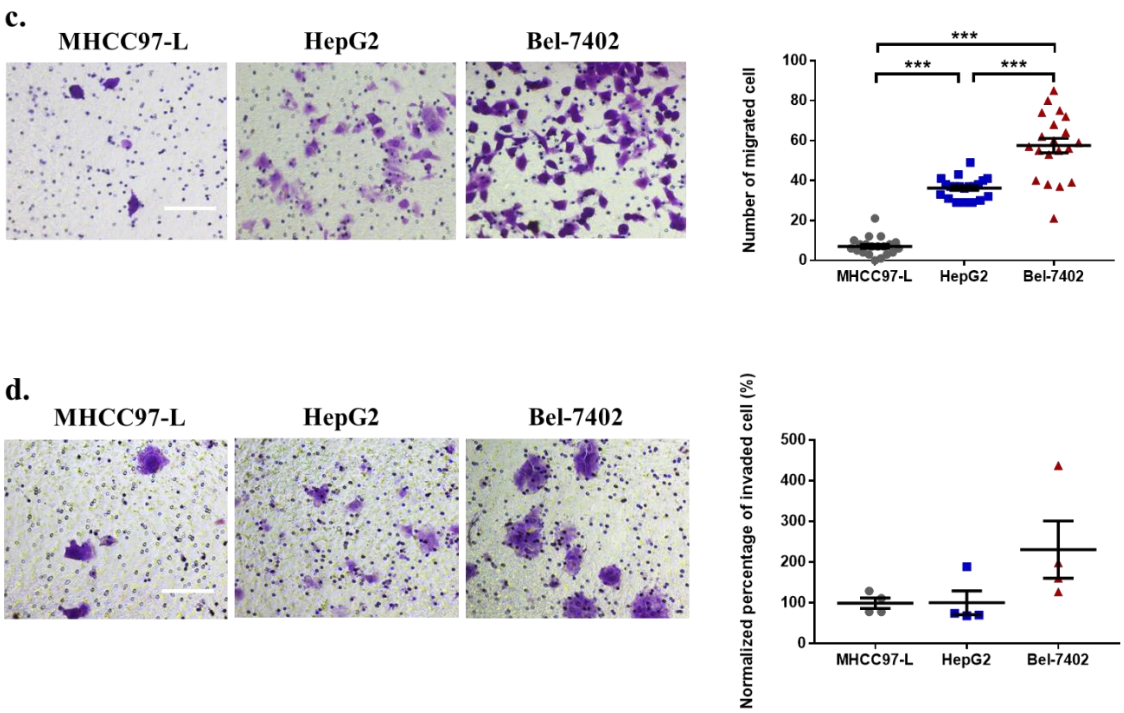

Figure 3.1 Establishment of the correlation between cellular stiffness and metastatic ability in HCC cell lines. (a) The cellular stiffness was measured by atomic force microscopy (AFM). The histograms of Young's modulus with Gaussian fittings were obtained from three HCC cell lines: MHCC97-L, HepG2 and Bel-7402. Above 150 force curves from more than 30 cells of each cell line were used for the statistics of Young's modulus. (b) Wound healing assay result between MHCC97-L and HepG2. The photos of three time points for two cell lines were shown on the left and the statistical result of the percentage of wound closure was shown on the right. (c) Transwell migration assay. Transwell migration assay was conducted on MHCC97-L, HepG2 and Bel-7402 with 3×10^5 cells/well for 24h. (d) Transwell invasion assay. Transwell invasion assay was conducted on MHCC97-L, HepG2 and Bel-7402 with 3×10^5 cells/well for 48h. The dyed cells were washed by glacial acetic acid and then the absorption values of the solution were record by microplate reader at 592nm and normalized for calculation, p=0.11. (* p<0.05, ** p<0.01, *** p<0.001)

3.2 Optimization of pharmacological treatment conditions

In order to modulate the mechanical stiffness of cells, two pharmacological inhibitors were used, including Blebbistatin and Y-27632. Blebbistatin is an inhibitor of myosin II and Y-27632 is an inhibitor of Rho-associated, coiled-coil containing protein kinase (ROCK). To optimize

the treatment conditions of Blebbistatin and Y-27632, wound healing assay was performed on HepG2 cells to determine the optimal time for pre-treatment. HCC cells were pre-treated with 10μM Blebbistatin and Y-27632 for 8, 12, 16 h and 6, 12, and 18 h, respectively. The wound healing process was analyzed and compared **(Figure 3.2a)**. The results showed that only when HepG2 cells were pre-treated by 10μM Blebbistatin for 12 hours, the migration capacity was obviously increased. The concentration of 10μM and the time of 12 hours were determined as the optimized pretreatment condition for Blebbistatin. For Y-27632, although the migration ability was enhanced when HepG2 cells were pre-treated for both 6 and 12 h **(Figure 3.2b)**, 12-h pre-treatment had a more significant effect ($p<0.01$). The concentration of 10μM and the time of 12 h were determined as the optimized pretreatment condition for Y-27632.

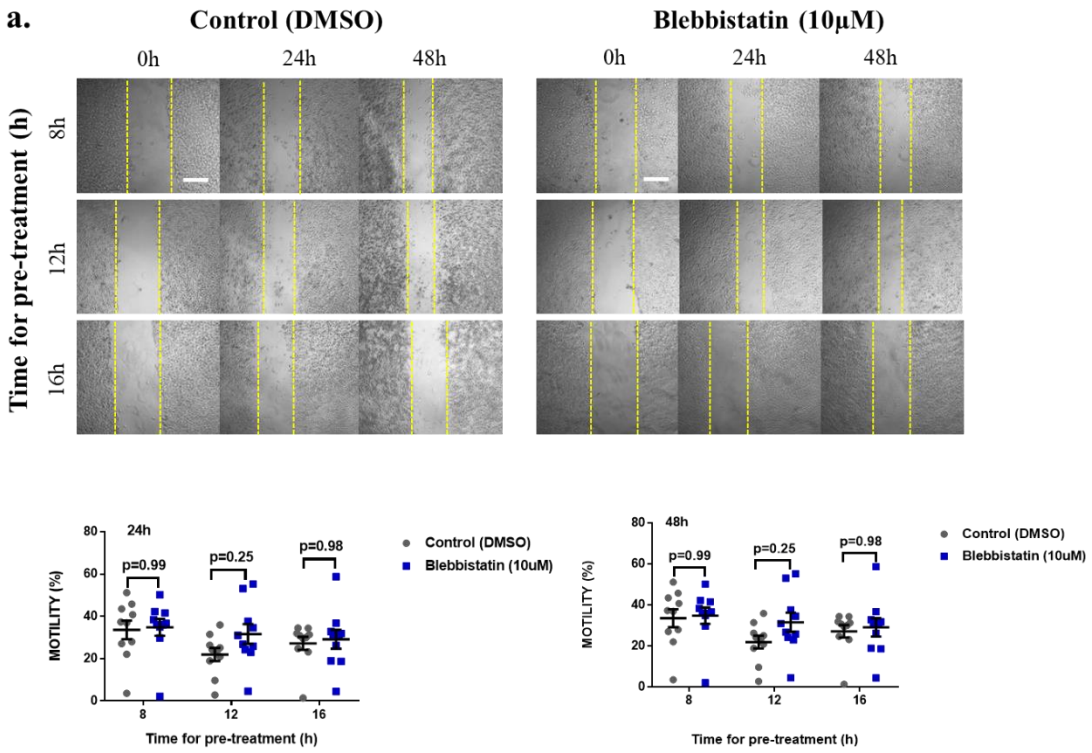

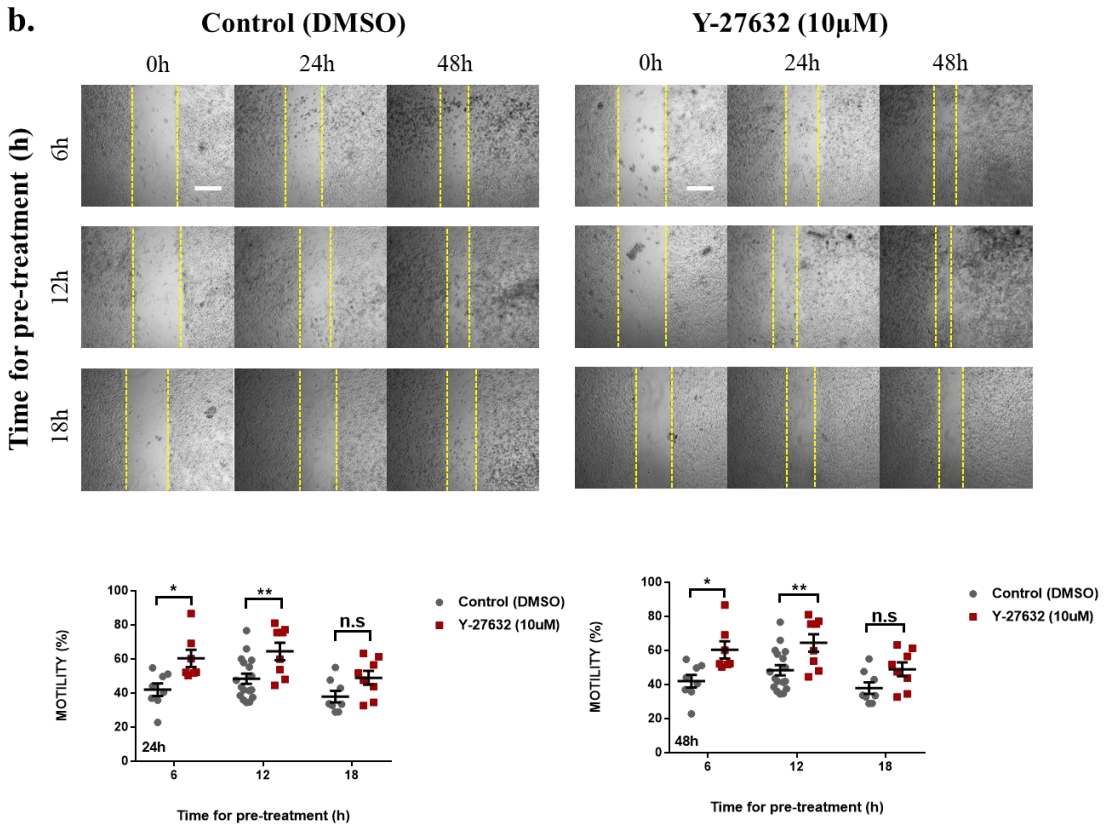

Figure 3.2 Optimization of pharmacological treatment conditions. (a) Wound healing assay for determination of the most optimized pre-treatment condition of Blebbistatin. HepG2 cells were pre-treated by Blebbistatin at 10μM while DMSO at the same concentration for control froup for 8 hours, 12 hours and 16 hours and then wound healing assay was performed. Photos of the scratch were taken at 0h, 24h and 48h. The statistical result was shown under the representative photos. (b) Wound healing assay for determination of the most optimized pre-treatment condition of Y-27632. HepG2 cells were pre-treated by Y-27632 at 10μM while DMSO at the same concentration for control group for 8 hours, 12 hours and 16 hours and then wound healing assay was performed. Photos of the scratch were taken at 0h, 24h and 48h. The statistical result was shown under the representative photos. (* $p<0.05$, ** $p<0.01$, *** $p<0.001$)

3.3 Pharmacologically inhibiting actomyosin decreases cellular stiffness but promotes metastatic ability

The regulatory role of cellular stiffness in metastatic ability was investigated by examining the effect of cellular stiffness on the migration and invasion of HCC cells. After HepG2 cells

were pre-treated by Blebbistatin and Y-27632 under optimized conditions, the amount of F-actin filament was measured by immunofluorescence staining and quantified by ImageJ software **(Figure 3.3a)**. The amount of F-actin was obviously decreased after treatment, which indicates that cellular stiffness was reduced. After HCC cells were softened by Blebbistatin or Y-27632, wound healing was performed to explore the migratory capacity. The results showed that there was an increasing trend of migration at 24 h and the increase was significant ($P<0.001$) at 48 h **(Figure 3.3b)**. In addition, when applying Y-27632 to soften the cells, there was an obvious increase ($P<0.05$) of migration at 24 h **(Figure 3.3b)**. Except for 2D migration, we also investigated the effect of cell softening on tumor cell migration/invasion. The results of transwell migration and invasion assay showed that both migration and invasion ability were promoted significantly after HepG2 cells were softened by Blebbistatin (10μM, 12h) **(Figure 3.3c**, $p<0.001$**)**. Similar results were also observed in HepG2 cells softened by Y-27632 (10μM, 12h) **(Fig. 3.3c)**. These results demonstrate that decreasing cellular stiffness promotes metastatic ability in HepG2 cells.

In order to confirm the findings, the influence of cell softening on MHCC97-L and Huh-7 cells was also examined. After Blebbistatin and Y-27632 treatment, both MHCC97-L and Huh-7 cells showed decrease in the amount of F-actin filament, which indicates the reduction in cellular stiffness **(Figure 3.3d, Figure 3.3f)**. The migration ability was enhanced ($P<0.05$) at 24 h when MHCC97-L cells were softened by Blebbistatin (10μM, 12h). Besides, when Y-

27632 (10μM, 12h) was utilized to soften MHCC97-L and Huh-7 cells, migration was significantly facilitated at 24 h ($P<0.05$) and 48 h ($P<0.01$). To further confirm that decreasing cellular stiffness promotes metastasis, we performed 3D tumor spheroid invasion assay on Huh-7 cells. The invasion rate showed an increase trend after the Blebbistatin treatment and was enhanced significantly ($P<0.01$) after cell softening by Y-27632 **(Figure3.3h)**. These results demonstrate that softening cells by pharmacological treatment promotes metastatic potential of HCC cells.

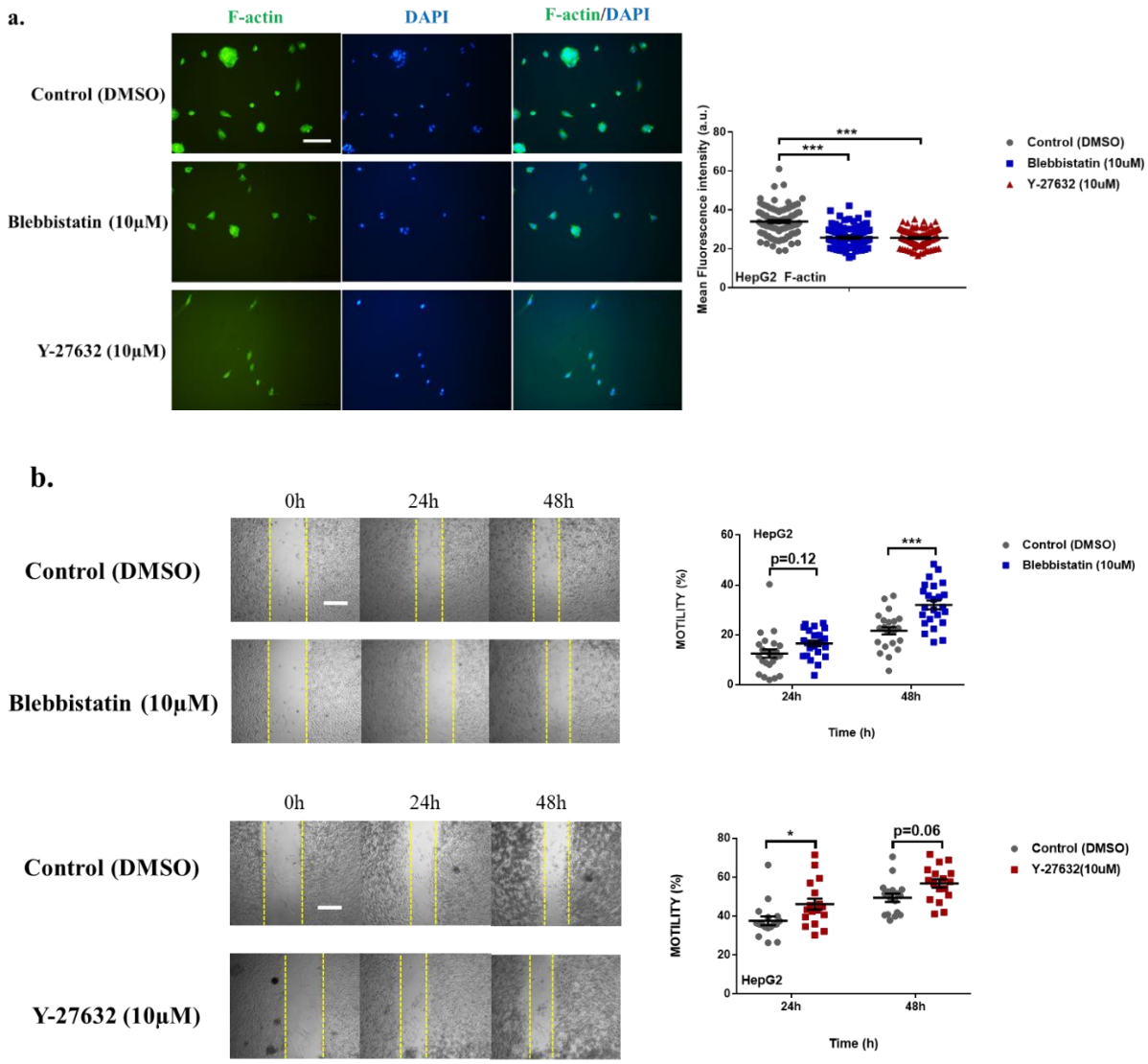

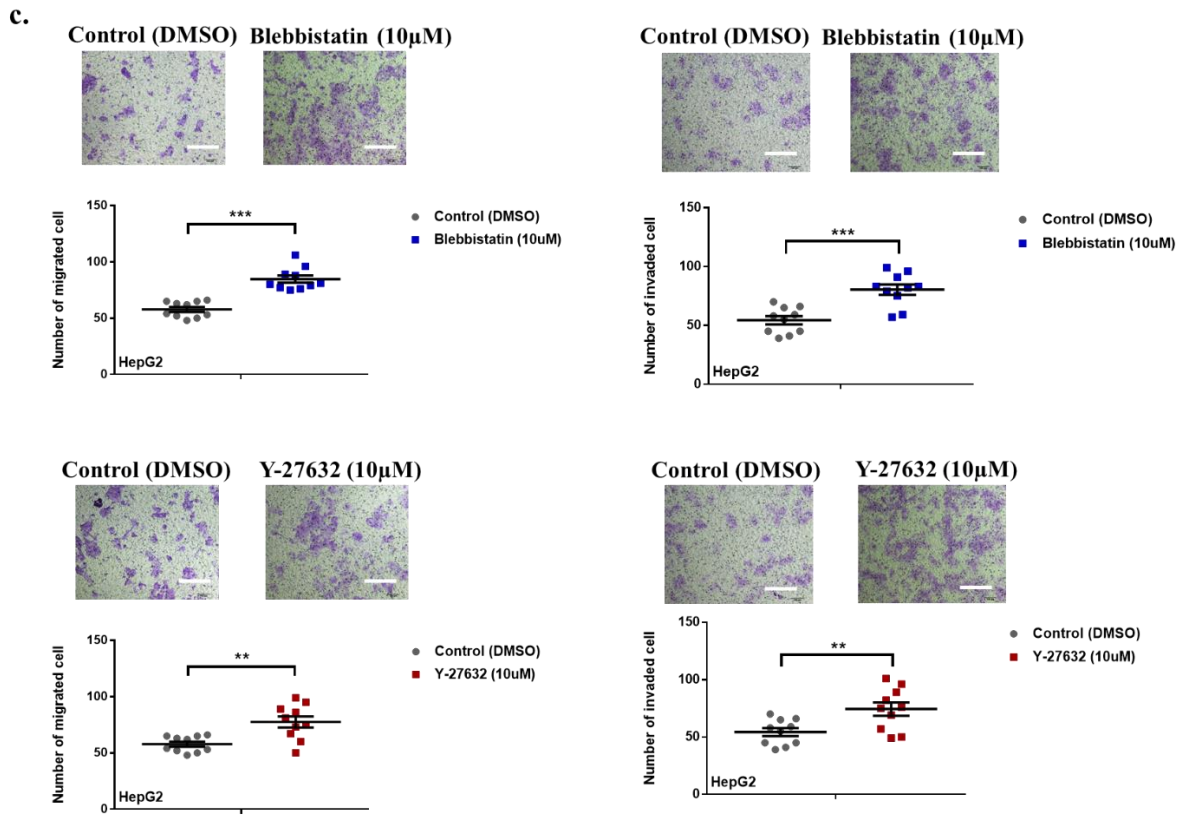
c.
Control (DMSO)
Blebbistatin (10μM)
Number of migrated cell
HepG2
***
Control (DMSO)
Blebbistatin (10uM)
Number of invaded cell
HepG2
***
Control (DMSO)
Blebbistatin (10uM)
Control (DMSO)
Y-27632 (10μM)
Number of migrated cell
HepG2
**
Control (DMSO)
Y-27632 (10uM)
Control (DMSO)
Y-27632 (10μM)
Number of invaded cell
HepG2
**
Control (DMSO)
Y-27632 (10uM)

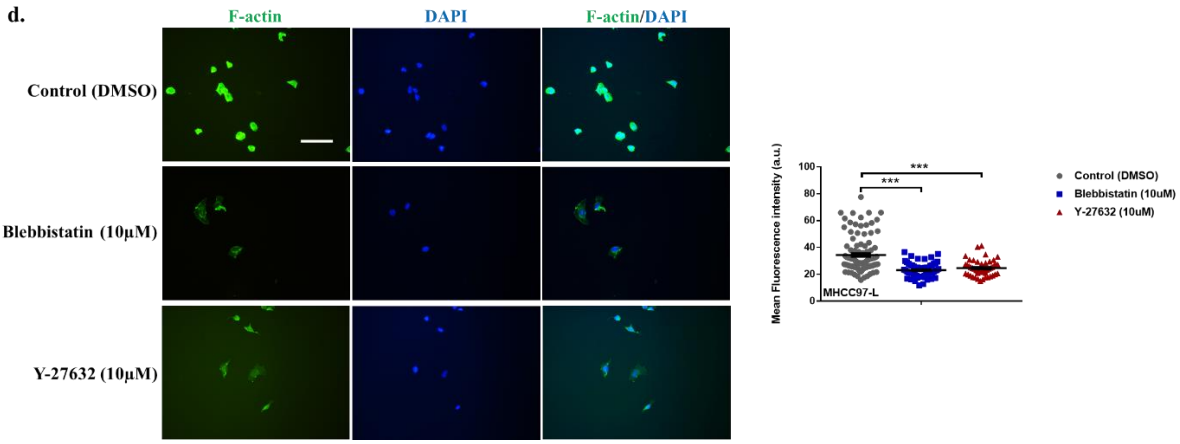
d.
F-actin
DAPI
F-actin/DAPI
Control (DMSO)
Blebbistatin (10μM)
Y-27632 (10μM)
Mean Fluorescence intensity (a.u.)
MHCC97-L
***
***
Control (DMSO)
Blebbistatin (10uM)
Y-27632 (10uM)

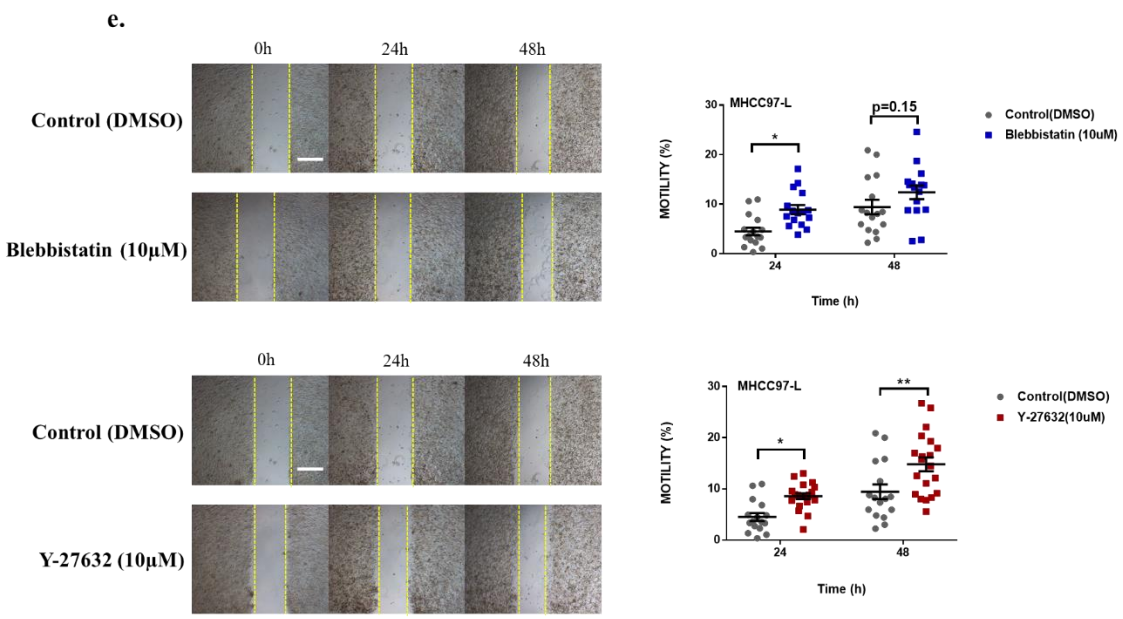
e.
0h
24h
48h
Control (DMSO)
Blebbistatin (10μM)
MHCC97-L
p=0.15
MOTILITY (%)
Time (h)
Control(DMSO)
Blebbistatin (10uM)
Y-27632 (10μM)
Y-27632(10uM)

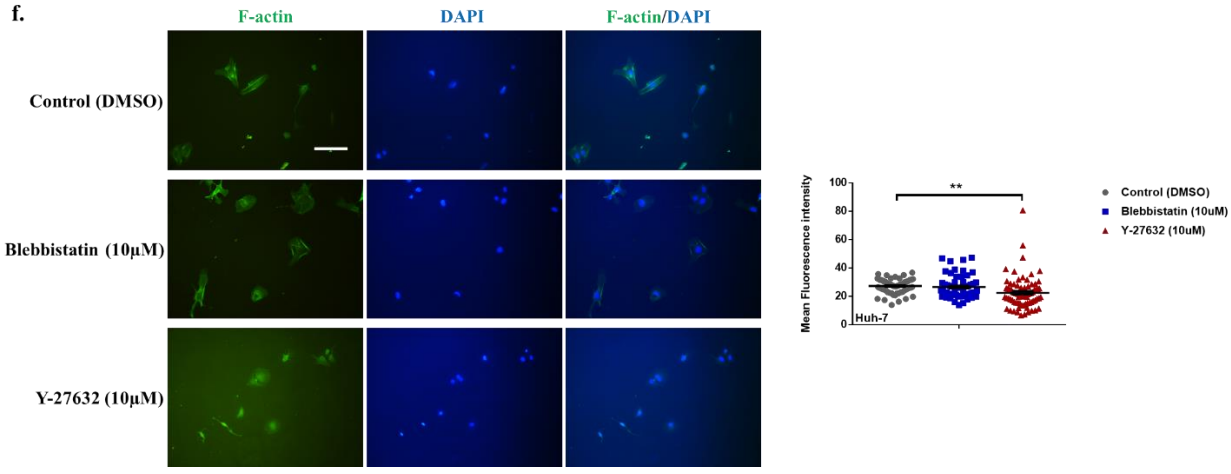
f.
F-actin
DAPI
F-actin/DAPI
Control (DMSO)
Blebbistatin (10μM)
Y-27632 (10μM)
Mean Fluorescence intensity
Huh-7
Control (DMSO)
Blebbistatin (10uM)
Y-27632 (10uM)

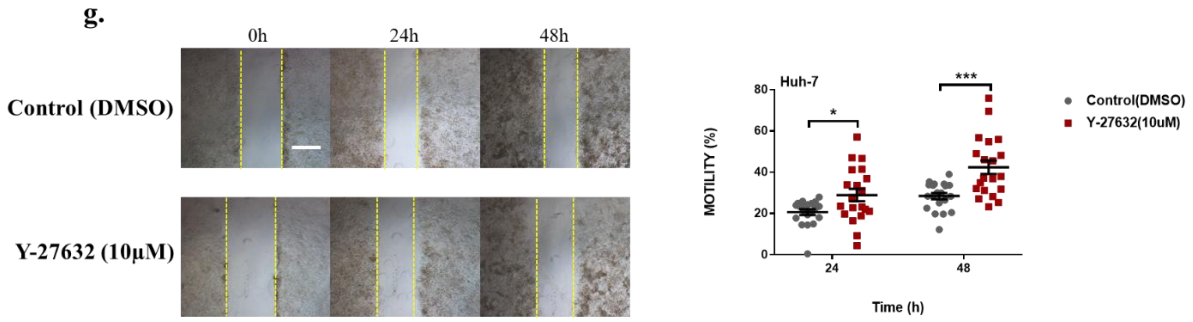
g.
0h
24h
48h
Control (DMSO)
Y-27632 (10μM)
Huh-7
MOTILITY (%)
Time (h)
Control(DMSO)
Y-27632(10uM)

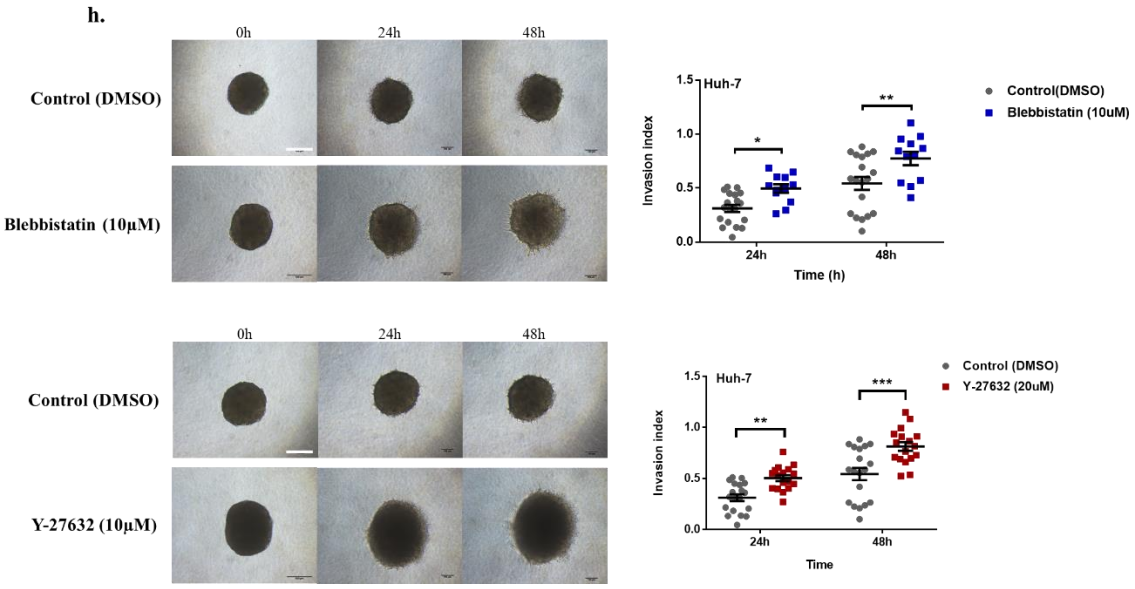

Figure 3.3 Decrease of cellular stiffness by pharmacological treatment promotes metastatic ability. (a) Representative immunofluorescence images of F-actin and the statistical results. HepG2 cells was pre-treated by DMSO for control, Blebbistatin at 10μM and Y-27632 at 10μM for 12h. Photos were taken by fluorescence microscope with 20×objective lens. The mean fluorescence intensity was calculated by ImageJ software. (b) Wound healing assay for comparison of migratory ability at 2D level. HepG2 cells were pre-treated by Blebbistatin, Y-27632 at 10uM while DMSO at the same concentration for control group for 12h and then wound healing assay was performed. Photos of the scratch were taken at 0h, 24h and 48h. The statistical result was shown under the representative photos. (c) Transwell migration and transwell invasion assay for HepG2 cells pre-treated by Blebbistatin and Y-27632. Transwell migration and transwell invasion assay were performed after cells pre-treated by Blebbistatin and Y-27632 for 12h, 3×10^5 cells were seeded in each well for 24h and 48h, the number of migrated cells were calculated. (d) Representative immunofluorescence images of F-actin and the statistical results of MHCC97-L cells pre-treated by Blebbistatin and Y-27632. (e) Wound healing assay after pre-treated by Blebbistatin and Y-27632 was repeated in MHCC97-L cell line. (f) Representative immunofluorescence images of F-actin and the statistical results of Huh-7 cells pre-treated by Blebbistatin and Y-27632. (g) Wound healing assay after pre-treated by Y-27632 was repeated in Huh-7 cell line. (h) 3D Collagen invasion assay for tumor spheroids formed by Huh-7 cell. Tumor spheroids were formed by inverted suspension methods. The tumor spheroids were seeded in 3D collagen gels and treated by Blebbistatin and Y-27632 at 10μM. The invasion process was observed and record at 0h, 24h and 48h. The fibroblast-like invasive pseudopodia was calculated by ImageJ software and normalized for statistics. p=0.2 for 24h and p=0.3 for 48h. (* $p<0.05$, ** $p<0.01$, *** $p<0.001$)

3.4 Inhibiting actomyosin by siRNAs decreases cellular stiffness and promotes metastatic ability

Except for pharmacological treatment, we also utilized siRNAs to knock down the expressions of cytoskeleton regulatory genes MLCK and mDia1. The knockdown efficiency of siRNA was measured by qPCR at mRNA level and by western blot at protein level **(Figure 3.4b)**. It was obvious that the expression of MLCK was decreased to approximately 20% while the expression of mDia1 was almost totally inhibited. The phosphorylation of myosin light chain was significantly decreased. Cellular stiffness was measured after HepG2 cells were transfected by siRNAs with concentration of 100nM for 48 h **(Figure 3.4a, right)**. Compared to control cells, the expressions of MLCK and mDia1 were inhibited by siRNAs and cellular stiffness was also remarkably decreased ($P<0.001$). The distribution of cell stiffness showed that silencing MLCK or mDia1 significantly shifted the peak point of stiffness to the value lower than 2 kPa **(Figure 3.4a, left)**. Further, the effect on metastatic ability was compared. Wound healing assay was performed on HepG2 cells that were transfected by siRNA of MLCK and mDia1. Inhibiting MLCK or mDia1 remarkably promoted cell migration in 2D condition. This effect was further verified by transwell migration and invasion assay. Similarly, knocking down MLCK or mDia1 elevated the ability of migration and invasion by nearly 50% **(Figure 3.4c, Figure 3.4d)**. We also tested whether cell softening promoted metastatic ability in another HCC cell line MHCC97-L. Consistently, when MHCC97-L cells were softened by knocking

down MLCK and mDia1, their migration and invasion abilities were significantly enhanced (Fig. 3.4e, f).

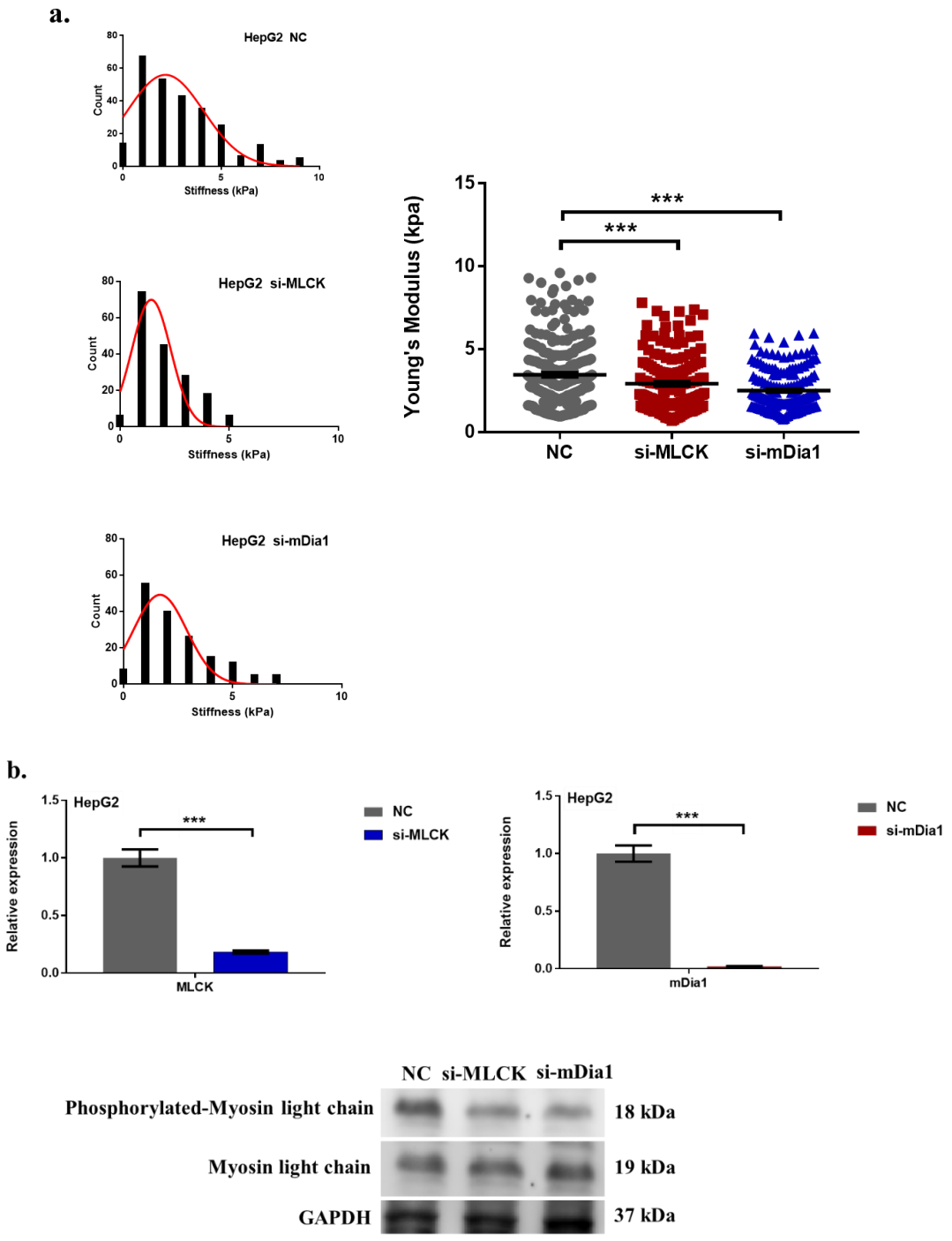

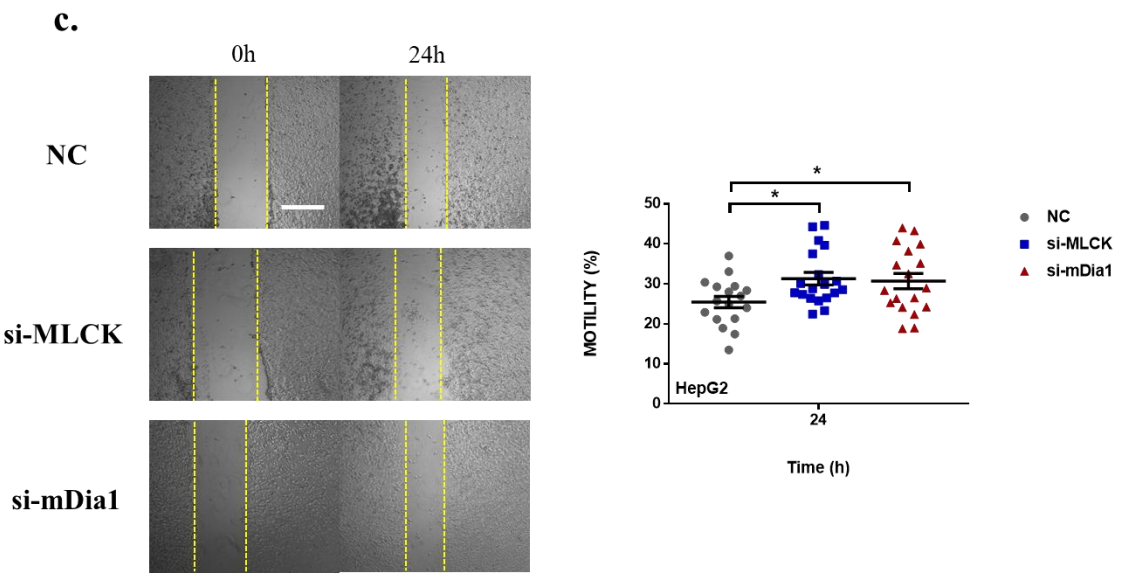
c.
0h
24h
NC
si-MLCK
si-mDia1
MOTILITY (%)
HepG2
24
Time (h)
NC
si-MLCK
si-mDia1

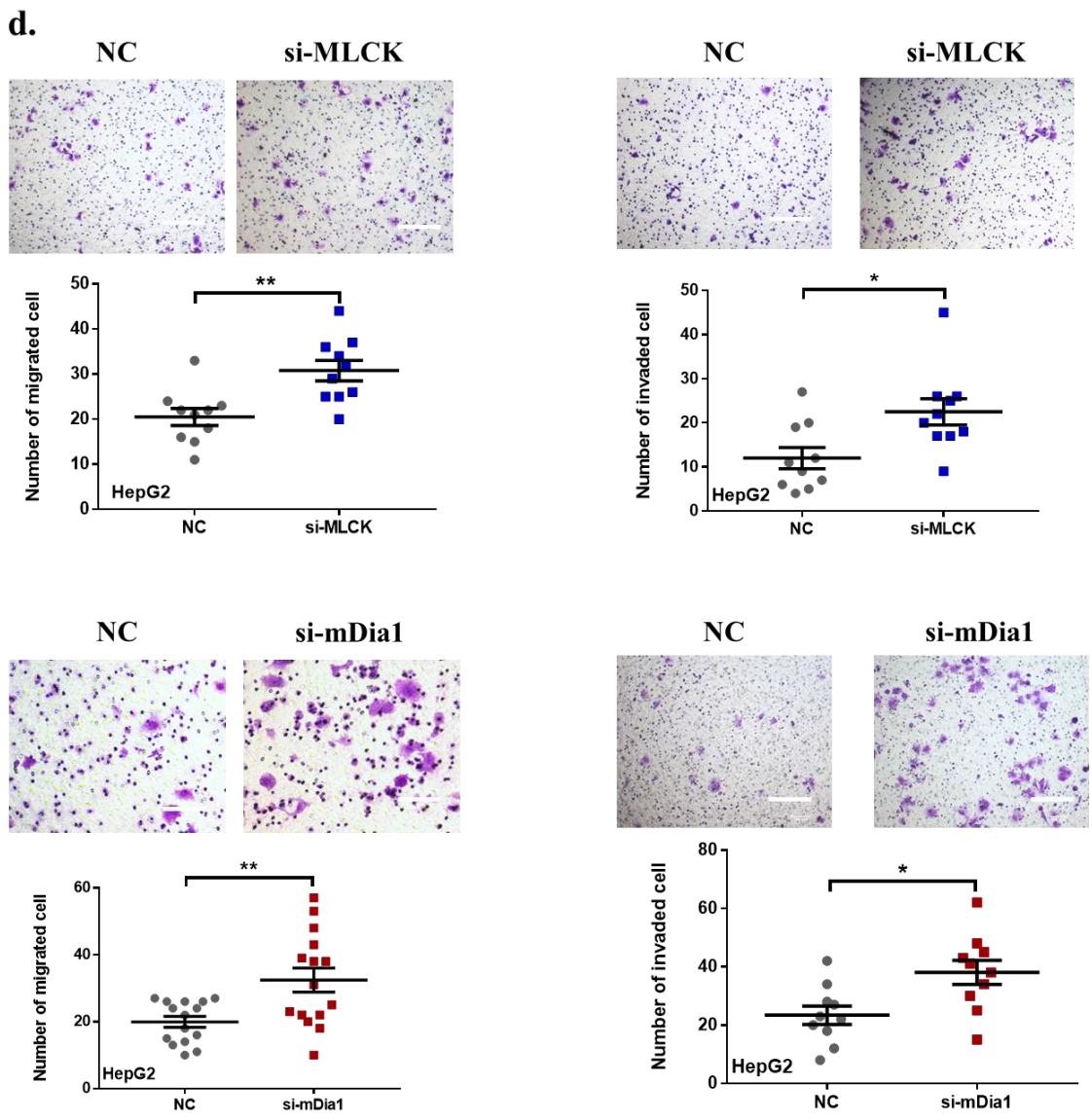
d.
NC
si-MLCK
Number of migrated cell
HepG2
NC
si-MLCK
Number of invaded cell
HepG2
NC
si-mDia1
Number of migrated cell
HepG2
NC
si-mDia1
Number of invaded cell
HepG2

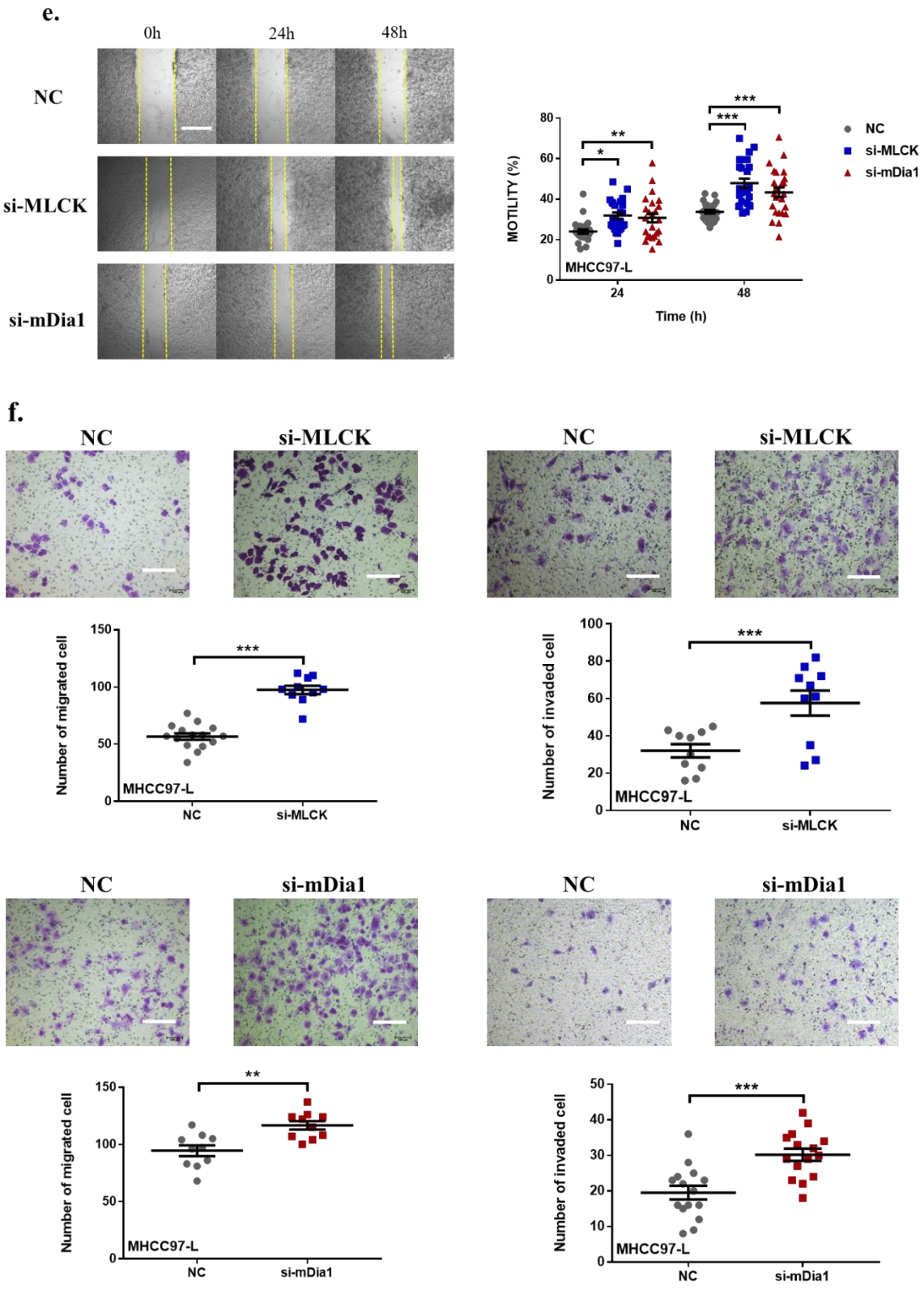

Figure 3.4 Decrease of cellular stiffness by siRNAs facilitates metastatic ability of HCC cells. (a) The cellular stiffness was measured by AFM. The histograms of Young's modulus with Gaussian fittings were obtained from HepG2 cells transfected by siRNAs knocking down

MLCK and mDia1 at the concentration of 100nM. Above 150 force curves from more than 30 cells of each group were used for the statistics of Young's modulus. (b) Quantitative Real-time Polymerase Chain Reaction (qPCR) results after HepG2 cells were transfected by siRNAs of MLCK and mDia1. Western blotting assay to prove the changes at protein level of myosin light chain and phosphorylated myosin light chain after knocking down MLCK and mDia1. (c) Wound healing assay. HepG2 cells were transfected by siRNAs downregulating MLCK and mDia1 for 48h and then wound healing assay was performed. Photos of the scratch were taken at 0h and 24h. The statistical result was shown on the right. (d) Transwell migration and transwell invasion assay for HepG2 cells that was downregulated of MLCK and mDia1. Transwell migration and transwell invasion assay were performed after cells transfected by siRNAs of MLCK and mDia1 for 48h, 3×10^5 cells were seeded in each well for 24h and 48h, the number of migrated or invaded cells were calculated. (e-f) Wound healing, transwell migration and transwell invasion assay after knocking down MLCK and mDia1 by siRNAs were repeated in MHCC97-L cells. (* $p<0.05$, ** $p<0.01$, *** $p<0.001$)

3.5 Cancer stem cells exhibit reduced cellular stiffness and enhanced metastatic ability

Compared to conventional cancer cells, cancer stem cells (CSCs) pose a serious challenge to cancer therapy due to the high malignancy, drug resistance, and high metastatic potential. We further established the correlation between mechanical stiffness of CSCs and their metastatic ability. HepG2-derived CSCs were obtained by 3D soft fibrin culture. Cellular stiffness of CSCs and non-CSCs was analyzed and calculated **(Figure 3.5a, right)**. It was found that cellular stiffness of non-CSCs was around 3kPa, while CSCs had a lower mechanical stiffness (2kPa). The histogram of CSCs and non-CSCs is very different **(Figure 3.5a, left)**. The distribution of non-CSC stiffness was broad and the peak value was close to 2kPa. However, the distribution of CSC stiffness was much narrower and the peak point was 1kPa. The results

indicated that CSCs are softer than non-CSCs.

The metastatic ability was compared between CSCs and non-CSCs through transwell migration and invasion assays **(Figure 3.5b)**. The number of migrated cells was analyzed and compared. The migratory ability was enhanced by 50% in CSCs compared to non-CSCs. A similar phenomenon was also observed in transwell invasion assay and CSCs had significantly higher invasion potential than non-CSCs. The results above indicated that CSCs had higher metastatic potential while lower mechanical stiffness than non-CSCs. (I prefer to demonstrate CSC part alone, because (1) CSC is different from general HCC cells, it might not be suitable to mix them together; (2) CSC is more malignant than HCC cells, so I want to emphasize the significance of studying CSC by make it as an individual case.)

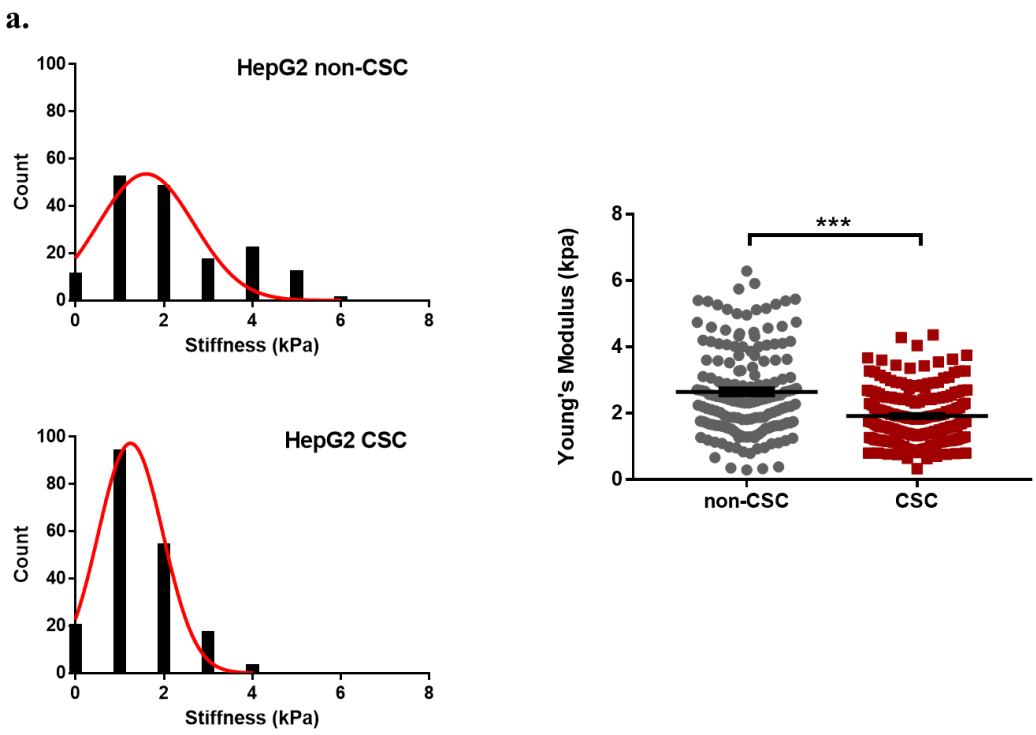

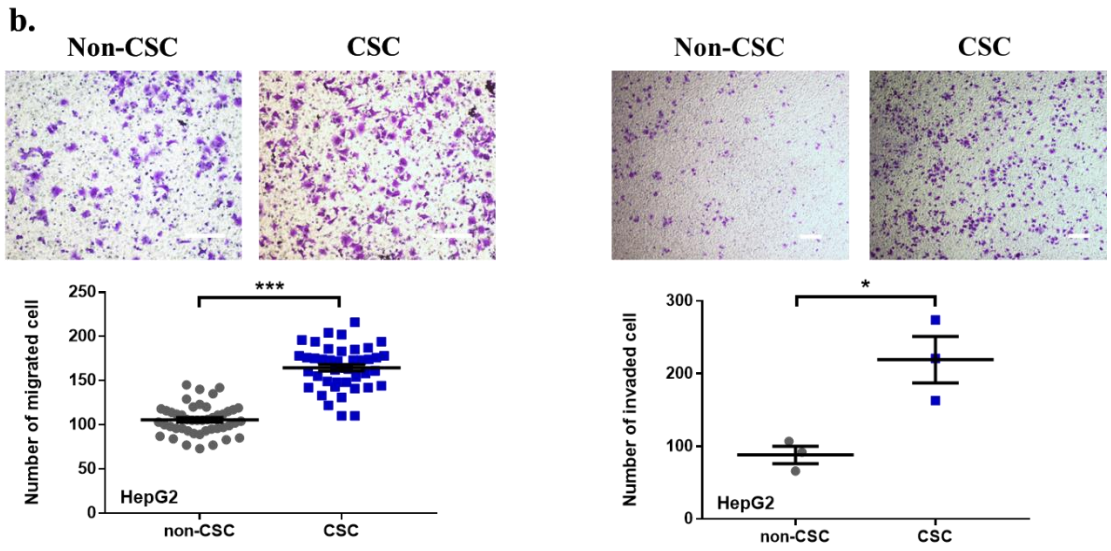

Figure 3.5 Cellular stiffness and metastasis has an inverted correlation in cancer stem cells. (a) The cellular stiffness was measured by AFM. The histograms of Young's modulus with Gaussian fittings were obtained from non-CSCs and CSCs derived from HepG2 cells. Above 150 force curves approximately 30 cells of non-CSC and CSC respectively were used for the statistics of Young's modulus. (b) Transwell migration and transwell invasion assay. Transwell migration and invasion assay was conducted on non-CSCs and CSCs with 3×10^5 cells/well for 24h and 48h. For transwell migration assay, the number of migrated cells were counted and calculated. For transwell invasion assay, the dyed cells were washed by glacial acetic acid and then the absorption values of the solution were record by microplate reader at 592nm and normalized for calculation. (* $p<0.05$, ** $p<0.01$, *** $p<0.001$)

Chapter 4 Increasing cellular stiffness inhibits HCC metastasis

In Chapter 3, we established the inverse correlation between cellular stiffness and metastatic ability in HCC cells and found that softening cells enhanced metastatic potential of tumor cells. Based on what has been done in Chapter 3, we further explored whether stiffening HCC cells could inhibit tumor cell metastasis. In this chapter, several activators of cytoskeleton protein or cytoskeleton regulators were applied to stiffen HCC cells, including Jasplakinolide and Narciclasine. Except pharmacological treatments, constitutive active (CA) MLCK and ROCK plasmids were used to over-express cytoskeleton-related genes in order to increase cellular stiffness. The effect of cellular stiffening on metastatic ability in HCC cells was investigated in vitro.

4.1 Pharmacologically activating actomyosin increases cellular stiffness but inhibits metastatic ability in HCC cells

The regulatory role of cellular stiffness in metastatic ability was further investigated by examining the effect of cellular stiffening on metastatic potential of HCC cells. In order to stiffen HCC cells, two activators were utilized, Jasplakinolide and Narciclasine. Jasplakinolide is an activator that is commonly used to promote polymerization and stabilization of F-actin filaments. Narciclasine is an activator of Ras homolog family member A (RhoA). After HepG2 cells were pre-treated by Jasplakinolide (50nM,12h) and Narciclasine (5nM, 12h), the amount

of F-actin filament was measured by immunofluorescence staining and quantified by ImageJ software **(Figure 4.1a)**. The results showed that the amount of F-actin filament was obviously increased after the treatment by Jasplakinolide and Narciclasine, which indicated the elevation of cellular stiffness. HepG2 cells were treated with three different concentrations of Jasplakinolide (10, 20, and 50 nM) and their migratory capacity was measured by wound healing assay. There was a decreasing trend of migration at 24 and 48 h at different concentrations, and the decrease was significant ($p<0.05$) at 48 h under the concentration of 50 nM **(Figure 4.1b)**. Transwell migration and invasion assay were also adopted to examine metastatic ability of these treated tumor cells. After HepG2 cells were stiffened by Jasplakinolide (0.1μM, 12h), both migration and invasion ability were inhibited significantly **(Figure 4.1c**, $P<0.01$, $P<0.001$**)**. Similarly, when HepG2 cells were stiffened by Narciclasine (5nM, 12h), cellular stiffness was increased while migration and invasion were decreased **(Figure 4.1c**, $P<0.01$**)**. All these results demonstrate that increasing cellular stiffness impairs metastatic potential in HepG2 cells.

In order to confirm the findings, we also tested the influence of cell stiffening on MHCC97-L cells. After Jasplakinolide and Narciclasine treatment, MHCC97-L cells exhibited an increase in the amount of F-actin filament, which indicated cellular stiffening **(Figure 4.1d)**. Wound healing assay was performed to test the ability of migration. Three concentrations of Jasplakinolide (10, 20, and 50 nM) decreased the migration of MHCC97-L cells at 24 and 48

h. Only when MHCC97-L cells were stiffened by Jasplakinolide (10nM, 12h), there exhibited a significant inhibitory effect ($P<0.05$) at 48h. Transwell migration and invasion assay were also applied to examine metastatic ability. After MHCC97-L cells were stiffened by Jasplakinolide (0.1μM, 12h), both migration and invasion ability were inhibited significantly **(Figure 4.1f**, $P<0.001$**)**. Similar results were observed in MHCC97-L cells stiffened by Narciclasine (20nM, 12h), which showed that the cellular stiffness was increased while the number of migrated cells was decreased. The results above indicated that increasing cellular stiffness could reduce metastasis in MHCC97-L cells.

To further test the influence of cellular stiffening on tumor invasion, we performed 3D tumor spheroid invasion assay on Huh-7 cells. After stiffened by Jasplakinolide, the invasion rate showed a decrease trend at 24h and a significant decrease ($P<0.001$) at 48h **(Figure 4.1h)**. Further, tumor cell invasion was also inhibited significantly at 48h ($P<0.001$) after stiffened by Narciclasine **(Figure 4.1i)**. The results above indicated that stiffening cells by pharmacological treatment could inhibit metastasis in HCC cells.

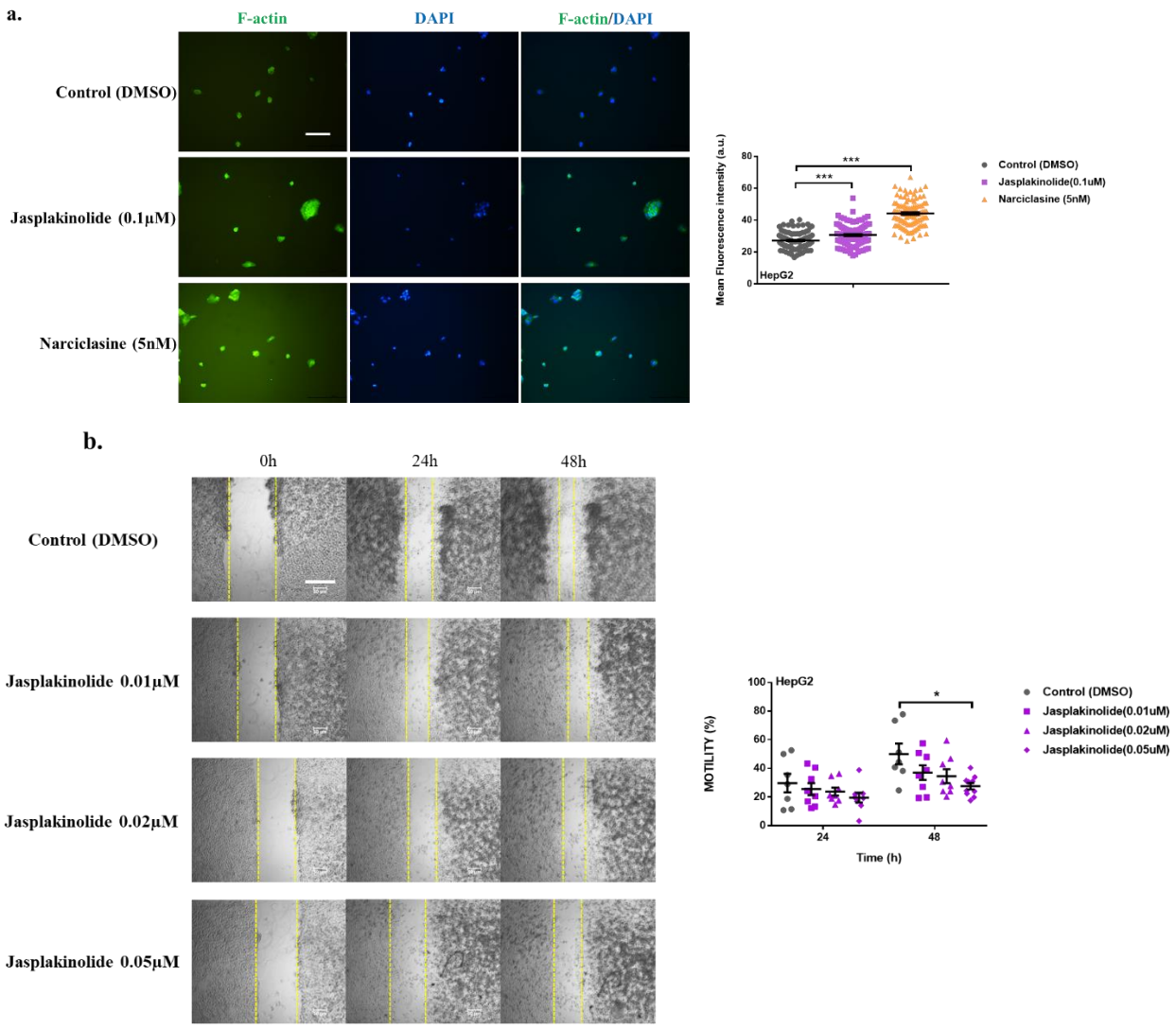
a.
F-actin
DAPI
F-actin/DAPI
Control (DMSO)
Jasplakinolide (0.1μM)
Narciclasine (5nM)
Mean Fluorescence intensity (a.u.)
HepG2
***
***
Control (DMSO)
Jasplakinolide(0.1uM)
Narciclasine (5nM)
b.
0h
24h
48h
Control (DMSO)
Jasplakinolide 0.01μM
Jasplakinolide 0.02μM
Jasplakinolide 0.05μM
MOTILITY (%)
HepG2
*
Time (h)
Control (DMSO)
Jasplakinolide(0.01uM)
Jasplakinolide(0.02uM)
Jasplakinolide(0.05uM)

c.

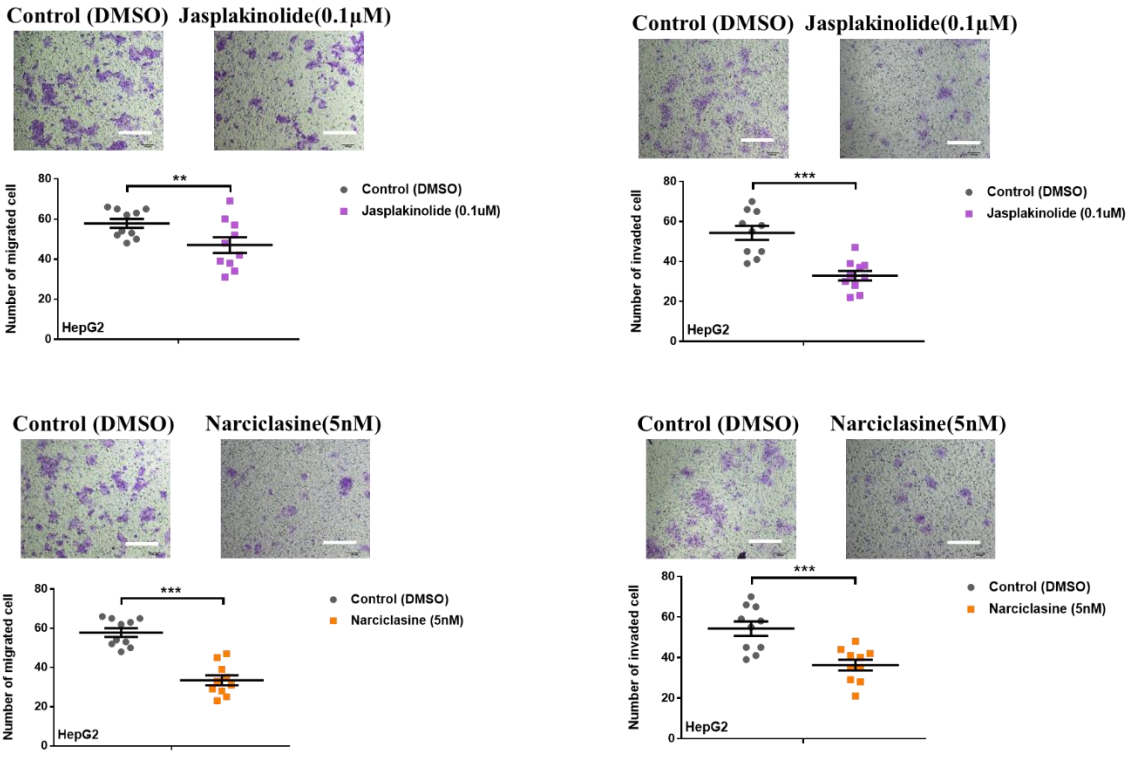
Control (DMSO)
Jasplakinolide(0.1μM)
Number of migrated cell
HepG2
**
Control (DMSO)
Jasplakinolide (0.1uM)
Number of invaded cell
***
Narciclasine(5nM)
Narciclasine (5nM)

d.

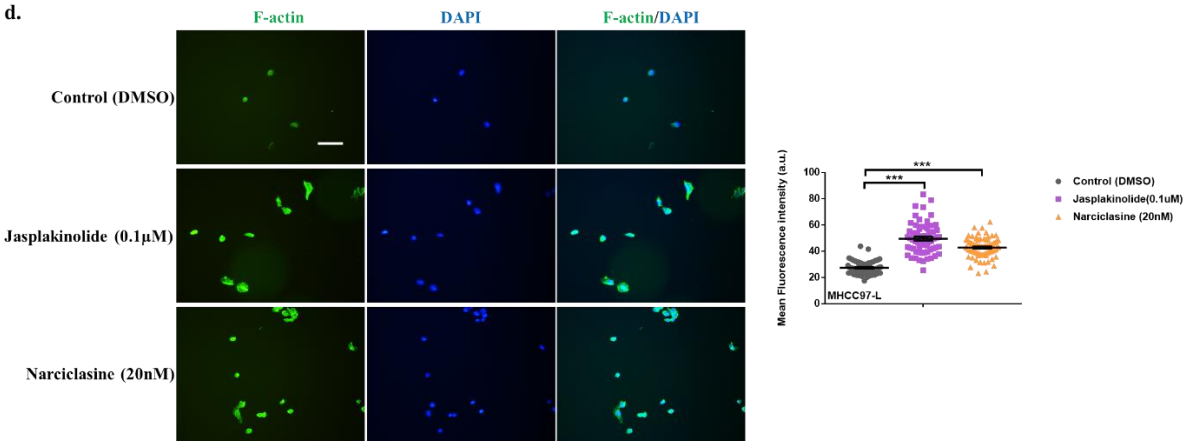
F-actin
DAPI
F-actin/DAPI
Control (DMSO)
Jasplakinolide (0.1μM)
Narciclasine (20nM)
Mean Fluorescence intensity (a.u.)
MHCC97-L
***
Jasplakinolide(0.1uM)

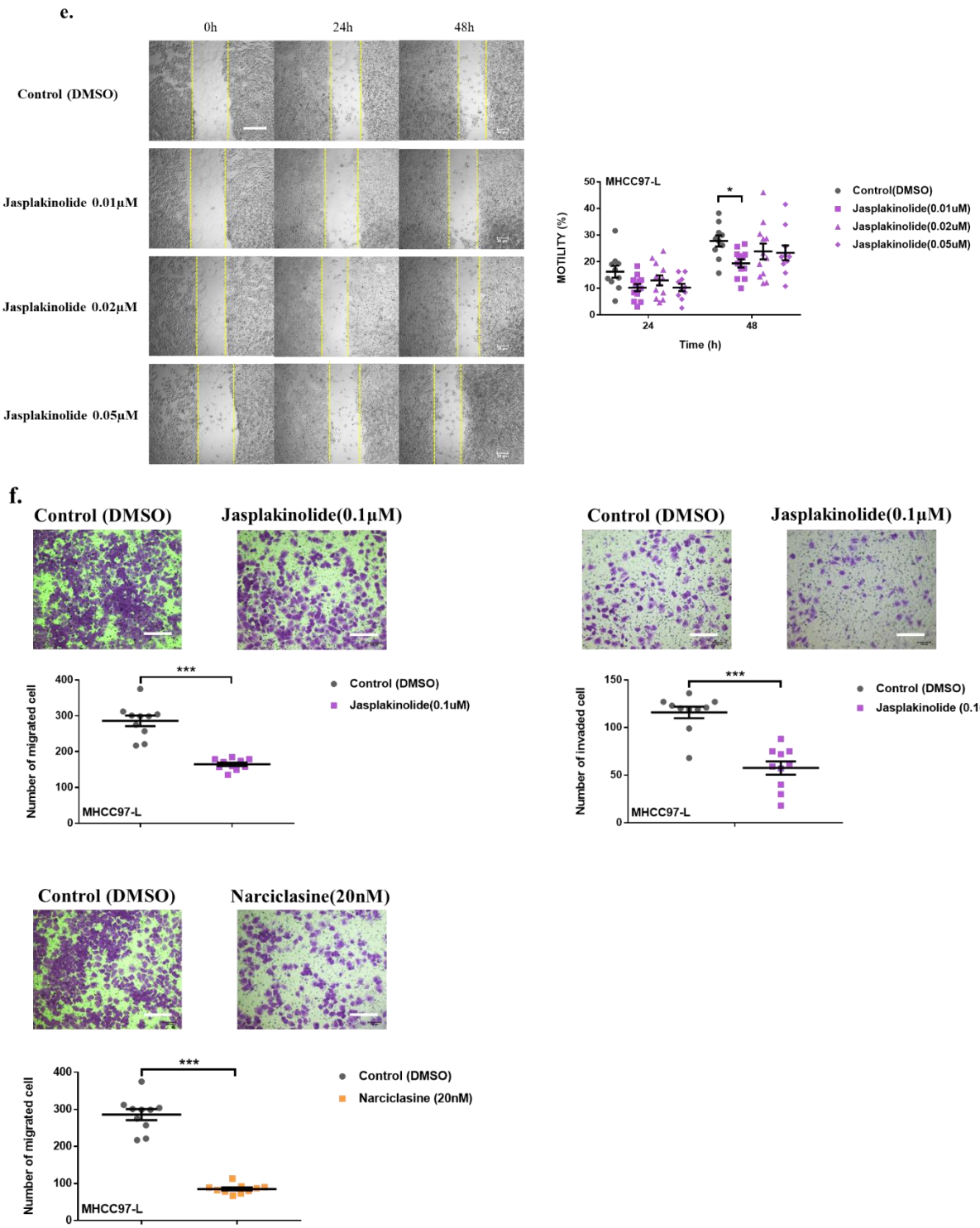
e.
0h
24h
48h
Control (DMSO)
Jasplakinolide 0.01μM
Jasplakinolide 0.02μM
Jasplakinolide 0.05μM
MHCC97-L
MOTILITY (%)
Time (h)
Control(DMSO)
Jasplakinolide(0.01uM)
Jasplakinolide(0.02uM)
Jasplakinolide(0.05uM)
f.
Control (DMSO)
Jasplakinolide(0.1μM)
Number of migrated cell
MHCC97-L
Control (DMSO)
Jasplakinolide(0.1uM)
Control (DMSO)
Jasplakinolide(0.1μM)
Number of invaded cell
MHCC97-L
Control (DMSO)
Jasplakinolide (0.1uM)
Control (DMSO)
Narciclasine(20nM)
Number of migrated cell
MHCC97-L
Control (DMSO)
Narciclasine (20nM)

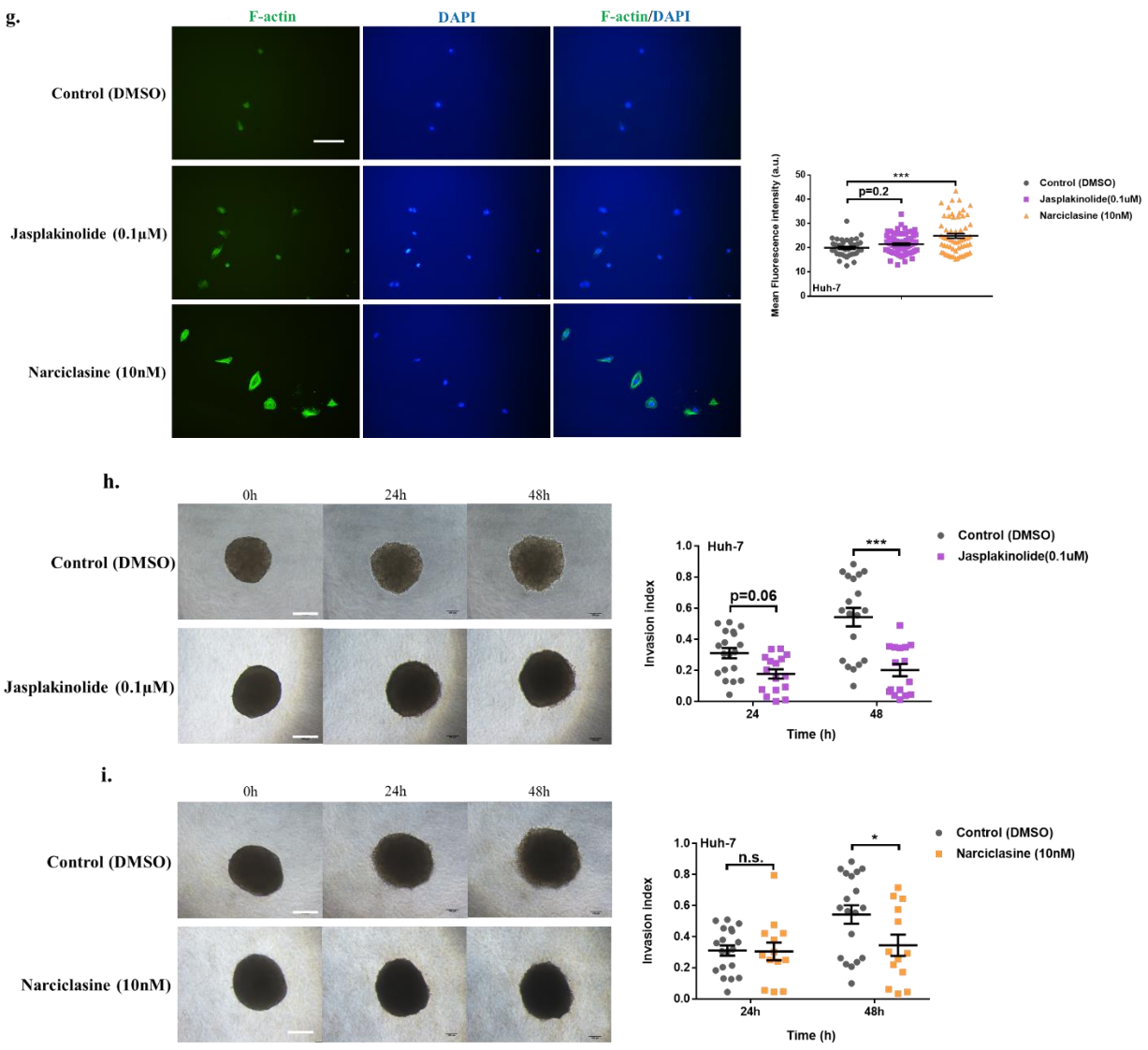

Figure 4.1 Increase of cellular stiffness by pharmacological treatment reduces metastatic ability. (a) Representative immunofluorescence images of F-actin staining and the statistical results. HepG2 cells was pre-treated by DMSO for control, Jasplakinolide at 0.1μM and Narciclasine at 5nM for 12h. Photos were taken by fluorescence microscope with 20×objective lens. The mean fluorescence intensity was calculated by ImageJ software. (b) Wound healing assay for comparison of migratory ability at 2D level. HepG2 cells were pre-treated by Jasplakinolide at 10nM, 20nM and 50nM while DMSO at the highest concentration for control group for 12h and then wound healing assay was performed. Images of the scratch were taken at 0h, 24h and 48h. The statistical result was shown under the representative photos. (c) Transwell migration and transwell invasion assay for HepG2 cells pre-treated by Jasplakinolide and Narciclasine. Transwell migration and transwell invasion assay were performed after cells pre-treated by Jasplakinolide (0.1μM) and Narciclasine (5nM) for 12h, 3×10^5 cells were seeded

in each well for 24h and 48h, the number of migrated or invaded cells were calculated. (d) Representative immunofluorescence images of F-actin and the statistical results of MHCC97-L cells pre-treated by Jasplakinolide and Narciclasine. (e) Wound healing assay after pre-treated by Jasplakinolide and Narciclasine was repeated in MHCC97-L cell line. (f) Transwell migration and transwell invasion assay for MHCC97-L cells pre-treated by Jasplakinolide and Narciclasine. Transwell migration and transwell invasion assay were performed after cells pre-treated by Jasplakinolide (0.1μM) and Narciclasine (20nM) for 12h, 3×10^5 cells were seeded in each well for 24h and 48h, the number of migrated or invaded cells were calculated. (g) Representative immunofluorescence images of F-actin and the statistical results of Huh-7 cells pre-treated by Jasplakinolide and Narciclasine. (h-i) 3D Collagen invasion assay for tumor spheroids formed by Huh-7 cell. Tumor spheroids were formed by inverted suspension methods. The tumor spheroids were seeded in 3D collagen gels and treated by Jasplakinolide (0.1μM) and Narciclasine (10nM). The invasion process was observed and record at 0h, 24h and 48h. The fibroblast-like invasive pseudopodia was calculated by ImageJ software and normalized for statistics. (* $p<0.05$, ** $p<0.01$, *** $p<0.001$)

4.2 Overexpression of actomyosin-related genes increases cellular stiffness and reduces metastatic ability

Except for pharmacological treatment, we further overexpressed constitutive active (CA) forms of cytoskeleton regulatory genes MLCK and ROCK, which could increase cellular stiffness. CA MLCK and ROCK were subcloned into the lentiviral vector pSLIK containing the TRE tight doxycycline inducible promoter, ampicillin bacterial resistance and the YFP variant Venus, while empty vector was used as a control (Wong et al., 2015). These viral particles were packaged into 293T cells and used to infect HCC cells and control cell lines were transfected by CA-Empty vector. The CA vectors were activated by 50ng/ml doxycycline for 2 days, when cellular stiffness was measured **(Figure 4.2a, right)**. The control group of HepG2 cells exhibited the lowest mechanical stiffness, and overexpressing CA-MLCK and ROCK

remarkably increased cellular stiffness (P<0.001). Histograms of cell Young's modulus were fitted by Gaussian function in control and MLCK and ROCK overexpression group **(Figure 4.2a, left)**. After HepG2 cells were stiffened by overexpression of CA-MLCK and ROCK, the distribution of cell stiffness became broader and the peak point shifted to the value close to 3 kPa. The results indicated that the mechanical stiffness was increased after overexpression of MLCK and ROCK. We also verified the efficiency of CA plasmids transfection through western blot at protein level **(Figure 4.2b)**. It was obvious that the protein content of phosphorylated myosin light chain was significantly increased. After confirmation of the effect of CA plasmids on stiffening cells, the metastatic ability was compared. Wound healing assay was performed on HepG2 cells that were transfected by CA plasmids of MLCK and ROCK. Stiffening cells obviously inhibited migration in 2D condition **(Figure 4.2c)**. We also verified these findings by transwell migration and invasion assay. Overexpression of MLCK or ROCK significantly decreased the ability of migration and invasion in HepG2 cells **(Figure 4.2d,** P<0.001**)**.

We also tested whether cellular stiffening could reduce metastatic ability in other HCC cells. Huh-7 and Bel-7402 were stiffened similarly by overexpressing CA-MLCK or ROCK. The results of transwell migration and invasion assay showed that stiffening cells by overexpression of MLCK and ROCK significantly inhibited metastatic potential in Huh-7 and Bel-7402 cells **(Fig. 4.2 e, f)**.

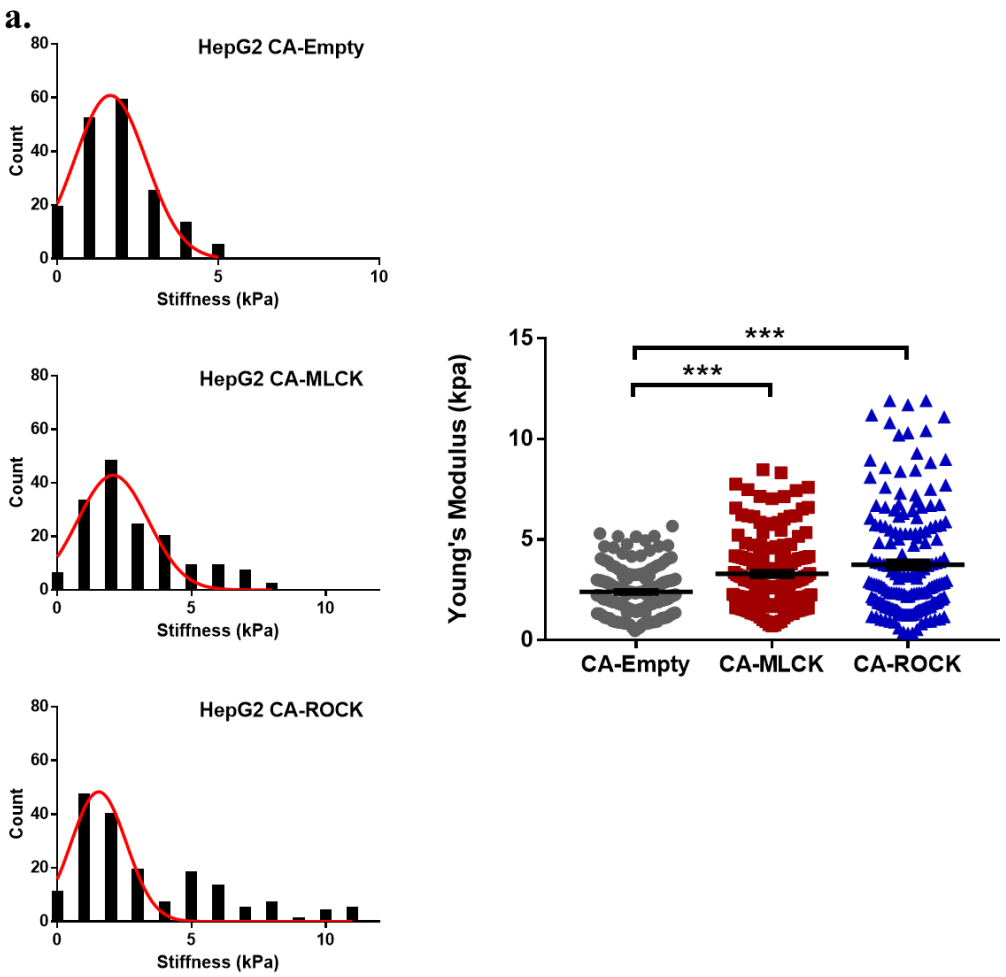
a.
HepG2 CA-Empty
HepG2 CA-MLCK
HepG2 CA-ROCK
Count
Stiffness (kPa)
Young's Modulus (kpa)
***
***
CA-Empty
CA-MLCK
CA-ROCK

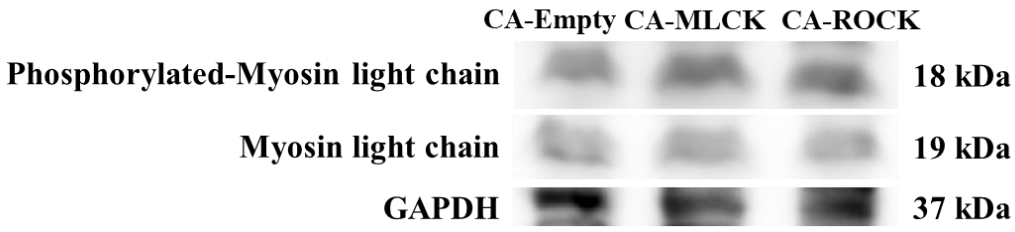
b.
CA-Empty CA-MLCK CA-ROCK
Phosphorylated-Myosin light chain
18 kDa
Myosin light chain
19 kDa
GAPDH
37 kDa

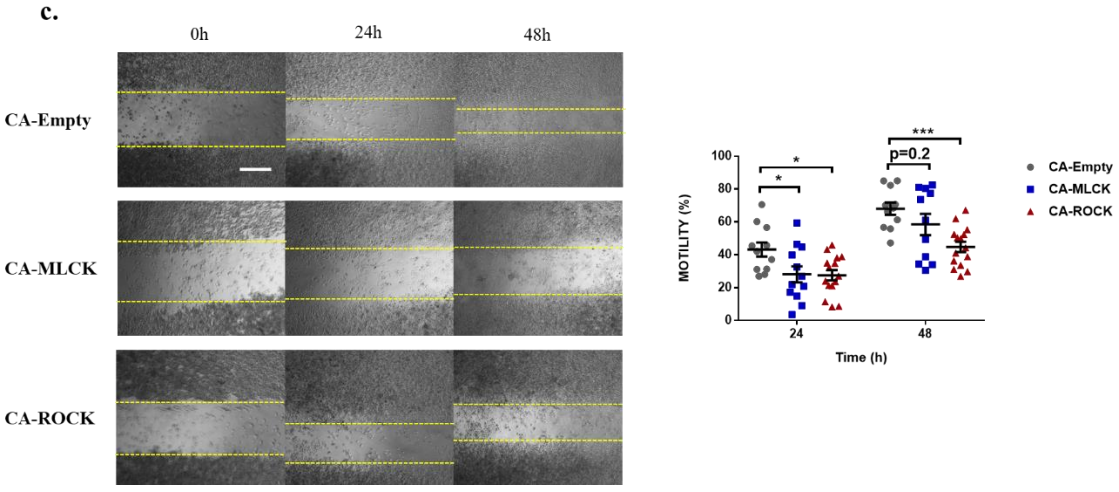
c.
0h
24h
48h
CA-Empty
CA-MLCK
CA-ROCK
MOTILITY (%)
Time (h)
p=0.2
CA-Empty
CA-MLCK
CA-ROCK

d.

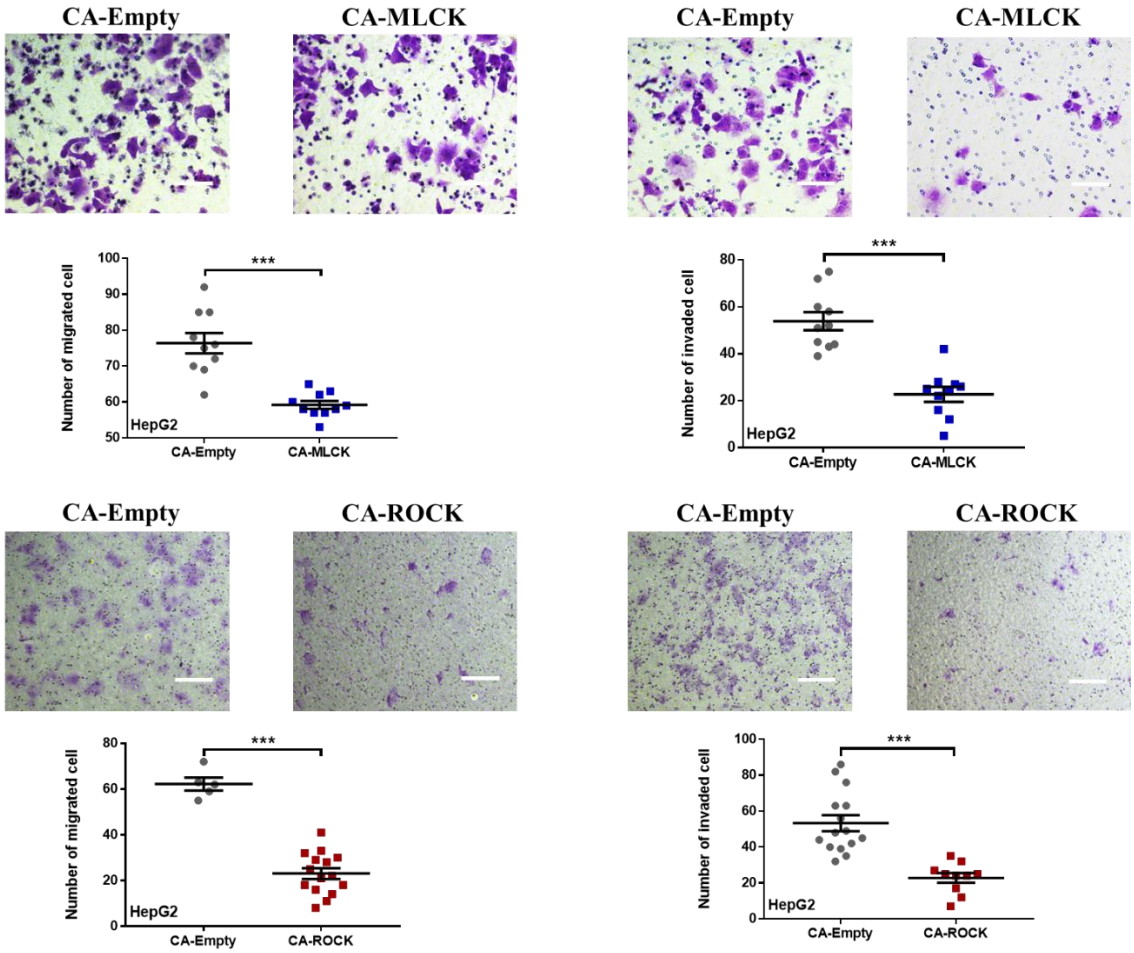
CA-Empty
CA-MLCK
CA-Empty
CA-MLCK
Number of migrated cell
***
HepG2
CA-Empty
CA-MLCK
Number of invaded cell
***
HepG2
CA-Empty
CA-MLCK
CA-Empty
CA-ROCK
CA-Empty
CA-ROCK
Number of migrated cell
***
HepG2
CA-Empty
CA-ROCK
Number of invaded cell
***
HepG2
CA-Empty
CA-ROCK

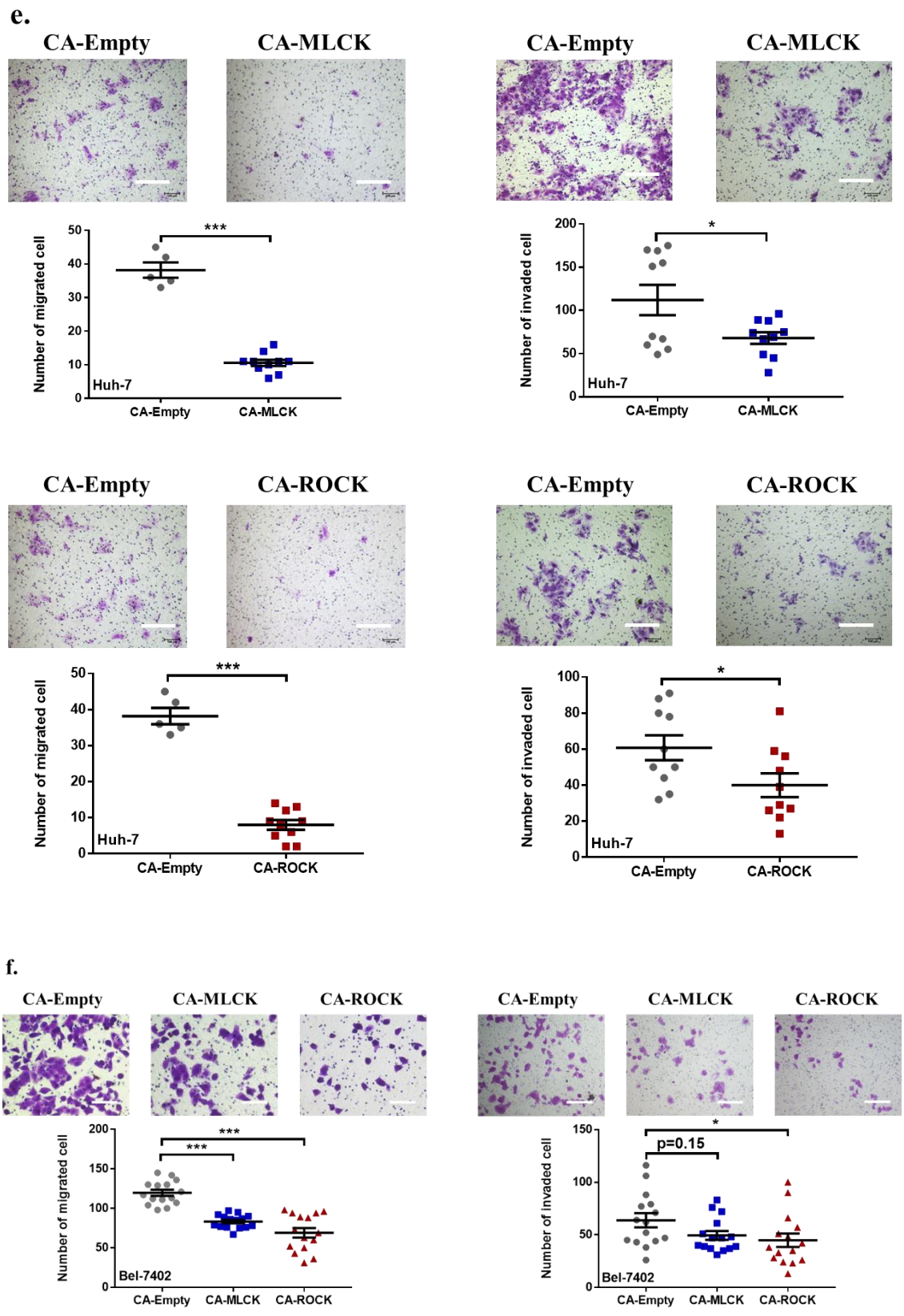

Figure 4.2 Increase of cellular stiffness by CA plasmids decreases metastatic ability of HCC cells. (a) The cellular stiffness was measured by AFM. The histograms of Young's

modulus with Gaussian fittings were obtained from HepG2 cells transfected by CA vectors overexpression of MLCK and ROCK. Above 150 force curves from more than 30 cells of each group were used for the statistics of Young's modulus. (b) Western blotting assay to prove the changes at protein level of myosin light chain and phosphorylated myosin light chain after overexpression of MLCK and ROCK. (c) Wound healing assay. HepG2 cells were transfected by CA vectors upregulating MLCK and ROCK for 48h, then doxycycline (50ng/ml) was added for 48h to activate the expression of MLCK and ROCK and then wound healing assay was performed. Photos of the scratch were taken at 0h, 24h and 48h. The statistical result was shown on the right. (d) Transwell migration and transwell invasion assay for HepG2 cells that overexpressed MLCK and ROCK. Transwell migration assay and transwell invasion assay were performed after cells transfected by CA vectors of MLCK and ROCK for 48h and activated by doxycycline (50ng/ml) for 48h, 3×10^5 cells were seeded in each well for 24h and 48h, the number of migrated or invaded cells were calculated. (e-f) Transwell migration and transwell invasion assay after overexpression of MLCK and ROCK by CA vectors were repeated in Huh-7cells and Bel-7402 cells. (* $p<0.05$, ** $p<0.01$, *** $p<0.001$)

4.3 Myosin mediated cellular stiffness regulates metastatic potential

Together with the findings in Chapter 3, we have demonstrated that softening cells promotes metastatic ability of HCC cells, while stiffening cells inhibits this ability. Since cell stiffness was altered by modulating actomyosin activity, we further tested whether the influence of actomyosin on metastatic potential was through the effect on cell mechanics. To answer this question, we designed four rescue experiments to prove that cellular stiffness regulates metastatic potential.

The first rescue experiment was designed to verify that cellular stiffness could regulate metastasis through MLCK. MLCK was silenced in HepG2 cells with 100nM siRNA and then re-expressed with CA plasmids of MLCK. Transwell migration and invasion assay were performed to examine the change of metastatic ability **(Figure 4.3a)**. After HepG2 cells were

softened by silencing MLCK, both migratory and invasion ability was enhanced **(Figure 4.3a, left,** P<0.01**) (Figure 4.3a, right,** P<0.001**)**. However, when the softened HepG2 cells were stiffened by overexpression of MLCK, the metastatic ability was decreased to the control level **(Figure 4.3a,** n.s**)**. This finding suggest that cellular stiffness regulates metastasis through MLCK.

The second rescue experiment was designed to prove that myosin-mediated cellular stiffness could alter metastatic capacity. HepG2 cells were transfected with CA plasmids of MLCK ROCK, and then were treated by Blebbistatin at 10μM for 12 h. Transwell migration and invasion assay were performed to examine the change of metastatic ability **(Figure 4.3b)**. It was showed that after HepG2 cells were stiffened by overexpression of MLCK and ROCK, the migration and invasion were inhibited significantly **(Figure 4.3b,** P<0.001**)**. However, when the stiffened HepG2 cells were softened by Blebbistatin treatment, the metastatic ability was increased to the control level **(Figure 4.3b,** n.s**)**. These results indicated that myosin mediated cellular stiffness regulates metastatic potential.

The last two rescue experiments were designed to prove that actomyosin-mediated cellular stiffness could alter metastatic capacity. At first, MLCK and mDia1 were silenced in HepG2 cells with 100nM siRNA and then treated with Jasplakinolide to enhance F-actin polymerization. Transwell migration and invasion assay were performed to examine the change of metastatic ability **(Figure 4.3c)**. After HepG2 cells were softened by silencing MLCK and

mDia1, both migratory and invasion ability was enhanced **(Figure 4.3c, left,** P<0.001**) (Figure 4.3c, right,** P<0.01**)**. However, when the softened HepG2 cells were stiffened by increasing F-actin polymerization, the metastatic ability was decreased to the control level **(Figure 4.3c,** n.s**)**. Inversely, HepG2 cells were transfected with CA plasmids of MLCK and ROCK, and then were treated by CytoD at 0.5μM for 12 h. Transwell migration and invasion assay were performed to examine the change of metastatic ability **(Figure 4.3d)**. It was showed that after HepG2 cells were stiffened by overexpression of MLCK and ROCK, the metastatic ability was inhibited **(Figure 4.3d,** P<0.05**)**. However, when the stiffened HepG2 cells were softened by CytoD treatment, the metastatic ability was rescued back **(Figure 4.3d,** n.s**)**. These findings suggest that it is actomyosin-mediated cellular stiffness regulates metastasis.

a.

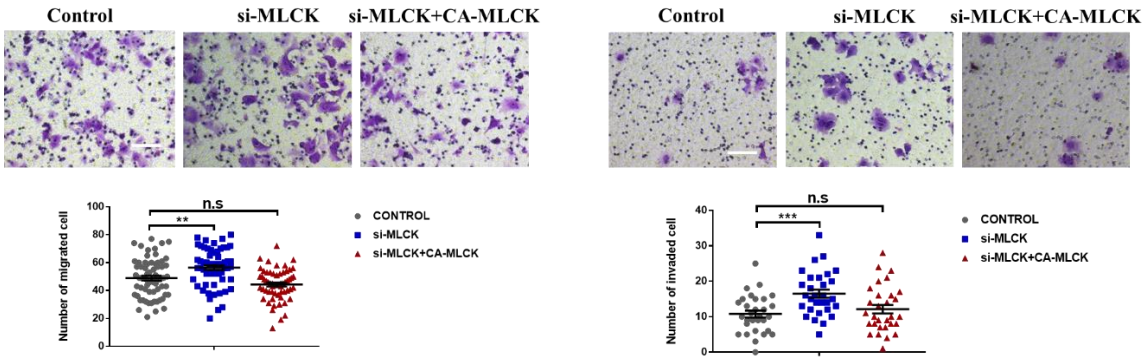

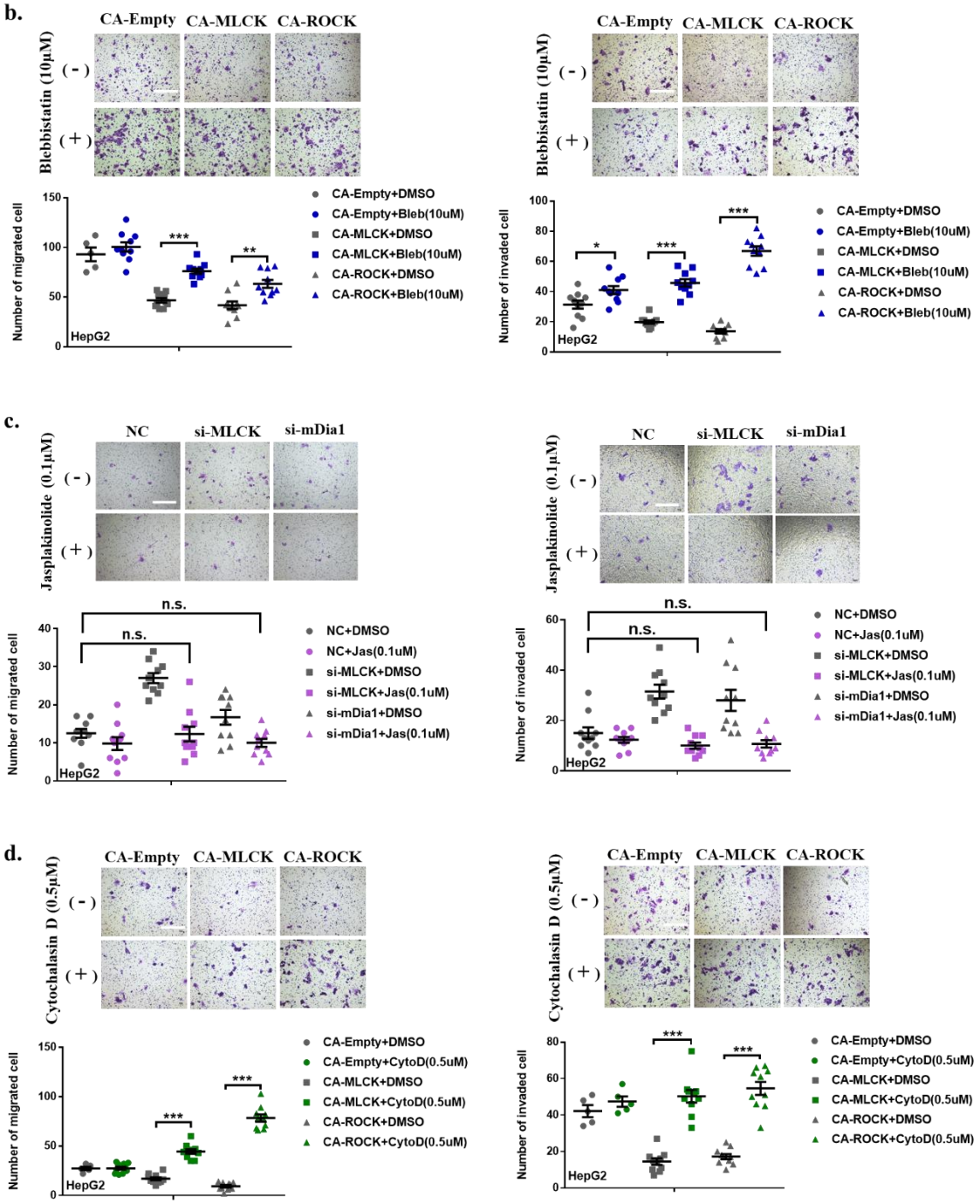

Figure 4.3 Myosin mediated cellular stiffness regulates metastatic potential. (a) HepG2 cells were transfected by siRNA of MLCK to downregulate the expression of MLCK for 48h, and then transfected by CA plasmids of MLCK to rescue the expression level of MLCK. Transwell migration assay and transwell invasion assay were performed on the pretreated cells, 3×10^5 cells were seeded in each well for 24h and 48h, the number of migrated or invaded cells were calculated. (b) HepG2 cells were transfected by CA plasmids of MLCK and ROCK for 48h and activated by doxycycline (50ng/ml) for 48h to overexpress MLCK and ROCK, after that, Blebbistatin was applied to the cells to decrease the expression level of myosinII.

Transwell invasion assay was performed on the pretreated cells, 3×10^5 cells were seeded in each well for 24h and 48h, the number of migrated or invaded cells were calculated. (c) HepG2 cells were transfected by siRNA of MLCK and mDia1 to downregulate the expression of MLCK and mDia1 for 48h, and then Jasplakinolide was applied to the cells to enhance F-actin polymerization. Transwell migration assay and transwell invasion assay were performed on the pretreated cells, 3×10^5 cells were seeded in each well for 24h and 48h, the number of migrated or invaded cells were calculated. (d) HepG2 cells were transfected by CA plasmids of MLCK and ROCK for 48h and activated by doxycycline (50ng/ml) for 48h to overexpress MLCK and ROCK, after that, CytoD was applied to the cells to decrease F-actin polymerization. Transwell invasion assay was performed on the pretreated cells, 3×10^5 cells were seeded in each well for 24h and 48h, the number of migrated or invaded cells were calculated. (* $p<0.05$, ** $p<0.01$, *** $p<0.001$)

4.4 Stiffening CSCs by overexpression of actomyosin-related genes impairs their metastatic ability

In Chapter 3, we have found that CSCs exhibit high metastatic ability but low mechanical stiffness compared to non-CSCs. Therefore, we further explored whether stiffening CSCs impaired their metastatic potential. CSCs were obtained by culturing HCC cells in 90-Pa 3D soft fibrin gel for 7 days (Liu et al., 2012). To stiffen cells, HCC cells were transfected with CA plasmids of MLCK and ROCK and then seeded into 3D soft fibrin gels without the induction of doxycycline. After 5 days, 50 ng/ml doxycycline were added to the gels and the derived CSCs were stiffened due to the activation of CA plasmids.

Cellular stiffness was measured after the induction of CSCs transfected with CA plasmids under 50ng/ml doxycycline for 2 days **(Figure 4.4a, right)**. The control CSCs exhibited low mechanical stiffness, while cellular stiffness was also remarkably increased when the

expression of MLCK or ROCK was activated (P<0.001). The distribution of cell stiffness became broader after the overexpression of MLCK and ROCK and the peak value shifted to ~3kPa, suggesting that HepG2-derived CSCs are stiffened **(Figure 4.2a, left)**. After confirmation of the effect of CA plasmids on the stiffness of CSCs, the metastatic ability was measured and compared. The results showed that the migratory ability of stiffened CSCs was decreased by approximately 50% **(Figure 4.4b, left,** P<0.001**)** and the invasion of CSCs was reduced by nearly 75%. **(Figure 4.4b, right,** P<0.001**)**. These results demonstrate that cellular stiffening significantly inhibited the metastatic ability of HepG2-derived CSCs **(Figure 4.4b)**.

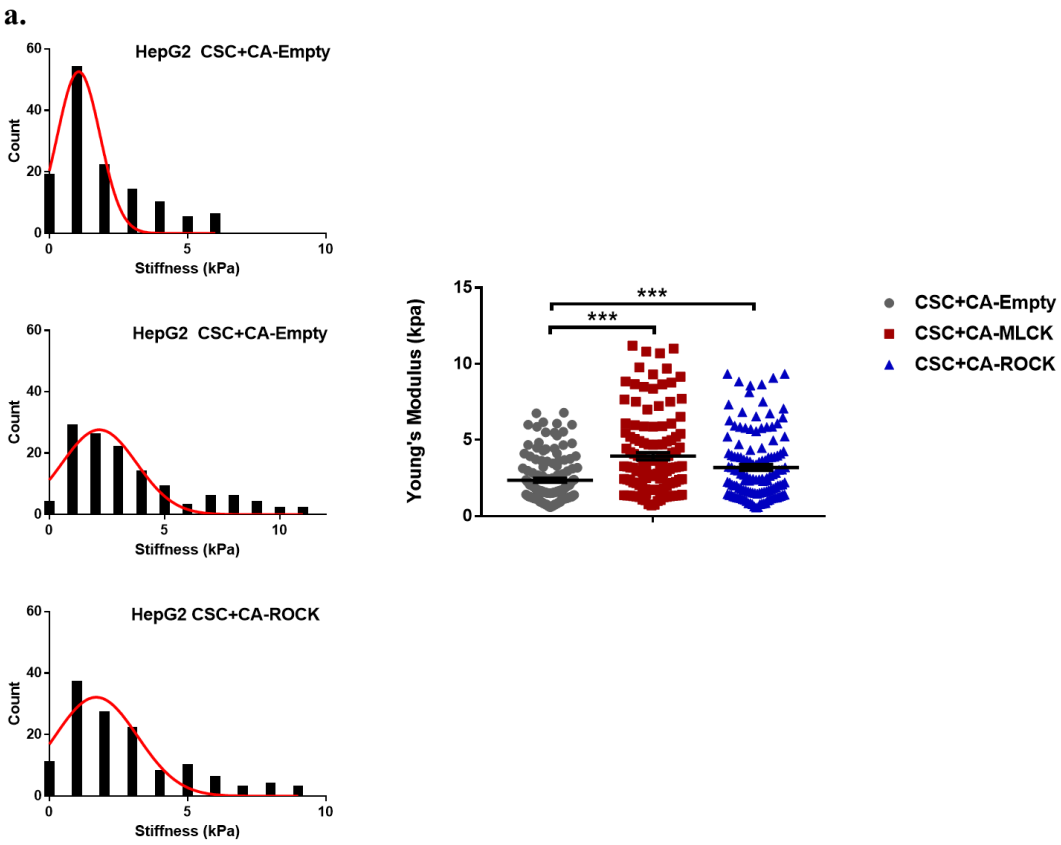

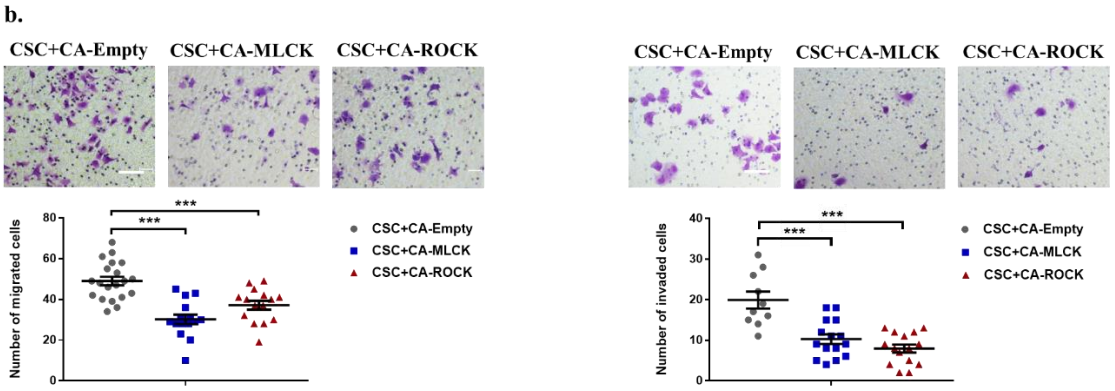

Figure 4.4 Stiffen CSCs could impair their metastasis. (a) The cellular stiffness was measured by AFM. The histograms of Young's modulus with Gaussian fittings were obtained from CSCs and non-CSCs derived from HepG2 cells. Above 150 force curves from more than 30 cells of each group were used for the statistics of Young's modulus. (b) Transwell migration and transwell invasion assay for CSCs and non-CSCs derived from HepG2 cells that overexpressed MLCK and ROCK. 3×10^5 cells were seeded in each well for 24h and 48h, the number of migrated or invaded cells were calculated. (* $p<0.05$, ** $p<0.01$, *** $p<0.001$)

Chapter 5 Cellular stiffness regulates metastatic ability of HCC cells through JNK signaling pathway

In Chapter 3 and 4, we have demonstrated that cellular stiffness regulates metastatic ability of HCC cells and CSCs. However, the mechanism underlying the effect of cellular stiffness on metastasis is still unknown.

In order to unveil the underlying mechanism, we explored several possible or classical pathways. The first one was epithelial to mesenchymal transition (EMT). EMT is an evolutionarily conserved process that commonly happens during development (D. H. Kim et al., 2017). Importantly, EMT has been demonstrated to play a crucial role in carcinogenesis, especially tumor metastasis (Lambert et al., 2017). EMT can confer cancer cells metastatic properties. Therefore, we explored whether cell mechanics impact metastatic potential through EMT. The results showed that softening cells down-regulated both epithelial markers (E-cadherin and EpCam) and mesenchymal markers (N-cadherin, Twist, Slug and Snail) **(Fig. 5a)**. On the other hand, stiffening cells up regulated both epithelial markers and mesenchymal markers. Therefore, EMT may not play an essential role, or their role is very complex in the regulation of metastatic potential by cell mechanics. The second mechanism we tested was nuclear stiffness and the distribution of F-actin. To test the effect of cellular stiffness on nuclear stiffness, we examined the expression level of lamin A/C. The results showed that the alteration in

cell stiffness did not have significant influence on lamin A/C **(Fig. 5b)**. Then we tested whether cellular stiffness could influence the distribution of F-actin. It was reported that F-actin was located at the front of migratory antennary, especially at lamellipodia (Perone et al., 2019). Our data showed that there were not obvious accumulations of F-actin at the edge of migratory antennary after cell softening **(Fig. 5c)**, suggesting that cell mechanics may not directly influence the distribution of F-actin in lamellipodia. The third mechanism we explored included Wnt/β-catenin pathway, Notch pathway and some other essential genes modulating cell activities through qPCR after cellular stiffness was changed. The results showed that the changes on expression level of these genes were contradictory between softened and stiffened cells **(Fig. 5d)**, suggesting no significant influence of cell mechanics on these pathways.

Finally, we explored the role of JNK signaling, since JNK, RhoA and F-actin remodeling could form a positive feedback network (Rudrapatna, Bangi, & Cagan, 2014). Besides, phosphorylated JNK was increased when MLCK was lost in breast cancer (D. Y. Kim & Helfman, 2016). In this chapter, we demonstrated that cellular stiffness regulated metastatic potential through JNK and identified JNK as a potential signaling pathway which participated in the regulation of high metastatic ability in soft CSCs. At first, we did qPCR assay and western blotting assay to examine whether the alteration in cellular stiffness affected the total and phosphorylated amount of JNK.

Softening/stiffening tumor cells inhibited/activated JNK signaling and the upstream genes MKK4 and MKK7 that could directly activate JNK. So far, JNK was identified as the potential signaling pathway mediated by cellular stiffness. The influence of cell mechanics on metastatic ability could be blocked by modulating JNK signaling, suggesting that cellular stiffness regulated metastatic ability through JNK signaling.

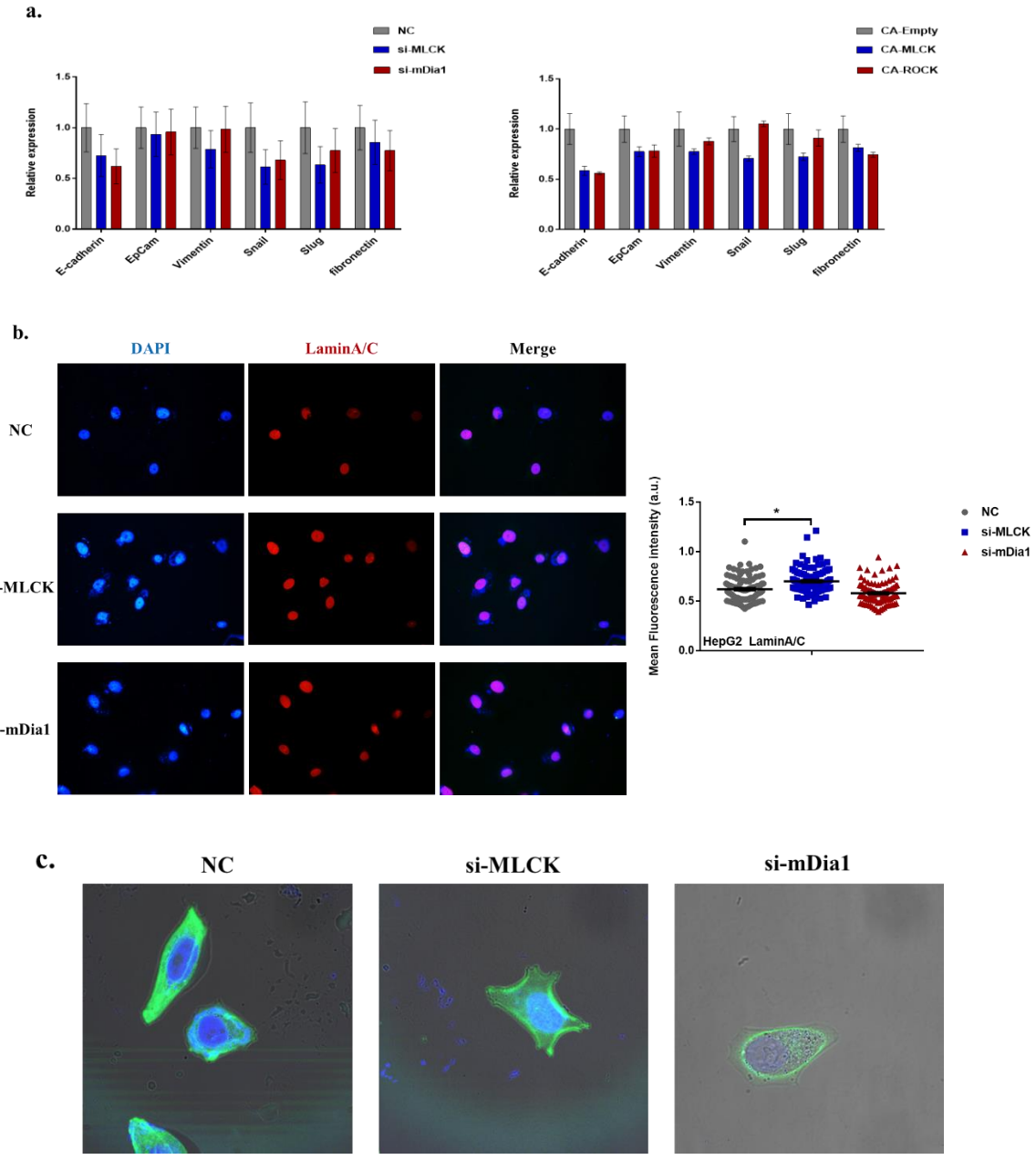

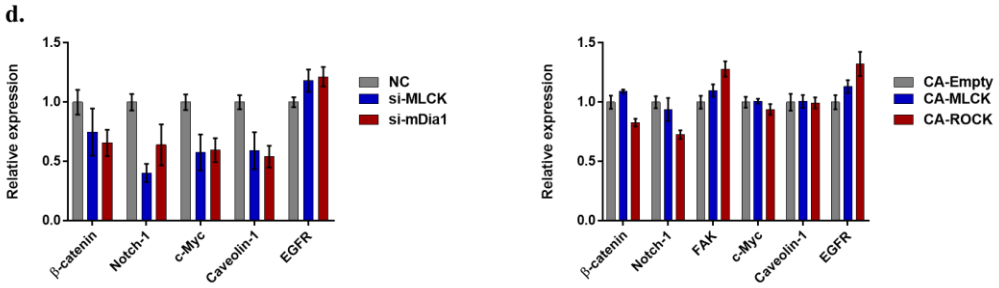

Figure 5 The tried mechanisms did not work in our case. (a) Epithelial-Mesenchymal Transition pathway. EMT related marker genes were tested by qPCR in softened and stiffened cells, respectively. (b) Nulear stiffness alteration. The amount of nuclear skeleton protein LaminA/C was examined by immunofluorescence. The mean fluorescence intensity was analyzed by ImageJ and the ratio of phosphorylated LaminA/C and total LaminA/C was calculated. (c) F-actin distribution alteration. Representative images were taken by confocal microscope with 63× objective lens including DAPI, FITC and bright channels. (d) Essential pathways modulating cellular activities. Related genes were tested by qPCR in softened and stiffened cells, respectively.

5.1 JNK is the potential signaling pathway that mediates the effect of cellular stiffness on metastatic ability

We performed qPCR assay to detect whether cellular stiffness influenced the expression of JNK and JNK-related genes. HepG2 cells were softened by knocking down the expression of MLCK and mDia1 through transfection of siRNAs for 2 days. Total RNA was extracted for qPCR assay. The expression levels of JNK and JNK-related genes MKK4 and MKK7 were downregulated after cellular stiffness was decreased **(Figure 5.1a)**. On the contrary, HepG2 cells were transfected with CA plasmids of MLCK and ROCK for 2 days and activated by doxycycline (50ng/ml) for another 2 days. After HepG2 cells were stiffened, total RNA was extracted for qPCR

detection. It was found that the expression levels of JNK and JNK-related gene MKK4 and MKK7 were increased **(Figure 5.1b)**.

Further, we also examined the changes of JNK signaling at the protein level through western blotting assay. Total proteins were extracted from HepG2 cells softened by silencing MLCK and mDia1 and stiffened by overexpression of MLCK and ROCK. It was found that softening cells had no significant effect on total amount of JNK1 and JNK2 but significantly decreased the phosphorylated JNK1 and JNK2 **(Figure 5.1c)**. On the contrary, stiffening cells significantly increased the amount of phosphorylated JNK1 and JNK2 **(Figure 5.1d)**. All these results above suggest that JNK is the downstream of cellular stiffness and might be a potential signaling that mediates the effect of cellular stiffness on metastatic potential.

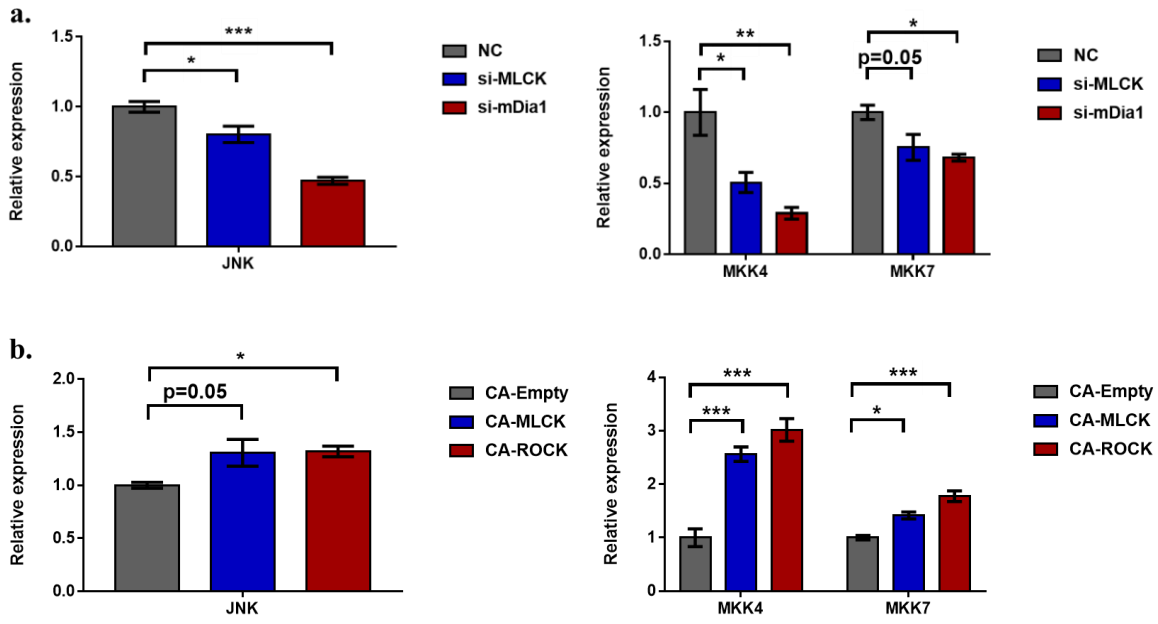

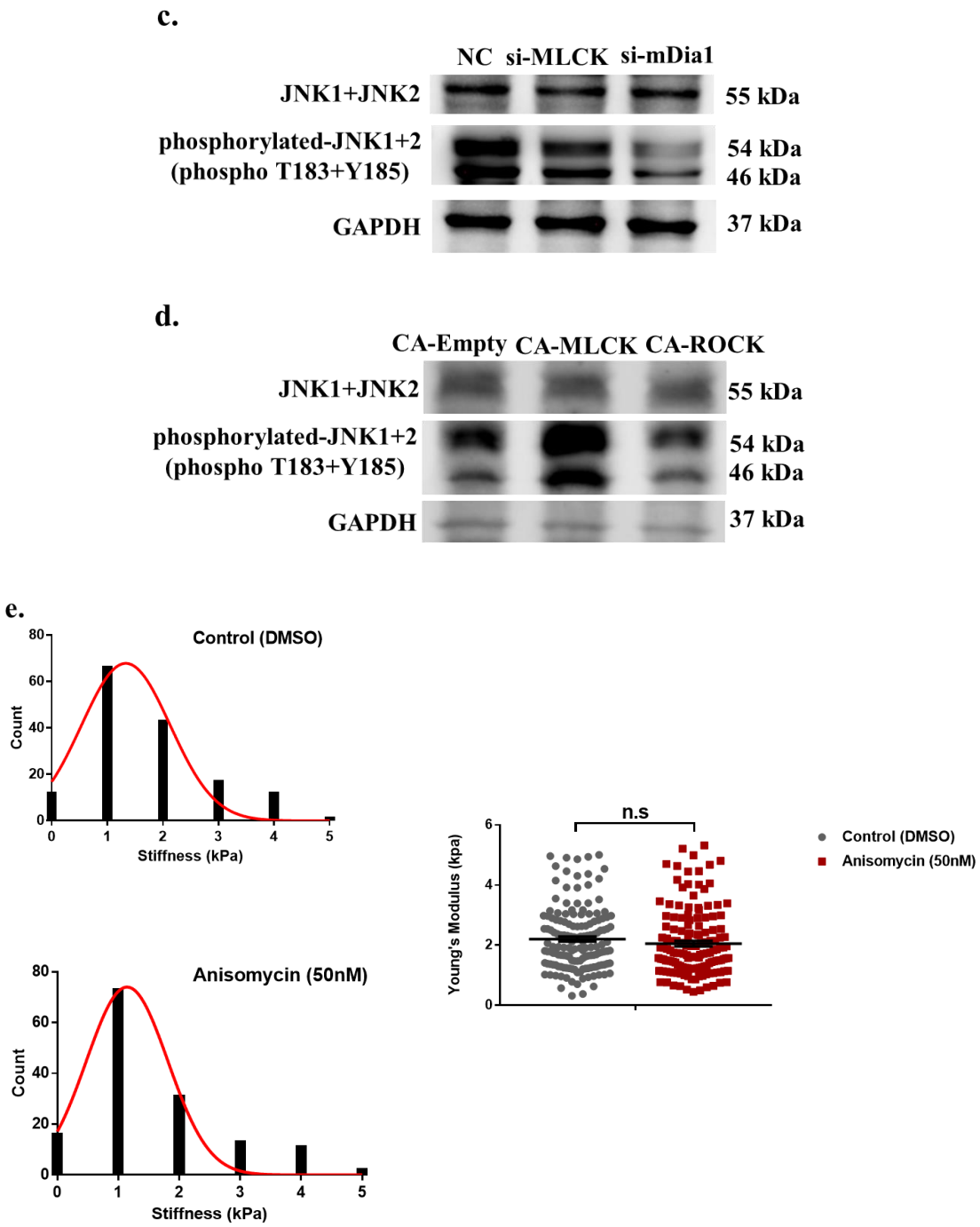

Figure 5.1 JNK signaling is the downstream of cellular stiffness alteration. (a) Huh-7 cells were softened by knocking down MLCK and mDia1, the expression of JNK and JNK related gene MKK4, MKK7 was examined by quantitative Real Time Polymerase Chain Reaction (qPCR). GAPDH was used as a reference gene and the expression level was normalized and calculated. JNK, MKK4 and MKK7 was downregulated after Huh-7 cells softness. (b) HepG2 cells were stiffened by overexpression of MLCK and ROCK, the expression of JNK and JNK related gene MKK4, MKK7 was examined by qPCR. GAPDH was used as a reference gene and the expression level was normalized and

calculated. JNK, MKK4 and MKK7 was upregulated after HepG2 cells stiffening. (c) HepG2 cells were softened by silencing MLCK and mDia1, the amount of total JNK and phosphorylated JNK1 and JNK2 were detected by western blotting assay, respectively. GAPDH was used as the reference. The amount of phosphorylated JNK1 and phosphorylated JNK2 was decreased after HepG2 cell softness. (d) HepG2 cells were stiffened by overexpression of MLCK and ROCK, the amount of total JNK and phosphorylated JNK1 and JNK2 were detected by western blotting assay, respectively. GAPDH was used as the reference. The amount of phosphorylated JNK1 and phosphorylated JNK2 was increased after HepG2 cells were stiffened. (e) Cellular stiffness was measured by AFM. The histograms of Young's modulus with Gaussian fittings were obtained from HepG2 cells treated by JNK activator Anisomycin. Above 150 force curves from more than 30 cells of each group were used for the statistics of Young's modulus. JNK activated level did not influence cellular stiffness.

5.2 Cellular stiffness regulates metastatic ability of HCC cells through JNK signaling pathway

We have demonstrated that cellular stiffness influences JNK signaling at both mRNA and protein level. However, it is still not clear whether cellular stiffness regulates metastatic ability through JNK signaling. In order to address this question, we designed two rescue experiments.

The first rescue experiment was designed to prove that decrease of cellular stiffness promotes metastasis through suppressing JNK signaling. HepG2 cells were softened by knocking down MLCK and mDia1, and after cells were softened, the capacity of migration and invasion was enhanced obviously, which was similar to the previous findings **(Figure 5.2a)**. Then the softened HepG2 cells were treated by JNK activator Anisomycin at the concentration of 50 nM for 12 h. It was found that activating JNK

signaling in the softened cells decreased the ability of migration and invasion to the level lower than that of control group **(Figure 5.2a)**. In order to confirm this finding, similar experiments were also conducted in Huh-7 cells. We found that the increase in metastatic potential induced by decrease of cellular stiffness could be inhibited significantly through activating JNK **(Figure 5.2b)**. These findings suggest that softening tumor cells enhances metastatic ability via inhibiting JNK signaling.

The second rescue experiment was designed to prove that increase of cellular stiffness inhibits metastasis through activating JNK signaling. HepG2 cells were stiffened by overexpression of MLCK and ROCK, and after cells were stiffened, the capacity of migration and invasion was reduced obviously, which was similar to the previous findings **(Figure 5.2c)**. Then the stiffened HepG2 cells were treated by JNK inhibitor SP600125 at the concentration of 20nM for 12 h. It was found that inhibiting JNK signaling in the stiffened cells dramatically increased the ability of migration and invasion **(Figure 5.2c)**. The findings were further verified in Huh-7 cells, the results supported that the suppressed metastatic ability by stiffening the cells could be rescued back by inhibition JNK phosphorylation **(Figure 5.2d)**. These data suggest that stiffening tumor cells suppresses metastatic ability via activating JNK signaling.

Therefore, all these findings together conclude that cellular stiffness regulates metastatic ability of HCC cells through JNK signaling.

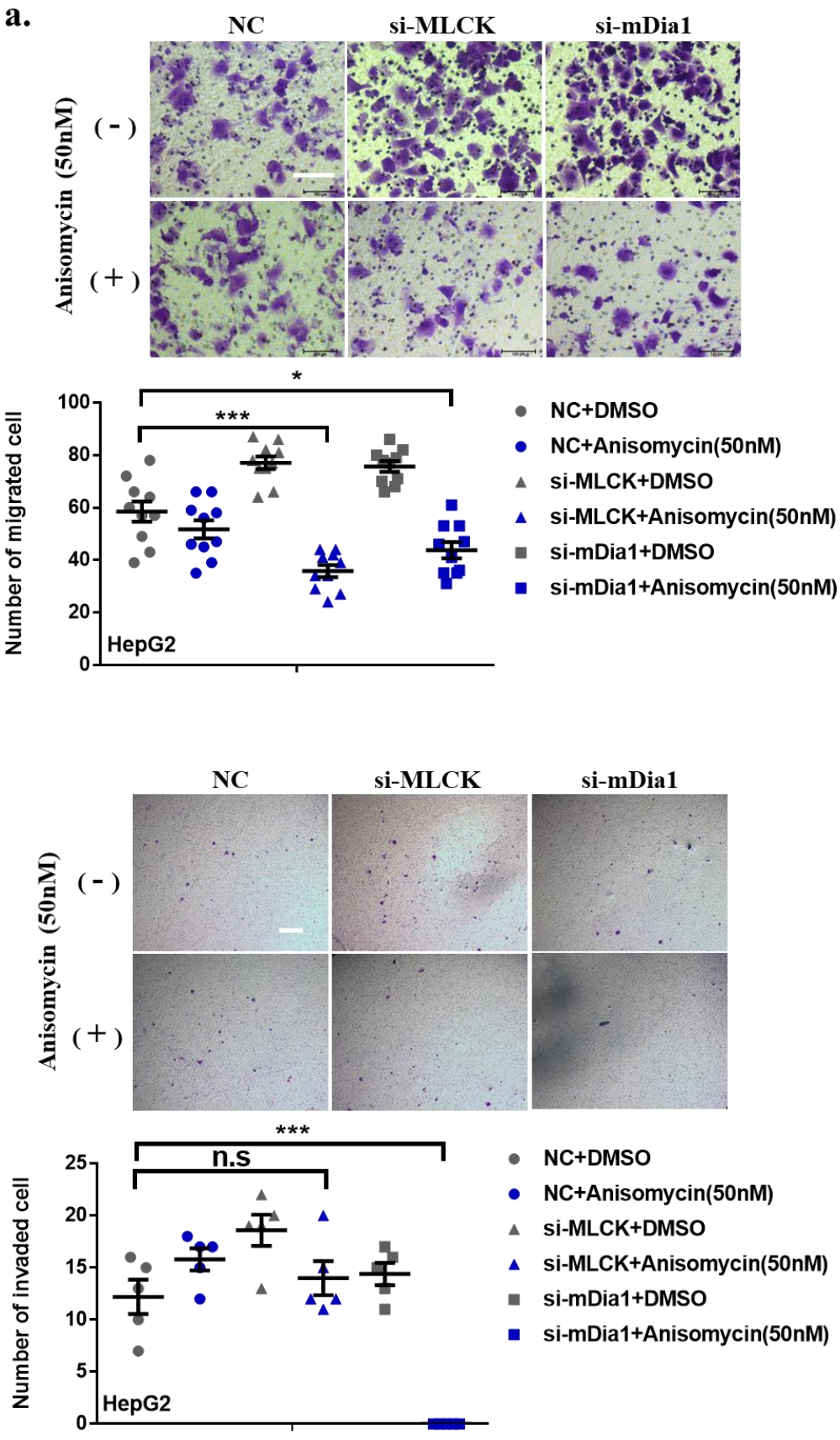
a.
NC
si-MLCK
si-mDia1
Anisomycin (50nM)
(-)
(+)
Number of migrated cell
HepG2
*
***
NC+DMSO
NC+Anisomycin(50nM)
si-MLCK+DMSO
si-MLCK+Anisomycin(50nM)
si-mDia1+DMSO
si-mDia1+Anisomycin(50nM)
Number of invaded cell
n.s

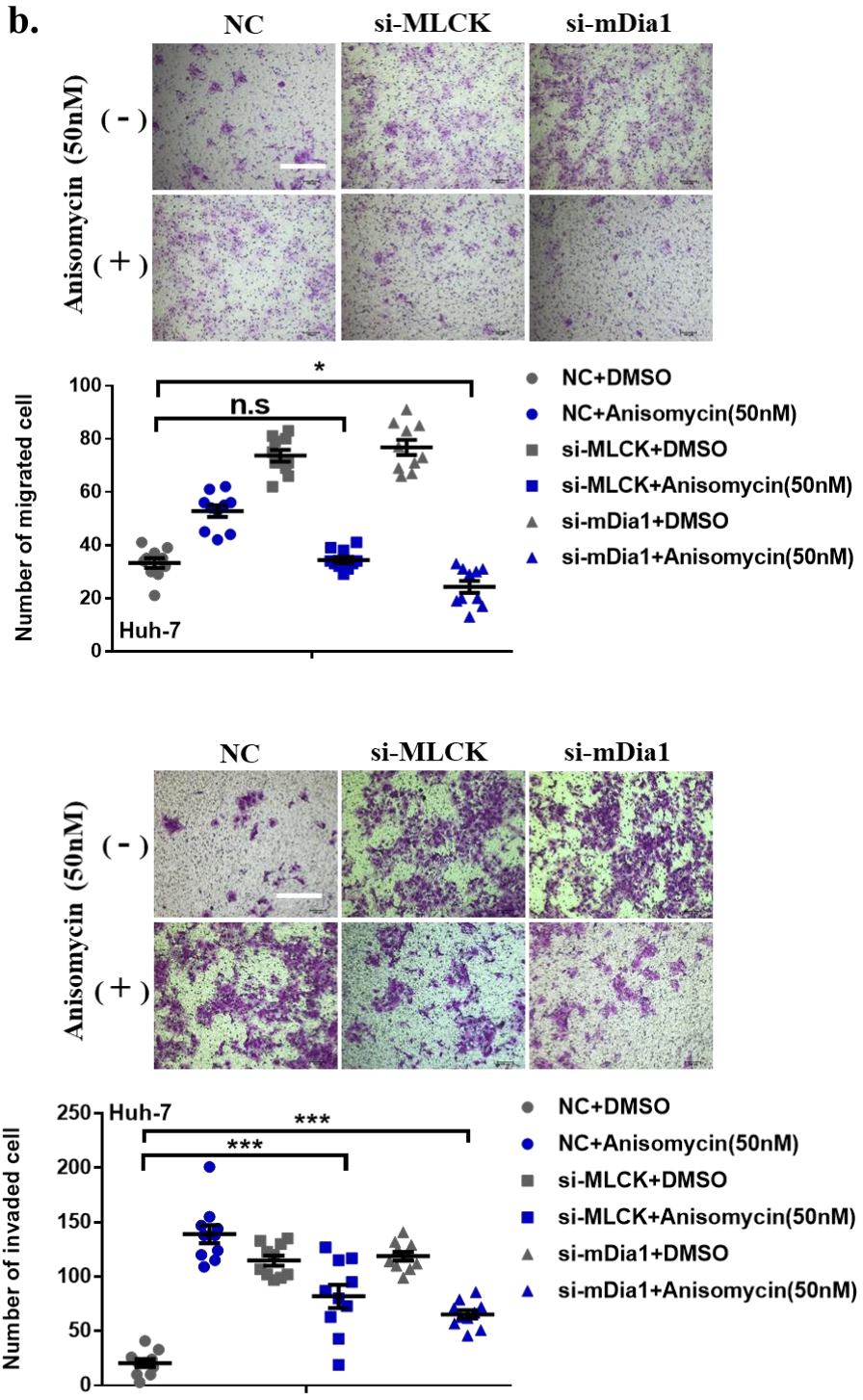
b.
NC
si-MLCK
si-mDia1
Anisomycin (50nM)
(-)
(+)
Number of migrated cell
Huh-7
n.s
*
NC+DMSO
NC+Anisomycin(50nM)
si-MLCK+DMSO
si-MLCK+Anisomycin(50nM)
si-mDia1+DMSO
si-mDia1+Anisomycin(50nM)
Number of invaded cell
***
***

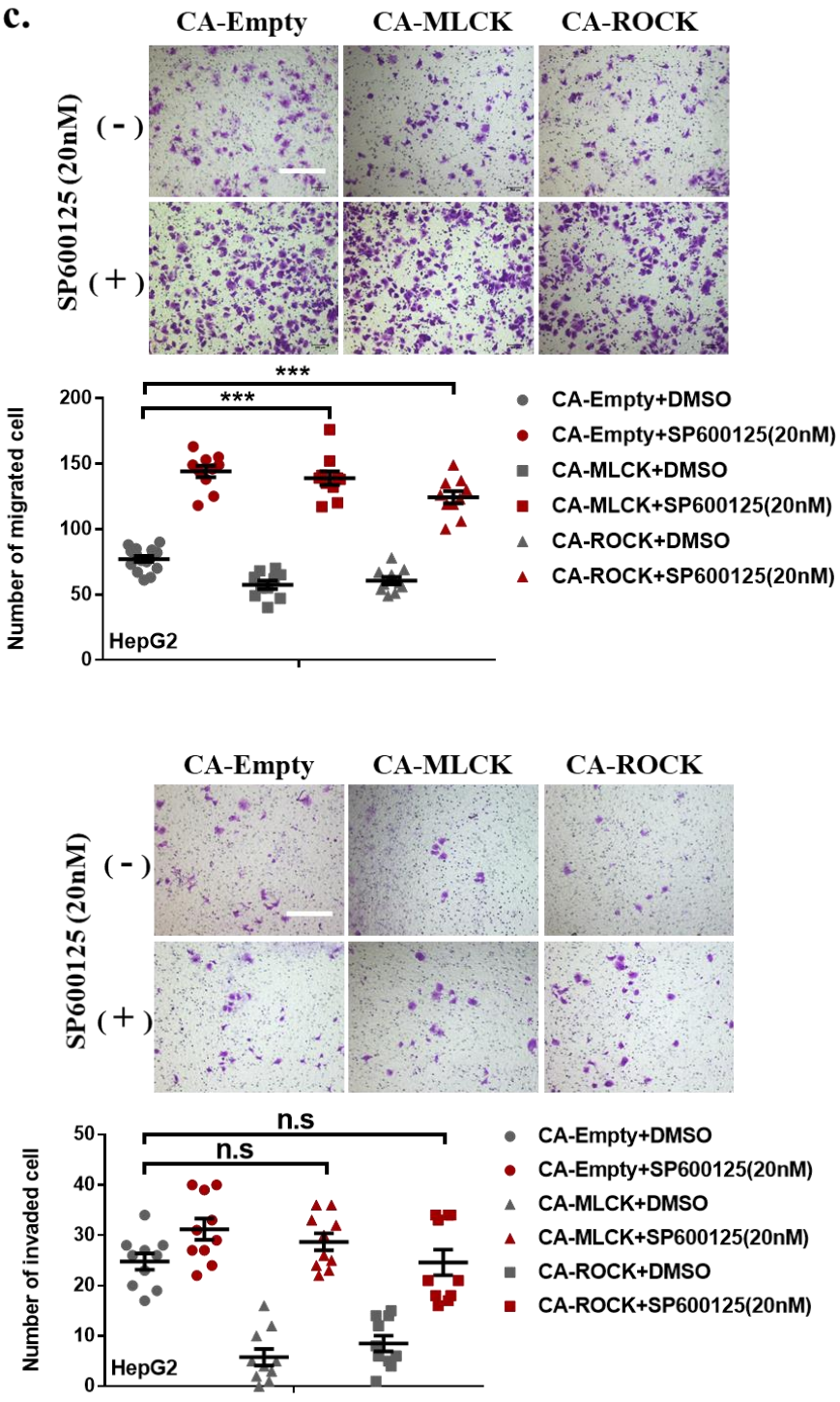
c.
CA-Empty
CA-MLCK
CA-ROCK
SP600125 (20nM)
(-)
(+)
***
***
Number of migrated cell
200
150
100
50
0
HepG2
CA-Empty+DMSO
CA-Empty+SP600125(20nM)
CA-MLCK+DMSO
CA-MLCK+SP600125(20nM)
CA-ROCK+DMSO
CA-ROCK+SP600125(20nM)
CA-Empty
CA-MLCK
CA-ROCK
SP600125 (20nM)
(-)
(+)
n.s
n.s
Number of invaded cell
50
40
30
20
10
0
HepG2
CA-Empty+DMSO
CA-Empty+SP600125(20nM)
CA-MLCK+DMSO
CA-MLCK+SP600125(20nM)
CA-ROCK+DMSO
CA-ROCK+SP600125(20nM)

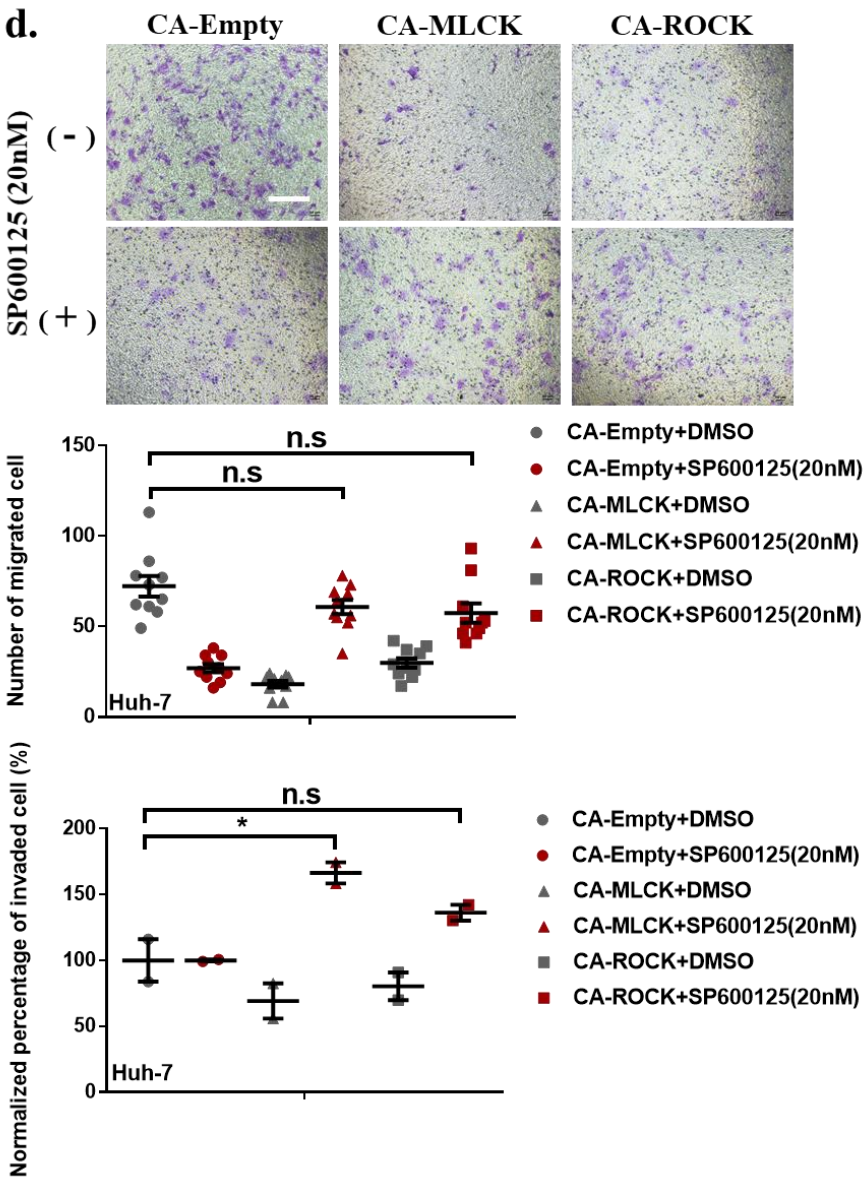

Figure 5.2 Cellular stiffness regulated metastasis through JNK. (a) The increase of metastatic ability caused by cell softness could be impaied by JNK activating in HepG2 cells. Transwell migration assay and transwell invasion assay was performed on HepG2 cells. HepG2 cells were softened by knocking down MLCK and mDia1, and the softened cells were treated by JNK activator Anisomycin at the concentration of 50nM for 12 hours while treated by DMSO as control. 3×10^5 cells were seeded in each well for 24h and 48h, the number of migrated or invaded cells were calculated. (b) The increase of metastatic ability caused by cell softness could be impaied by JNK activating in Huh-7 cells. Transwell migration assay and transwell invasion assay was performed on Huh-7 cells. Huh-7 cells were softened by knocking down MLCK and mDia1, and the softened cells were treated by JNK activator Anisomycin at the concentration of 50nM for 12 hours while treated by DMSO as control. 3×10^5 cells

were seeded in each well for 24h and 48h, the number of migrated or invaded cells were calculated. (c) The decrease of metastatic ability caused by cell stiffening could be enhanced by JNK inhibiting in HepG2 cells. Transwell migration assay and transwell invasion assay was performed on HepG2 cells. HepG2 cells were stiffened by overexpression of MLCK and ROCK, and the stiffened cells were treated by JNK inhibitor SP600125 at the concentration of 20nM for 12 hours while treated by DMSO as control. 3×10^5 cells were seeded in each well for 24h and 48h, the number of migrated or invaded cells were calculated. (d) The decrease of metastatic ability caused by cell softness could be enhanced by JNK inhibiting in Huh-7 cells. Transwell migration assay and transwell invasion assay was performed on Huh-7 cells. Huh-7 cells were stiffened by overexpression of MLCK and ROCK, and the stiffened cells were treated by JNK inhibitor SP600125 at the concentration of 20nM for 12 hours while treated by DMSO as control. 3×10^5 cells were seeded in each well for 24h and 48h, the number of migrated cells were counted and the percentage of invaded cells were calculated by the absorption value of crystal violet. (*$p<0.05$, **$p<0.01$, ***$p<0.001$)

5.3 Cell mechanics regulate metastatic potential of liver CSCs via JNK signaling

Except for HCC cells, we also explored the role of JNK signaling in cellular stiffness mediated metastasis in cancer stem cells (CSCs). HepG2-derived CSCs were obtained by 3D soft fibrin culture and stiffened by overexpression of MLCK and ROCK. At first, we examined the expression of phosphorylated JNK by immunofluorescence staining **(Figure 5.3a)**. On the one hand, F-actin polymerization was increased, supporting the stiffening of CSCs, on the other hand, the results showed that JNK phosphorylation was activated after CSCs stiffening. To further confirm the role of JNK phosphorylation in regulation of CSC metastasis, we performed functional rescue experiments. The results of transwell migration assay showed that the migratory ability was significantly inhibited by 70% after HepG2-derived CSCs were stiffened **(Figure 5.3b)**, which is

similar to the results of conventional HCC cells. Meanwhile, in transwell invasion assay, stiffening liver CSCs dramatically inhibited tumor cell invasion by more than 50%, and even reached at over 90% when CSC cells stiffened by overexpression of ROCK **(Figure 5.3c)**. However, when JNK was inhibited by the treatment of inhibitor SP600125 at the concentration of 20nM for 12 h, both migration and invasion of the stiffened CSCs were increased dramatically, especially for invasion, where inhibiting JNK signaling enhanced the invasive ability of stiffened CSCs to the level of control cells **(Figure 5.3c)**. These rescue experiments demonstrate that cellular stiffening inhibits CSC metastasis through activating JNK.

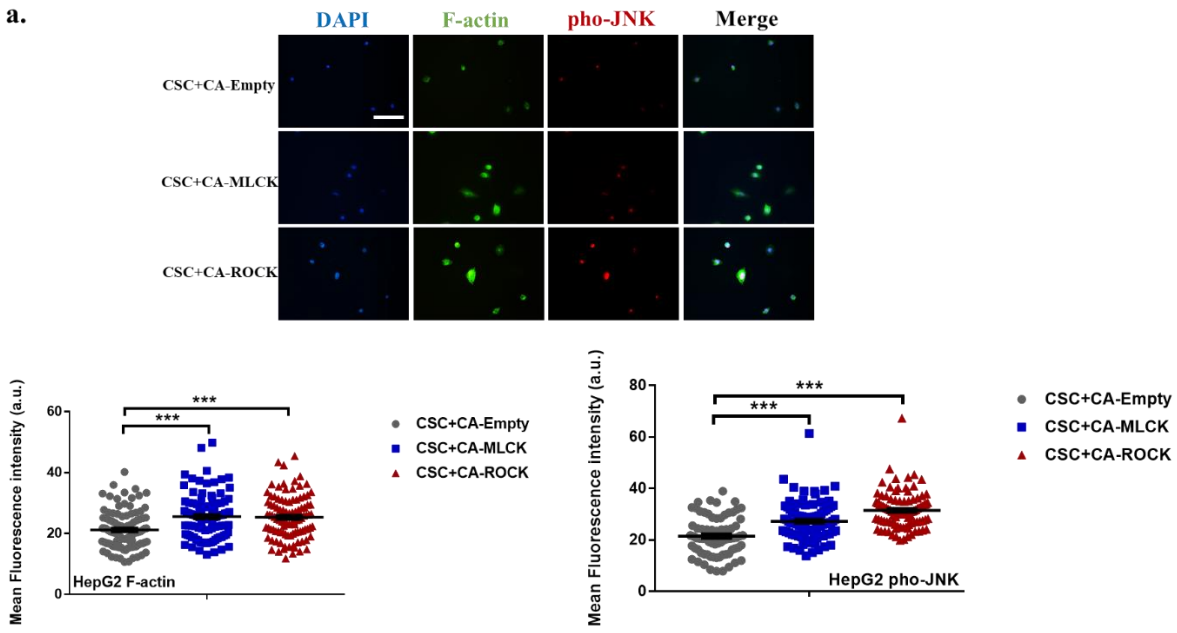

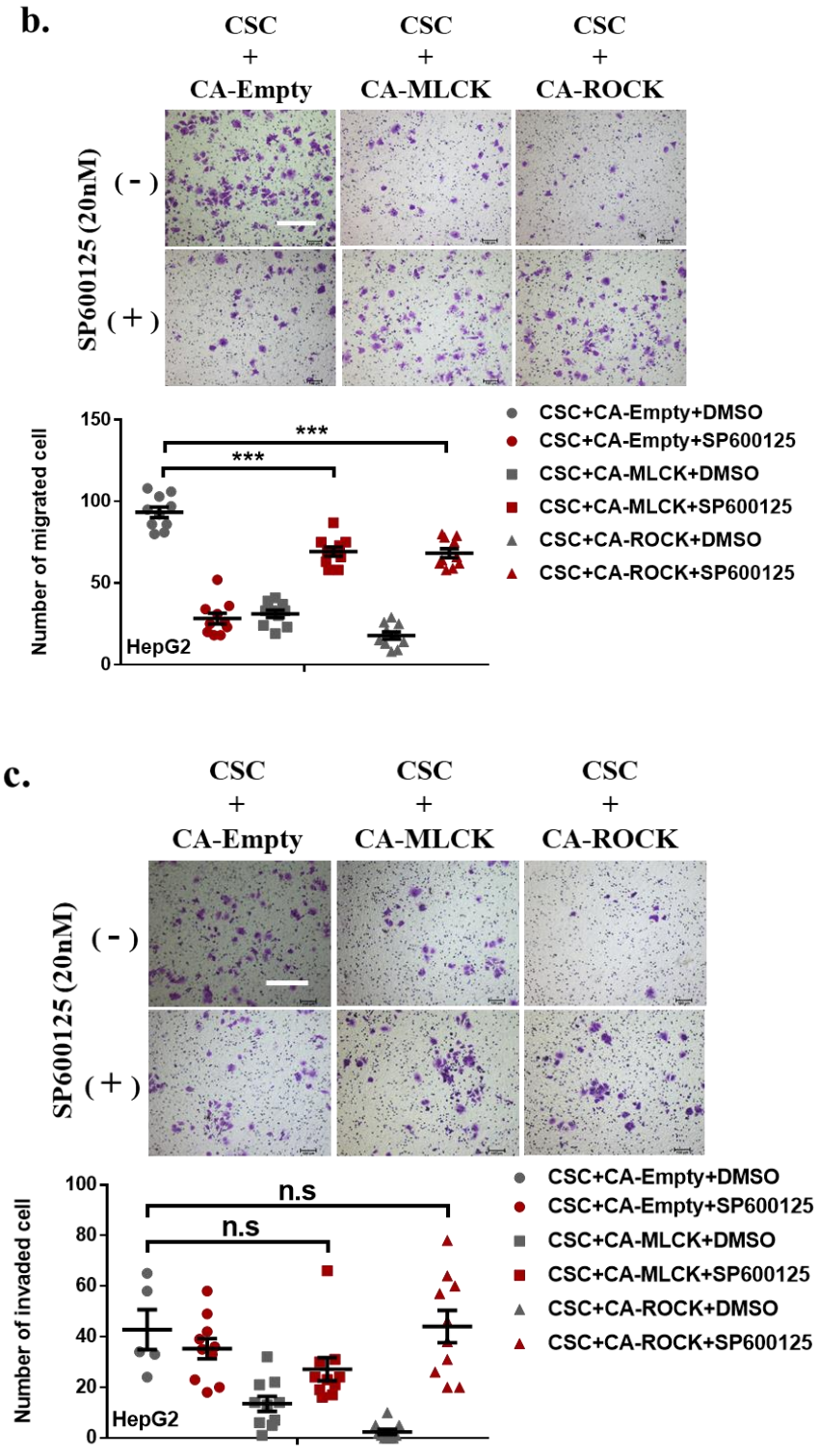

Figure 5.3 Cellular stiffness regulated metastatic potential through JNK in CSCs. (a) The expression level of phosphorylated JNK and the extent of F-actin polymerization was measured by immunofluorescence staining assay in CSCs. (b) The decrease of migratory ability caused by cell stiffening could be rescues by JNK activating in HepG2 derived CSCs. Transwell migration assay was performed on

HepG2 derived CSCs. HepG2 derived CSCs were stiffened by overexpression of MLCK and ROCK, and the stiffened cells were treated by JNK inhibitor SP600125 at the concentration of 20nM for 12 hours while treated by DMSO as control. 3×10^5 cells were seeded in each well for 24h and 48h, the number of migrated cells were calculated. (c) The decrease of invasion caused by cell stiffening could be enhanced by JNK inhibiting in HepG2 derived CSCs. Transwell invasion assay was performed on HepG2 derived CSCs. HepG2 derived CSCs were stiffened by overexpression of MLCK and ROCK, and the stiffened cells were treated by JNK inhibitor SP600125 at the concentration of 20nM for 12 hours while treated by DMSO as control. 3×10^5 cells were seeded in each well for 24h and 48h, the number of migrated or invaded cells were calculated. (*$p<0.05$, **$p<0.01$, ***$p<0.001$)

Chapter 6 Conclusion, Limitations and Future perspective

6.1 Conclusion

Liver cancer ranked as the third leading cause of cancer-related death around the whole world. Among four sub-types of liver cancer, HCC is regarded as the biggest threaten because approximately 80% diagnosed cases are HCC worldwide (El-Serag, 2012). The nature of high chemoresistance, cancer recurrence, and metastasis in HCC builds up a barrier to between HCC therapeutics and expectations of patient survival. Metastasis is the major cause of cancer death and it is responsible for over 90% of cancer-related death. Unless diagnosed at earlier stage, liver cancer threatens lives owing to its extremely malignancy, especially metastasis. Although cancer metastasis has already been studied for nearly 200 years, there are still many debatable key points unclear. Besides, the majority of the studies on metastasis have been focusing on genetic mutation. Although considerable advance has been achieved, metastasis, however, is still far away from being treated or avoided effectively. CSCs are commonly regarded as the origin of metastasis in various types of cancer, and CSCs also play an important role in facilitating cancer progression. It is reported in many studies that the characteristics of CSCs help them to escape and survive from the therapies. It is an urgent need to find out new thinking and methods on therapeutics of cancer metastasis, especially inhibition of metastasis of CSCs. The current situation may suggest that it is necessary to study tumor metastasis from new perspectives, which may be distinct from traditional notions. It has been widely accepted that

the cause of cancer is accumulation of genetic mutations. However, in recent years, more and more studies indicated that not only genetic mutation, the alterations of cell mechanics such as cellular stiffness also play a critical role in tumor progression, especially metastasis. Although the phenomenon of cellular softness could promote metastasis have been found, whether the decrease of cellular stiffness is the consequence or cause of promoting metastasis and the underlying mechanisms are still not clear. Besides, how we could extend these findings to clinical applications and what new thinking would these experimental data provide to cancer therapies are still waiting for answers.

In our study, we first established the correlation between cellular stiffness and metastatic ability in several HCC cell lines, and it showed that they had an inverted correlation. This finding was agreed to the reported studies associated with melanoma cancer, breast cancer, ovarian cancer and so on (Cross, Jin et al. 2008, Swaminathan, Mythreye et al. 2011, Fenner, Stacer et al. 2014, Tatsuro Watanabe et al, 2012). However, it is still not clear whether the cellular alteration is the reason of cancer metastasis.

Firstly, we designed experiments to soften HCC cells and wanted to know what influence that decrease of cellular stiffness would bring to metastatic capacity. The methods we applied to soften HCC cells mainly targeted at cytoskeleton, including RhoA/ROCK-myosin-F-actin network. Pharmacological inhibitors and small RNA interference were applied, and the metastatic ability was examined not only in 2D migratory condition, 3D invasive ability was

also tested. The results obtained suggested that decrease of cellular stiffness could promote metastasis in HCC, and these findings were confirmed in different HCC cell lines.

Based on what we observed in softened HCC cells, we think about whether the metastasis could be inhibited or avoid by stiffening the cells? In order to answer this question, we performed the experiments that were on the opposite of what we did to soften cells. The pharmacological activator of RhoA and F-actin assembly were used to stiffen HCC cells. Besides, we also applied constitutive active vector of MLCK and ROCK to transfect HCC cells, and overexpressed MLCK and ROCK to stiffen the cells. After the HCC cells were stiffened by different approaches, the same results appeared, which is that metastasis was inhibited after HCC cells were stiffened.

Compared to other HCC cells, cancer stem cells (CSCs) showed much more malignancy and metastatic ability, which is a big challenge to cancer therapy. We also explore the mechanical stiffness alteration in CSCs and the influence of cellular stiffness alterations on metastasis. We firstly found that CSCs was much softer than non-CSCs, while the metastatic ability was significantly enhanced. Based on the mechanical characterizations, we proposed to stiffen CSCs and examine whether metastatic ability could be impaired by stiffening CSCs. The results we obtained proved that metastasis could be inhibited after CSCs were stiffened. This finding might contribute to treatments targeting CSCs.

After confirmation of cellular stiffness could regulate metastatic ability in HCC, we further

explored which signaling pathway participated in the regulatory effect of cellular stiffness had on metastasis. JNK was finally identified as the signaling pathway after a lot of attempts. We examined JNK signaling not only from mRNA and protein expression level, but we also verified the function of JNK signaling in cellular mediated metastasis. The rescue experiments were designed and performed, we found no matter in HCC cells or CSCs, the changes of metastasis caused by alteration of cellular stiffness could be rescued by alteration of JNK. It suggested that cellular stiffness regulated metastatic ability through JNK in HCC.

Taken together, our study revealed that cellular stiffness regulates hepatocellular carcinoma metastasis through JNK signaling. Our finding contributes to better understanding the role of cellular stiffness in regulation of metastasis in HCC. We also provided some evidence for cell mechanics as a new potential target for cancer therapeutics. However, there are some limitations of this study and some questions should be further explored to strengthen and support the conclusion of this study.

6.2 Limitations

Firstly, what we have done are only performed in vitro, including cellular experiments, biochemical analysis and so on. However, experiments carried on in vitro might not reflect the real situation in vivo. So, all the proposed hypothesis should be also verified in vivo, which means mouse model should be applied.

Secondly, all the HCC cells we used in our study were commercialized HCC cell lines,

including HepG2, Huh-7, MHCC97-L and Bel-7402. Commercialized HCC cell lines have been applied for several decades, there might be some differences from the primary cells gained from HCC patient. In order to approach closer to actual HCC cells and further explore the regulatory effect of cellular stiffness on metastasis, it is better to use primary cells of patient sample.

Thirdly, the survival curves of cellular stiffness related genes should be analyzed. The survival curves could indicate prognosis of cellular stiffness alterations. In order to increase the clinical value of this study, it is better to directly analyze the HCC patient survival curves of cellular stiffness related genes, such as RhoA, ROCK, MLCK and mDia1.

6.3 Future perspective

Firstly, we are going to establish mice model to explore whether cellular stiffness could influence metastasis of HCC in vivo. The first choice of mice model is spontaneous metastasis model. Nude mice will be used in this study. Mice will be kept in cages under specific pathogen-free condition. In brief, the luciferase labelled HCC cells will be subjected to treatment to change cellular stiffness in vitro which mimic the alterations of cellular stiffness during HCC progression. The softened or stiffened HCC cells will be orthotopically injected into the left lobes of the livers of 4 to 6-week-old nude mice. All animals will be inspected, and their health conditions will be monitored daily throughout the experiment period. Six to eight weeks after implantation, organs will be harvested for ex vivo imaging and histologic analysis. Metastatic nodules will be counted. However, spontaneous metastasis model will take a very long time and the failure risk is a little bit high. There is another alternative, tail vein injection model. Nude mice will be used in this experiment. The luciferase labelled HCC cells will also be subjected to treatment to change cellular stiffness in vitro and the pre-treated HCC cells will be injected intravenously into lateral tail vein for the 3~6 weeks old nude mice. The luciferase signal will be monitored daily to observe metastasis. Mice blood and tissue will be collected for analysis.

Secondly, JNK signalling worth digging deeper. In our present study, we only preliminarily identified JNK as the downstream of cellular stiffness and proved that cellular stiffness

regulated metastasis through JNK. However, JNK participates in so many signalling transduction pathways, it is necessary to find out other effective factors of this signalling pathway. In our study, we have demonstrated that the upstream of JNK MKK4 and MKK7 significantly changed after cellular stiffness alterations, but we still did not know whether indeed MKK4 and MKK7 are playing a role from functional level. It will be significant if we find out what links cellular stiffness to JNK and how JNK links to metastatic ability alterations.

Thirdly, the mechanism underlying cellular stiffening could inhibit metastasis of CSCs has been tentatively investigated. For further investigation of the underlying mechanism, RNA-sequence analysis could be considered in the future. It is commonly accepted that CSCs are the biggest challenge of cancer therapy, so, it is very important and significant to further investigate the mechanism of cellular stiffness regulating metastasis in CSCs. It may provide more fresh thinking and method on clinical application targeting CSCs.

Finally, what we have done are still staying at experimental level, it is necessary to make this study be closer to clinical application. The first step we need to take is to establish the correlation between what we have done and patient survival. So, the essential one is to analyse the survival curve of cellular stiffness related genes. Therefore, we could know clear whether cellular stiffness would be a better indicator of metastasis and a potential target for HCC therapies.

Reference

Aragonès, G., Saavedra, P., Heras, M., Cabré, A., Girona, J., & Masana, L. (2012). Fatty acid binding protein 4 impairs the insulin-dependent nitric oxide pathway in vascular endothelial cells. *Cardiovasc Diabetol, 11*, 72. doi:10.1186/1475-2840-11-72

Behrens, A., Sibilia, M., & Wagner, E. F. (1999). Amino-terminal phosphorylation of c-Jun regulates stress-induced apoptosis and cellular proliferation. *Nat Genet, 21*(3), 326-329. doi:10.1038/6854

Betapudi, V., Licate, L. S., & Egelhoff, T. T. (2006). Distinct roles of nonmuscle myosin II isoforms in the regulation of MDA-MB-231 breast cancer cell spreading and migration. *Cancer Res, 66*(9), 4725-4733. doi:10.1158/0008-5472.Can-05-4236

Bode, A. M., & Dong, Z. (2007). The functional contrariety of JNK. *Mol Carcinog, 46*(8), 591-598. doi:10.1002/mc.20348

Bogoyevitch, M. A., & Kobe, B. (2006). Uses for JNK: the many and varied substrates of the c-Jun N-terminal kinases. *Microbiol Mol Biol Rev, 70*(4), 1061-1095. doi:10.1128/mmbr.00025-06

Bray, F., Ferlay, J., Soerjomataram, I., Siegel, R. L., Torre, L. A., & Jemal, A. (2018). Global cancer statistics 2018: GLOBOCAN estimates of incidence and mortality worldwide for 36 cancers in 185 countries. *CA Cancer J Clin, 68*(6), 394-424. doi:10.3322/caac.21492

Bubici, C., & Papa, S. (2014). JNK signalling in cancer: in need of new, smarter therapeutic targets. *Br J Pharmacol, 171*(1), 24-37. doi:10.1111/bph.12432

Chang, L., Jones, Y., Ellisman, M. H., Goldstein, L. S., & Karin, M. (2003). JNK1 is required for maintenance of neuronal microtubules and controls phosphorylation of microtubule-associated proteins. *Dev Cell, 4*(4), 521-533. doi:10.1016/s1534-5807(03)00094-7

Chen, J., Sun, W. L., Wasylyk, B., Wang, Y. P., & Zheng, H. (2012). c-Jun N-terminal kinase mediates microtubule-depolymerizing agent-induced microtubule depolymerization and G2/M arrest in MCF-7 breast cancer cells. *Anticancer Drugs, 23*(1), 98-107. doi:10.1097/CAD.0b013e32834bc978

Chen, Y. Q., Lan, H. Y., Wu, Y. C., Yang, W. H., Chiou, A., & Yang, M. H. (2018). Epithelial-

mesenchymal transition softens head and neck cancer cells to facilitate migration in 3D environments. *J Cell Mol Med, 22*(8), 3837-3846. doi:10.1111/jcmm.13656

Cheng, M., Wu, J., Liu, X., Li, Y., Nie, Y., Li, L., & Chen, H. (2007). Low shear stress-induced interleukin-8 mRNA expression in endothelial cells is mechanotransduced by integrins and the cytoskeleton. *Endothelium, 14*(6), 265-273. doi:10.1080/10623320701678169

Cross, S. E., Jin, Y. S., Rao, J., & Gimzewski, J. K. (2007). Nanomechanical analysis of cells from cancer patients. *Nat Nanotechnol, 2*(12), 780-783. doi:10.1038/nnano.2007.388

Cross, S. E., Jin, Y. S., Tondre, J., Wong, R., Rao, J., & Gimzewski, J. K. (2008). AFM-based analysis of human metastatic cancer cells. *Nanotechnology, 19*(38), 384003. doi:10.1088/0957-4484/19/38/384003

Davis, R. J. (2000). Signal transduction by the JNK group of MAP kinases. *Cell, 103*(2), 239-252. doi:10.1016/s0092-8674(00)00116-1

Dhanasekaran, D. N., & Reddy, E. P. (2017). JNK-signaling: A multiplexing hub in programmed cell death. *Genes Cancer, 8*(9-10), 682-694. doi:10.18632/genesandcancer.155

Dhillon, A. S., Hagan, S., Rath, O., & Kolch, W. (2007). MAP kinase signalling pathways in cancer. *Oncogene, 26*(22), 3279-3290. doi:10.1038/sj.onc.1210421

Dou, Y., Jiang, X., Xie, H., He, J., & Xiao, S. (2019). The Jun N-terminal kinases signaling pathway plays a "seesaw" role in ovarian carcinoma: a molecular aspect. *J Ovarian Res, 12*(1), 99. doi:10.1186/s13048-019-0573-6

Fenner, J., Stacer, A. C., Winterroth, F., Johnson, T. D., Luker, K. E., & Luker, G. D. (2014). Macroscopic stiffness of breast tumors predicts metastasis. *Sci Rep, 4*, 5512. doi:10.1038/srep05512

Fernández-Sánchez, M. E., Barbier, S., Whitehead, J., Béalle, G., Michel, A., Latorre-Ossa, H., . . . Farge, E. (2015). Mechanical induction of the tumorigenic β-catenin pathway by tumour growth pressure. *Nature, 523*(7558), 92-95. doi:10.1038/nature14329

Forner, A., Reig, M., & Bruix, J. (2018). Hepatocellular carcinoma. *Lancet, 391*(10127), 1301-1314. doi:10.1016/s0140-6736(18)30010-2

Friedl, P., & Wolf, K. (2003). Tumour-cell invasion and migration: diversity and escape mechanisms. *Nat Rev Cancer, 3*(5), 362-374. doi:10.1038/nrc1075

Fritsch, A., Höckel, M., Kiessling, T., Nnetu, K. D., Wetzel, F., Zink, M., & Käs, J. A. (2010). Are biomechanical changes necessary for tumour progression? *Nature Physics, 6*(10), 730-732. doi:10.1038/nphys1800

Fuhrmann, A., Staunton, J. R., Nandakumar, V., Banyai, N., Davies, P. C., & Ros, R. (2011). AFM stiffness nanotomography of normal, metaplastic and dysplastic human esophageal cells. *Phys Biol, 8*(1), 015007. doi:10.1088/1478-3975/8/1/015007

Gupta, G. P., & Massagué, J. (2006). Cancer metastasis: building a framework. *Cell, 127*(4), 679-695. doi:10.1016/j.cell.2006.11.001

Haeusgen, W., Herdegen, T., & Waetzig, V. (2011). The bottleneck of JNK signaling: molecular and functional characteristics of MKK4 and MKK7. *Eur J Cell Biol, 90*(6-7), 536-544. doi:10.1016/j.ejcb.2010.11.008

Hsu, H. J., Lee, C. F., Locke, A., Vanderzyl, S. Q., & Kaunas, R. (2010). Stretch-induced stress fiber remodeling and the activations of JNK and ERK depend on mechanical strain rate, but not FAK. *PLoS One, 5*(8), e12470. doi:10.1371/journal.pone.0012470

Iyer, S., Gaikwad, R. M., Subba-Rao, V., Woodworth, C. D., & Sokolov, I. (2009). Atomic force microscopy detects differences in the surface brush of normal and cancerous cells. *Nat Nanotechnol, 4*(6), 389-393. doi:10.1038/nnano.2009.77

Jasper, H., Benes, V., Schwager, C., Sauer, S., Clauder-Münster, S., Ansorge, W., & Bohmann, D. (2001). The genomic response of the Drosophila embryo to JNK signaling. *Dev Cell, 1*(4), 579-586. doi:10.1016/s1534-5807(01)00045-4

Kaltschmidt, J. A., Lawrence, N., Morel, V., Balayo, T., Fernández, B. G., Pelissier, A., . . . Martinez Arias, A. (2002). Planar polarity and actin dynamics in the epidermis of Drosophila. *Nat Cell Biol, 4*(12), 937-944. doi:10.1038/ncb882

Kataoka, K., & Ogawa, S. (2016). Variegated RHOA mutations in human cancers. *Exp Hematol, 44*(12), 1123-1129. doi:10.1016/j.exphem.2016.09.002

Kim, D. H., Xing, T., Yang, Z., Dudek, R., Lu, Q., & Chen, Y. H. (2017). Epithelial

Mesenchymal Transition in Embryonic Development, Tissue Repair and Cancer: A Comprehensive Overview. *J Clin Med, 7*(1). doi:10.3390/jcm7010001

Kim, D. Y., & Helfman, D. M. (2016). Loss of MLCK leads to disruption of cell-cell adhesion and invasive behavior of breast epithelial cells via increased expression of EGFR and ERK/JNK signaling. *Oncogene, 35*(34), 4495-4508. doi:10.1038/onc.2015.508

Kulik, L., & El-Serag, H. B. (2019). Epidemiology and Management of Hepatocellular Carcinoma. *Gastroenterology, 156*(2), 477-491.e471. doi:10.1053/j.gastro.2018.08.065

Kumar, S., & Weaver, V. M. (2009). Mechanics, malignancy, and metastasis: the force journey of a tumor cell. *Cancer Metastasis Rev, 28*(1-2), 113-127. doi:10.1007/s10555-008-9173-4

Lai, C. L., Ratziu, V., Yuen, M. F., & Poynard, T. (2003). Viral hepatitis B. *Lancet, 362*(9401), 2089-2094. doi:10.1016/s0140-6736(03)15108-2

Lambert, A. W., Pattabiraman, D. R., & Weinberg, R. A. (2017). Emerging Biological Principles of Metastasis. *Cell, 168*(4), 670-691. doi:10.1016/j.cell.2016.11.037

Lauffenburger, D. A., & Horwitz, A. F. (1996). Cell migration: a physically integrated molecular process. *Cell, 84*(3), 359-369. doi:10.1016/s0092-8674(00)81280-5

Lessey, E. C., Guilluy, C., & Burridge, K. (2012). From mechanical force to RhoA activation. *Biochemistry, 51*(38), 7420-7432. doi:10.1021/bi300758e

Li, Q. S., Lee, G. Y., Ong, C. N., & Lim, C. T. (2008). AFM indentation study of breast cancer cells. *Biochem Biophys Res Commun, 374*(4), 609-613. doi:10.1016/j.bbrc.2008.07.078

Li, S., Kim, M., Hu, Y. L., Jalali, S., Schlaepfer, D. D., Hunter, T., . . . Shyy, J. Y. (1997). Fluid shear stress activation of focal adhesion kinase. Linking to mitogen-activated protein kinases. *J Biol Chem, 272*(48), 30455-30462. doi:10.1074/jbc.272.48.30455

Liu, J., Tan, Y., Zhang, H., Zhang, Y., Xu, P., Chen, J., . . . Huang, B. (2012). Soft fibrin gels promote selection and growth of tumorigenic cells. *Nat Mater, 11*(8), 734-741. doi:10.1038/nmat3361

Llovet, J. M., Zucman-Rossi, J., Pikarsky, E., Sangro, B., Schwartz, M., Sherman, M., & Gores, G. (2016). Hepatocellular carcinoma. *Nat Rev Dis Primers, 2*, 16018.

doi:10.1038/nrdp.2016.18

Martin-Blanco, E., Pastor-Pareja, J. C., & Garcia-Bellido, A. (2000). JNK and decapentaplegic signaling control adhesiveness and cytoskeleton dynamics during thorax closure in Drosophila. *Proc Natl Acad Sci U S A, 97*(14), 7888-7893. doi:10.1073/pnas.97.14.7888

Mehlen, P., & Puisieux, A. (2006). Metastasis: a question of life or death. *Nat Rev Cancer, 6*(6), 449-458. doi:10.1038/nrc1886

Nash, G. F., Turner, L. F., Scully, M. F., & Kakkar, A. K. (2002). Platelets and cancer. *Lancet Oncol, 3*(7), 425-430. doi:10.1016/s1470-2045(02)00789-1

Nelson, C. M., & Bissell, M. J. (2006). Of extracellular matrix, scaffolds, and signaling: tissue architecture regulates development, homeostasis, and cancer. *Annu Rev Cell Dev Biol, 22*, 287-309. doi:10.1146/annurev.cellbio.22.010305.104315

Noguchi, H. (2019). Regulation of c-Jun NH(2)-Terminal Kinase for Islet Transplantation. *J Clin Med, 8*(11). doi:10.3390/jcm8111763

Okada, M., Matsumori, A., Ono, K., Furukawa, Y., Shioi, T., Iwasaki, A., . . . Sasayama, S. (1998). Cyclic stretch upregulates production of interleukin-8 and monocyte chemotactic and activating factor/monocyte chemoattractant protein-1 in human endothelial cells. *Arterioscler Thromb Vasc Biol, 18*(6), 894-901. doi:10.1161/01.atv.18.6.894

Park, J. W., Chen, M., Colombo, M., Roberts, L. R., Schwartz, M., Chen, P. J., . . . Sherman, M. (2015). Global patterns of hepatocellular carcinoma management from diagnosis to death: the BRIDGE Study. *Liver Int, 35*(9), 2155-2166. doi:10.1111/liv.12818

Perone, Y., Farrugia, A. J., Rodríguez-Meira, A., Győrffy, B., Ion, C., Uggetti, A., . . . Magnani, L. (2019). SREBP1 drives Keratin-80-dependent cytoskeletal changes and invasive behavior in endocrine-resistant ERα breast cancer. *Nature Communications, 10*(1), 2115. doi:10.1038/s41467-019-09676-y

Plodinec, M., Loparic, M., Monnier, C. A., Obermann, E. C., Zanetti-Dallenbach, R., Oertle, P., . . . Schoenenberger, C. A. (2012). The nanomechanical signature of breast cancer. *Nat Nanotechnol, 7*(11), 757-765. doi:10.1038/nnano.2012.167

Polyak, K., & Weinberg, R. A. (2009). Transitions between epithelial and mesenchymal states:

acquisition of malignant and stem cell traits. *Nat Rev Cancer, 9*(4), 265-273. doi:10.1038/nrc2620

Rennefahrt, U. E., Illert, B., Kerkhoff, E., Troppmair, J., & Rapp, U. R. (2002). Constitutive JNK activation in NIH 3T3 fibroblasts induces a partially transformed phenotype. *J Biol Chem, 277*(33), 29510-29518. doi:10.1074/jbc.M203010200

Rudrapatna, V. A., Bangi, E., & Cagan, R. L. (2014). A Jnk-Rho-Actin remodeling positive feedback network directs Src-driven invasion. *Oncogene, 33*(21), 2801-2806. doi:10.1038/onc.2013.232

Sahai, E. (2005). Mechanisms of cancer cell invasion. *Curr Opin Genet Dev, 15*(1), 87-96. doi:10.1016/j.gde.2004.12.002

Seki, E., Brenner, D. A., & Karin, M. (2012). A liver full of JNK: signaling in regulation of cell function and disease pathogenesis, and clinical approaches. *Gastroenterology, 143*(2), 307-320. doi:10.1053/j.gastro.2012.06.004

Shi, C., Cai, Y., Li, Y., Li, Y., Hu, N., Ma, S., . . . Zhou, H. (2018). Yap promotes hepatocellular carcinoma metastasis and mobilization via governing cofilin/F-actin/lamellipodium axis by regulation of JNK/Bnip3/SERCA/CaMKII pathways. *Redox Biol, 14*, 59-71. doi:10.1016/j.redox.2017.08.013

Suresh, S. (2007). Biomechanics and biophysics of cancer cells. *Acta Biomater, 3*(4), 413-438. doi:10.1016/j.actbio.2007.04.002

Swaminathan, V., Mythreye, K., O'Brien, E. T., Berchuck, A., Blobe, G. C., & Superfine, R. (2011). Mechanical stiffness grades metastatic potential in patient tumor cells and in cancer cell lines. *Cancer Res, 71*(15), 5075-5080. doi:10.1158/0008-5472.Can-11-0247

Talmadge, J. E., & Fidler, I. J. (2010). AACR centennial series: the biology of cancer metastasis: historical perspective. *Cancer Res, 70*(14), 5649-5669. doi:10.1158/0008-5472.Can-10-1040

Thiery, J. P. (2002). Epithelial-mesenchymal transitions in tumour progression. *Nat Rev Cancer, 2*(6), 442-454. doi:10.1038/nrc822

Thomas, D., Thiagarajan, P. S., Rai, V., Reizes, O., Lathia, J., & Egelhoff, T. (2016). Increased cancer stem cell invasion is mediated by myosin IIB and nuclear translocation. *Oncotarget,*

7(30), 47586-47592. doi:10.18632/oncotarget.9896

Tian, M., Li, Y., Liu, W., Jin, L., Jiang, X., Wang, X., . . . Shi, Y. (2015). The nanomechanical signature of liver cancer tissues and its molecular origin. *Nanoscale, 7*(30), 12998-13010. doi:10.1039/c5nr02192h

Valastyan, S., & Weinberg, R. A. (2011). Tumor metastasis: molecular insights and evolving paradigms. *Cell, 147*(2), 275-292. doi:10.1016/j.cell.2011.09.024

Watanabe, T., Kuramochi, H., Takahashi, A., Imai, K., Katsuta, N., Nakayama, T., . . . Suganuma, M. (2012). Higher cell stiffness indicating lower metastatic potential in B16 melanoma cell variants and in (-)-epigallocatechin gallate-treated cells. *J Cancer Res Clin Oncol, 138*(5), 859-866. doi:10.1007/s00432-012-1159-5

Whitmarsh, A. J. (2006). The JIP family of MAPK scaffold proteins. *Biochem Soc Trans, 34*(Pt 5), 828-832. doi:10.1042/bst0340828

Wong, S. Y., Ulrich, T. A., Deleyrolle, L. P., MacKay, J. L., Lin, J. M., Martuscello, R. T., . . . Kumar, S. (2015). Constitutive activation of myosin-dependent contractility sensitizes glioma tumor-initiating cells to mechanical inputs and reduces tissue invasion. *Cancer Res, 75*(6), 1113-1122. doi:10.1158/0008-5472.Can-13-3426

Xu, R., & Hu, J. (2020). The role of JNK in prostate cancer progression and therapeutic strategies. *Biomed Pharmacother, 121*, 109679. doi:10.1016/j.biopha.2019.109679

Xu, W., Mezencev, R., Kim, B., Wang, L., McDonald, J., & Sulchek, T. (2012). Cell stiffness is a biomarker of the metastatic potential of ovarian cancer cells. *PLoS One, 7*(10), e46609. doi:10.1371/journal.pone.0046609

Zhang, L., Wang, W., Hayashi, Y., Jester, J. V., Birk, D. E., Gao, M., . . . Xia, Y. (2003). A role for MEK kinase 1 in TGF-beta/activin-induced epithelium movement and embryonic eyelid closure. *Embo j, 22*(17), 4443-4454. doi:10.1093/emboj/cdg440

Zhu, R. X., Seto, W. K., Lai, C. L., & Yuen, M. F. (2016). Epidemiology of Hepatocellular Carcinoma in the Asia-Pacific Region. *Gut Liver, 10*(3), 332-339. doi:10.5009/gnl15257